TECHNISCHE UNIVERSITÄT WIEN
Vienna University of Technology

Master Thesis

Investigation of Aged, Non-aged Bitumen and their Bitumen Fractions

Done at the Institute of Materials Chemistry, Vienna University of Technology
under supervision of Ao. Univ.-Prof.Dipl.-Chem. Dr. rer.nat. Hinrich Grothe

by
Daniel Großegger

Bsuch 97
5760 Saalfelden
Salzburg, Austria

Vienna, April 2015 Daniel Großegger

Abstract

In road construction the main application of bitumen is as binder for asphalt. The viscoelastic, adhesive and mostly black material is mainly obtained as a residue from petroleum distillation. Other origins for bitumen exist, but this thesis discusses only bitumen originating from crude oil.

Bitumen can be separated into four fractions. The separation takes place in two steps. The first step is the precipitation of asphaltenes, done by filtering bitumen dissolved in n-heptane. The remaining part, called maltenes, is then in the second step separated by liquid column chromatography into saturates, aromatics and resins. Polarity increases form saturates to resins and asphaltenes are in the polarity range of aromatics and resins.

Asphaltenes form a black powder and decompose when heated above 350 °C. The asphaltene fraction consists of large molecules containing hetero atoms like oxygen, nitrogen, sulphur and metal atoms. Due to fused aromatic rings asphaltenes can exhibit fluorescence, but they do not show fluorescence in the solid state, only when dissolved they fluoresce. Asphatenes have a major contribution on all physical properties, as they increase alongside of resins. During ageing bitumen gets stiffer (less viscous), so their fluorescence signal decreases.

Resins are a black solid at room temperature and liquefy at higher temperature. The exhibited fluorescence is contributed to its molecular structure containing aromatic rings. They increase during ageing.

Aromatics are viscous and appear dark red. They contribute the most to the fluorescence of bitumen. Other fractions (most resins) seem to quench the fluorescence of the aromatics leading to the spectrum of maltenes. Asphaltenes decreases the intensity further, but no additional change in curve progression takes place. Aromatics act as solution for asphaltenes and resins and are decreasing during ageing, probably changing to resins and asphaltenes, due to oxidation.

Saturates are a colourless liquid, which behaves purely viscous like aromatics. The saturate concentration is not altered during ageing, so their contribution to any property remains constant. A part fluoresces, but the main part shows fewer to no signals.

During ageing the fractions asphaltenes and resins increase in content as aromatics decrease. Due to the change in these three fractions the fluorescence signal lessens. Infrared spectroscopy indicates that oxygen is taken up during ageing – oxidation process. Effects on the microstructure are that the catana and peri-phase increase in size shown by atomic force microscopy.

The mechanism for laboratory liquid ageing is different from standard laboratory ageing methods or field ageing, indicated by fluorescence and infrared spectroscopy.

Preface and acknowledgements

Understanding a complex material like bitumen is a difficult task. Published researches did not study the same bitumen and thus found unique properties cannot be generalised. However, bitumen and similar obtained bitumen fractions feature properties that can be distinguished as uniform for all bitumen. It is assumed by the author that understanding the intricate mechanism of bitumen ageing and structural feature development is essential. By studying one bitumen sample and the reproducibility of all applied test methods should by verified. Then the study can be expanded to other, first similar then different, samples to identify and outline those mechanisms.

This thesis uses as decimal mark a comma and as delimiter a dot.

I would like to express my gratitude to my advisor Hinrich Grothe for the autonomy in my laboratory studies. I am also grateful for Susanna Neudl's introduction into laboratory work and guidance at the beginning of this project.

I would also like to thank all my colleges at the Institute of Materials Chemistry, who supported and helped me, my colleges at the Institute of Transportation, Research Centre of Road Engineering, my student colleges with whom I studied along and my friends who always had an open ear for my problems.

I appreciate the proofreading of my thesis, done by Martin Sigmund and Evelyn Kapeller.

And finally I am deeply thankful to my parents and my whole family for supporting me all these years.

Content

1. Introduction 1

2. Material 2

2.1. Introduction and terminology 2

2.2. Bitumen 2

2.2.1. Crude oil and bitumen production 2

2.2.2. Physical, chemical properties and structure of bitumen 7

2.2.3. Bitumen fractions 10

2.2.3.1. Asphaltenes 11

2.2.3.2. Maltenes 13

2.2.3.3. Saturates 13

2.2.3.4. Aromatics 13

2.2.3.5. Resins 14

2.3. Asphalt 14

2.4. Sample origin 16

3. Bitumen ageing 19

3.1. Introduction 19

3.2. Excerpt of atmospheric chemistry 19

3.3. Chemical ageing and evaporation 22

3.4. Steric hardening 25

3.5. Ageing stages 25

4. Methods 27

4.1. Introduction 27

4.2. Ageing methods 27

4.2.1. Laboratory ageing 27

4.2.1.1. Rolling Thin Film Oven Test (RTFOT) 27

4.2.1.2. Pressure Ageing Vessel (PAV) 28

4.2.1.3. Liquid ageing 29

4.2.2. Field ageing 30

4.2.2.1. Test field 30

4.2.2.2. Road sample 31

4.3. Analytical methods 31

4.3.1. Needle penetration 31

4.3.2. Dynamic Shear Rheometer (DSR) 32

4.3.3. Classical liquid column chromatography 34

4.3.4. Bitumen separation into four fractions 35

4.3.5. Liquid-liquid extraction 42

4.3.6. Optical and spectrochemical methods 42

4.3.6.1. Optical methods 42

4.3.6.2. Fluorescence spectroscopy 42

4.3.6.3. Infrared spectroscopy 45

5. Results and discussion 46
5.1. Bitumen separation 46
5.1.1. Gravimetrical analyses 46
5.1.2. Fluorescence analyses 51
5.1.3. Infrared analyses 54
5.1.4. Fractions analyses 58
5.1.5. Viscoelastic analyses 59
5.1.6. Water soluble compounds 62
5.2. Investigation of ageing by optical and spectrochemical methods 65
5.2.1. Fluorescence spectroscopy 65
5.2.2. Investigation of liquid aged bitumen 69
5.2.3. Infrared spectroscopy 72
5.3. Brief insight in bitumen microstructure 73
6. Summary and conclusions 77
7. List of tables 80
8. List of figures 81
9. References 84
Appendix: Details on bitumen separation 87

1. Introduction

A functional infrastructure is the backbone of an industrialised country. The whole economy and civil life rely on working roadway systems. Even if concrete may be used more often in higher roadway construction, asphalt has still its uses. In local roadways like in cities it is still the most often used building material. In Europe over 90% of the road network have an asphalt surface [1]. In Austria 95% of the road network, which is about 200.000 km long, are build out of asphalt [2].

With rising economic and environmental issues, like erratic oil price developments, governmental limitations on waste disposal and a concerned society, recycling of asphalt road constructions is inevitable. Asphalt is virtually 100% recyclable and a recycling rate of up to 70% is possible. In Austria a lesser part is recycled and done by down cycling [3] due to the effect that aged bitumen is more brittle compared to virgin binder and also shows a lesser favoured viscoelastic behaviour over the temperature range especially at low temperature. Still there is an advantage, which is the so-called self-healing ability of bitumen. With the understanding of the ageing process and the self-healing process it could be possible to recycle asphalt more efficiently or even regenerate it to a minor degree in situ.

The main objective of this study was to investigate the change of the chemical composition in bitumen with regard to four main fractions: saturates, aromatics, resins and asphaltenes.

The separation was accomplished in two steps. The first step was the precipitation of asphaltenes. The next step the division of the remaining fractions was preformed by liquid column chromatography. The different fractions were collected in snap-cap vials for determination of their weight distribution. Further the fraction were analysed with spectrochemical methods to verify that the obtained fractions were not adulterated.

Laboratory aged and field aged bitumen were analysed with the aim to control if the impact of ageing under natural or artificial conditions results in the same effects. Additionally first steps in understanding the interaction of bitumen and environment were made.

2. Material

2.1. Introduction and terminology

In this section the basic properties of bitumen are introduced. A general understanding of the complex nature of bitumen is defined with the aspect of dividing bitumen into four fractions. In regard to the origin of samples, as bitumen is the binding component in asphalt and is recovered from it, asphalt is shortly outlined.

In this study only the residue of the vacuum distillation from crude oil (petroleum) is studied and thus the term bitumen refers only to the origin from crude oil. Other origin for bitumen-like deposits, like natural asphalts, rock asphalts and oil sands, are noted when referred to these.

The European usage of the term bitumen, or asphaltic bitumen is used for this thesis. Synonyms in North America are asphalt or asphalt cement, but the term asphalt is used to describe the mixture of bitumen and mineral compounds [1,4].

2.2. Bitumen

Bitumen is a viscoelastic material, adhesive and appears mostly black. It can be obtained as a residue from petroleum distillation and can be further processed by air blowing process to alter its physical properties [1,4,5]. The term bitumen should not be confounded with coal tar or pitch. Due to carcinogenic effects coal tar is prohibited for road constructions. Natural bitumen, such as the occurrence in natural asphalt lakes, differs from industrial produced bitumen. They are unrefined and often contain more light compounds, mineral particles and occasionally water [4].

The first records of natural occurring bitumen (most likely petroleum mistaken for natural occurring bitumen) used as an adherent material to craft tool dates back to the Middle Palaeolithic [4]. Due to its adhesive and waterproof properties bitumen has been used since antiquity and was also deployed medically [4,5]. During that time the first road construction based on bitumen was built. Then over nearly two and a half centuries the broad use vanished and was then rediscovered in the 19th century. In the 1910s natural occurring bitumen started to diminish in use due to the vacuum distillation from crude oil [4]. Until nowadays (available data from 2007) 85% are applied in road construction as binder originated from crude oil [1].

2.2.1. Crude oil and bitumen production

The properties of bitumen depend on the properties of the crude oil from which it is manufactured and the treatment during manufacturing. Table 1 illustrates the similarities in relation to elemental composition between crude oil and bitumen. Nitrogen and sulphur contents are increasing, due to higher concentration of these elements in heavier compounds and hydrogen is decreasing, due to extraction of lighter hydrocarbon chains during refinery. The metal content varies in crude oil from 0,01 to 0,04wt%. About thirty different metals are

found in different crude oils [1]. The most common are vanadium, nickel, iron, zinc, mercury, boron, sodium, potassium, calcium and magnesium.

Table 1: Elemental analysis of crude oil and bitumen from various sources (wt%) [1,4–6]

element	crude oil	bitumen
carbon (C)	82,8 – 86,9	80,2 – 86,8
hydrogen (H)	10,4 – 14,2	9,8 – 11,3
nitrogen (N)	0,3 – 0,5	0,2 – 1,2
oxygen (O)	0,6 – 3,6	0,4 – 1,1
sulphur (S)	0,2 – 4,5	0,9 – 6,9
nickel (Ni)	n.d.	$10 \cdot 10^{-4}$ – $130 \cdot 10^{-4}$
vanadium (V)	n.d.	$7 \cdot 10^{-4}$ – $1590 \cdot 10^{-4}$
iron (Fe)	n.d.	$5 \cdot 10^{-4}$ – $147 \cdot 10^{-4}$
manganese (Mn)	n.d.	$0{,}1 \cdot 10^{-4}$ – $3{,}7 \cdot 10^{-4}$
calcium (Ca)	n.d.	$1 \cdot 10^{-4}$ – $335 \cdot 10^{-4}$
magnesium (Mg)	n.d.	$1 \cdot 10^{-4}$ – $134 \cdot 10^{-4}$
sodium (Na)	n.d.	$6 \cdot 10^{-4}$ – $159 \cdot 10^{-4}$

There are two hypotheses about the origin of crude oil. The inorganic petroleum origin is based on the formation of carbides (CaC_2) by the reaction of alkali metals with carbonates ($CaCO_3$), followed by a reaction with water (H_2O) producing ethylene (C_2H_2) [5]. At higher temperature and pressure petroleum is formed from ethylene. This hypothesis is not very common nowadays and is replaced by the organic petroleum origin hypothesis (modern concept). The carbon source in this hypothesis is the biomass (special microorganisms like phytoplankton) that inhabited the seas and oceans. The concentration of organic material increases with depth, so the highest concentration is found at the bottom. Due to mineral accumulation this organic material can be trapped and encapsulated from decomposition. With the build up of additional layers of minerals and the movements of the lithosphere plates, trapped organic material can pass in zones of rift or subduction where the temperature increases by 100 to 400 °C (minimum depth of 2 to 3 km). In that temperature range the dissociation of various compounds takes place and provides the necessary energy for the formation of petroleum [5].

Petroleum is either extracted from oil wells under the natural pressure of the layer, or by pumping. With both operation methods the petroleum layer and added water layer are concurrently extracted [5]. Petroleum and water then form an emulsion. The continuous phase is most frequently petroleum and the discontinuous phase is accordingly water. The emulsion intensifies depending on the extraction method and additionally during transportation through pipes. Further the presence of emulsifiers influences the formation and properties of an emulsion. The used method to dry petroleum depends on the amount and condition of water. Non-stabilized emulsion can be separated by settling methods or by settling with moderate heating. A stabilized emulsion is more difficult to separate. The methods include intense heating, chemical processing, electrical processing or a combination

of those methods. Often during drying a desalting takes place, by removing the water with the dissolved minerals (chemical or electrostatic separation at 110 to 160 °C) [5].

The first step in petroleum refinery is rectification. Since the boiling points of the compounds of petroleum are close to one another, differential distillation is employed for the primary separation. Differential distillation is based on distillation at differing levels and the counter-current flow principle [5].

The refinery involves one or more distillation towers, depending on the desired products. The classification into atmospheric towers and vacuum towers is according to the predominant pressure inside the operating tower [5]. Further on the basis of the internals tray towers and trickle or packed towers (not described) can be distinguished and on the basis of the function simple towers and complicated towers can be differed. Complicated towers have additional strippers (small towers with the same function as the main rectification tower) as side cuts that are used to obtain a purer product. The inducted petroleum, from storage tanks, is preheated to a temperature between 315 and 400 °C by a heat exchanger and oven, and fed at the lower part into the tower. This first tower operates close to ambient pressure till over pressure due to maintaining a pressure in the influx pipes. The towers are about 45 m high and contain 20 to 40 fractionating trays, which can be sieve (common used), bubble cap or valve trays (common used). The raising vapour is cooled by the descending liquid as it streams up the tower and due to this contact the liquid absorbs heavier constituents and lighter constituents migrate into the vapour phase. The descending liquid arises from the limited feed load of the tray where it condenses and runs off. The bottom of the tower is heated to assure that lighter constituents raises as vapour up again. On the top the vapour is partial condensed to a liquid in a water- or air-cooled condenser. The volatile part is piped into the refinery fuel gas system. Additionally, at several points from the tower intermediate products are drained. To receive higher purity side cut strippers are used, also a part is fed back into the tower as reflux to achieve a more efficient separation. The products obtained by atmospheric tower distillation are naphtha (rich in cycloalkane; head), heavy naphtha (side-stream), kerosene (side-stream), light gas oil or diesel (side-stream), heavy gas oil (side-stream) and residue (bottom). The residue can be further fractionated by a vacuum tower, but rather is thermal cracked before processed in the vacuum tower [5].

Vacuum towers are based on the same principles as atmospheric towers. The lower pressure (1.333 to 13.332 Pa), induced by vacuum pumps or steam ejectors, requires different tower geometry. The upper parts have larger diameters (about 15 m), which are tapered to the bottom. Due to lower pressure and temperature below 425 °C thermal cracking of components is avoided. For higher quality nowadays two-step vacuum rectification is used. Products from vacuum tower distillation are light vacuum gas oil, middle/heavy vacuum gas oil and vacuum distilled residue (formerly sometimes referred to as “goudron”). The residue from the vacuum rectification is used either as a feedstock for thermal cracking or coking units, or is used for bitumen products [5].

The first part described “primary processes”. During these treatments no chemical changes occur, it is based on the physical properties of petroleum. The “secondary processes” involve chemical changes and are thermal cracking, catalytic cracking, visbreaking, coking and hydroprocessing [5].

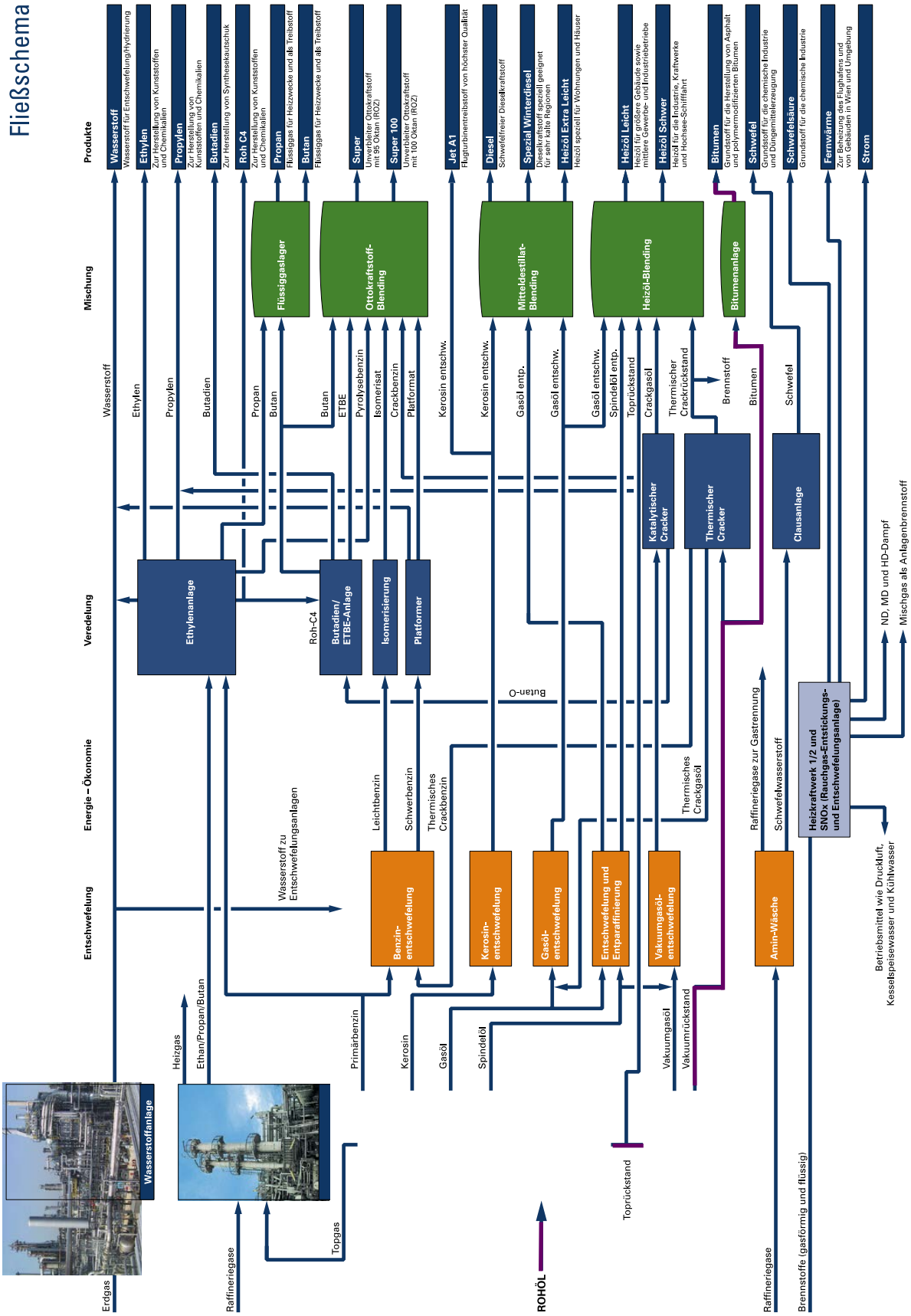

Figure 1: Flow chart of OMV refinery Schwechat; the production line for bitumen is marked purple [7]

The processes thermal cracking, catalytic cracking and visbreaking are applied to convert lager molecules into smaller molecules by breaking bounds. Thermal cracking is a radical

chain reaction preformed at about 400 to 450 °C. Side chains of aromatic rings are first to crack, due to the lower bonding energy (273 kJ·mol^{-1}), followed by the C-C bond (approximately 320 kJ·mol^{-1}). Also chain growths occur due to addition reaction and the formation of lager aromatic structures by polycondensation (coke formation). Thermal cracking converts about 50% of the feed into naphtha and light gas oil. Catalytic cracking, especially fluid catalytic cracking, has nearly completely replaced thermal cracking, due to a higher production rate of desired products. The catalysts are acidic such as zeolites and as a powder distributed in the oil vapour (500 to 550 °C). Visbreaking is an advancement of thermal cracking. The temperature used is between 450 and 500 °C and additionally, to avoid coke formation, higher pressure is applied. This leads to shorter molecules and lower viscosity [5].

In Figure 1 the petroleum refinery process is illustrated in reference to OMV. The vacuum residue is split into two line sections. Without further treatment the relevant line section (bitumen) is guided into bitumen processing. The whole refinery process is to be considered for bitumen production. Bitumen does not occur as a by-product, instead is specifically demand-oriented produced, beginning with selection of crude oil for the refinery and is thereby linked to all processes. Only about 10 to 15% of the worldwide crude oil delivery volume is suitable for bitumen production [8].

The vacuum residue does not always have the desired properties and so it is post-processed. To receive "harder" bitumen (decreasing needle penetration value (see subsection 4.3.1), change in temperature-viscosity property) the bitumen can be oxidized with air [1,4,5]. There are two grades of oxidised bitumen: semi-blown and blown bitumen. The blowing column is about 70% filled with 230 to 260 °C hot vacuum residue. The air is introduced at the bottom and occasionally for more intense mixing baffles or agitation systems are installed. In order to control the temperature of the generally exothermic reaction water can be sprayed from the top or injected laterally [1,4].

Further the vacuum residue can be deasphalted. With solvent (alkane) the asphaltene fraction is removed from bitumen [1].

For the final product bitumen is blended with itself or other compounds resulting in modified bitumen. The compounds for modified bitumen are, for example, emulsifier (for production of emulsion), petroleum distillates, polymers, sulphur or waxes [1]. The final product is stored in heated tanks at a temperature of about 185 °C. To avoid oxidation (oxidative hardening) the tanks are pressurised with nitrogen. The delivery, too, is done by tank lorries at a temperature of 185 °C ±5 °C [8].

2.2.2. Physical, chemical properties and structure of bitumen

All properties of bitumen can only be given in a range due to the different origins of petroleum, manufacturing processes and time dependent microstructure, which affects the properties of bitumen. As stated earlier bitumen is a viscoelastic material. The viscoelastic behaviour is temperature dependent [4,9]. At higher temperature it tends to be less viscous (generally, depending on the bitumen, >140 °C bitumen becomes liquid [1]), increasing

viscosity with decreasing temperature and at lower temperature elastic/brittle behaviour prevails [4]. This change in behaviour is marked by glass transition (change from liquid to amorphous solid (non-crystalline solid with no well-defined ordered structure [10]); not a sharp transition) which varies from +5 °C to -40 °C [4]. The thermo-viscous behaviour is the reason for its utilization; heating up for manipulation and showing the desired behaviour at service temperature. Some properties are regulated by national or international specifications, like the softening point, which is grade dependent or the solubility [1].

The density fluctuates in a small range from 1,01 to 1,04 $g \cdot cm^{-3}$ at room temperature [4]. The weight loss on heating is between 0,5 and 1wt% [1]. The solubility of bitumen in water is negligible, yet it is up to 99wt% soluble in trichloroethene, methylbenzene or dimethylbenzene [1,4]. The solubility in organic solvents, general methylbenzene, is sometimes used to define bitumen [4].

The elemental composition (Table 1) describes bitumen as consisting mainly of carbon and hydrogen as hydrocarbons and hydrocarbon derivatives [4,11]. The H/C ratio is about 1,5 and hence is between aromatic structures with the lowest ratio of 1 and saturated alkenes with a ratio of around 2 [4]. Additionally bitumen contains nitrogen, sulphur, oxygen and traces of other elements, mostly metals like iron, vanadium and nickel. All elements are present in the crude oil source but by manufacturing some are increased in content. Through abrasion of pumps and oil refining equipment by corrosive mineral salts in the water phase additional metal is introduced [5] and by the use of air blowing units the oxygen content is increased. The heavy metals agglomerate mostly in the residue and accordingly in bitumen. The average molecular weight of bitumen is in the range from 600 to 1500 $g \cdot mol^{-1}$ [4].

As a residue of petroleum refinery, which is not further separated under the applied conditions of temperature and pressure, bitumen is a complex solution of variant molecular species. Defining each molecule is impossible, due to the existence of proposed 10^5 to 10^6 different molecules, hence a general separation into different groups of chemically related compounds is practicable [4]. For this thesis the separation into four fractions (asphaltenes, saturates, aromatics and resins) was chosen. These fractions are described separately in the following subsections. Even though bitumen can be separated into fractions, these fractions cannot be seen as individual components of a mixture, which forms bitumen. It is more like a continuum with unsharp cut points for fractions (overlapping of elution in chromatographic separation) defined by separation methods [12,13].

The presents of heteroatoms, typically for asphaltenes and resins, within molecules makes them slightly polar. The interaction of the different molecules and the modest change in polarity by increasing oxygen content during ageing influence the physical properties of bitumen [12,14,15]. The dominant interaction between molecules is likely the London force, in addition there are polar interactions and π-π interactions present [4,12].

Different imaging methods have shown that bitumen is not a homogeneous mixture instead it shows structural features at the sub-microscopic level. These features are outlined on the

basis of two imaging techniques (confocal laser scanning microscopy and atomic force microscopy) in the following paragraphs.

Confocal laser scanning microscopy is a high-resolution optical technique. A laser with defined wavelength aims at one point at the time and excites a susceptible molecule. The emitted photon with a longer wavelength than introduced of the excited molecule when it returns to its ground state is detected also for this point (see additionally subsection 4.3.6.2, description of fluorescence). This process is repeated until all points of the image are scanned. Not all compounds of bitumen have the ability to fluorescence; so only those, which are capable, give a response. Bitumen shows distributed fluorescent centres (Figure 2) [16]. The spatial distribution, size and shape of the centres vary with origin, treatment state and ageing.

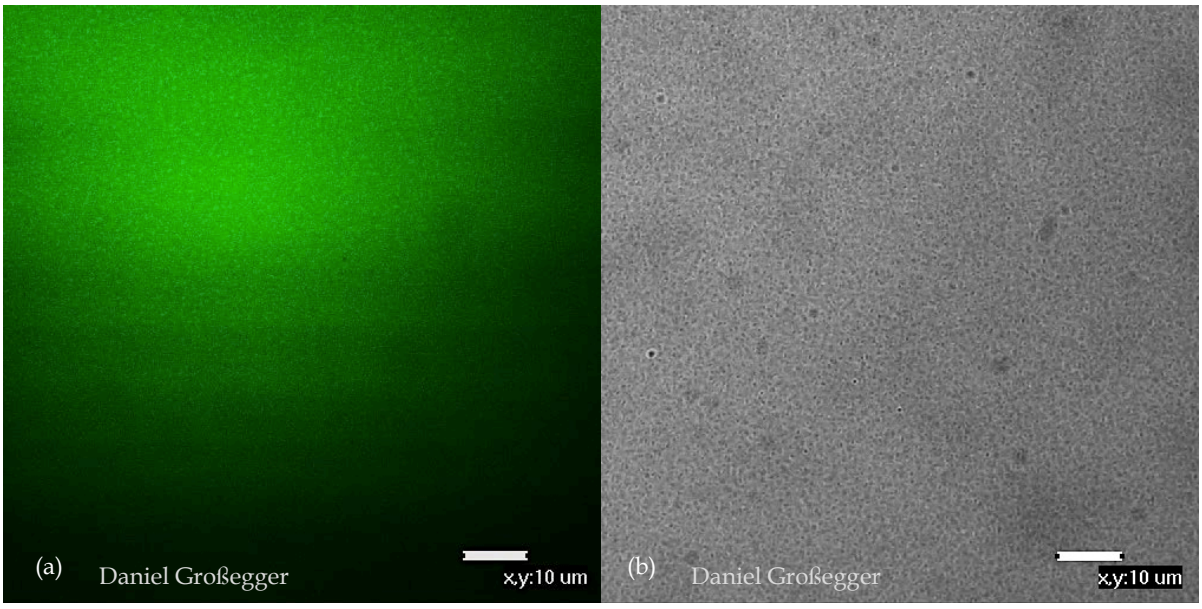

Figure 2: Confocal laser scanning microscopy image of B_LPAV: fluorescence image (a) and optical image (b)

Atomic force microscopy is a surface analytical technique. The tip, fixed on a cantilever, is brought close to the sample surface. The interaction of tip and surface atoms introduce a force, which bends the cantilever. The displacement of the cantilever from its initial position is measured, so topographical maps of the sample can be obtained. Various other modes can be applied for different results. Three phases for bitumen were identified by this method: the catana phase ("bee structure"), the peri-phase (surrounding the catana phase) and the para-phase (Figure 3). Sometimes a fourth phase, sal-phase, is observes within the para-phase, which does not freeze at very low temperature [17]. The observed structure does not occur directly after sample preparation (over 3 hours of delay is necessary). The structure also depends on the film thickness and starts to vanish with increasing temperature. It is possible that these structural formations can be introduced due to different thermal expansion coefficients.

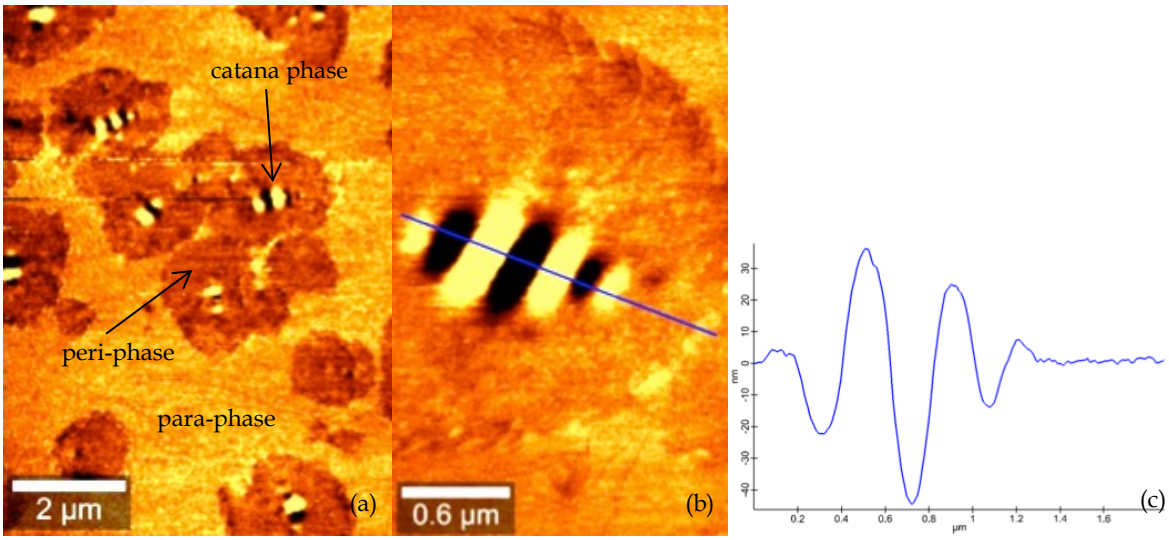

Figure 3: Atomic force microscopy images of B: topography (a, b) and cross profile of catana phase (c) [18]

Other techniques, like environmental scanning electron microscopy or cryo-transmission electron microscopy (contentious), showed structural features. But all imaging techniques should be considered with caution, due to the possibility of introduced artefacts (like bitumen sticking to the tip of the atomic force microscope cantilever). Though all observations display a structure on micrometre to nanometre level. The structure influences the physical properties (viscosity and elasticity) and depends on the origin of bitumen.

The correlation between structure and chemical fractions is not displayed in this subsection. An attempted is made in subsection 5.3. It is noted that different models are stated in the literature, which are partly vexed.

2.2.3. Bitumen fractions

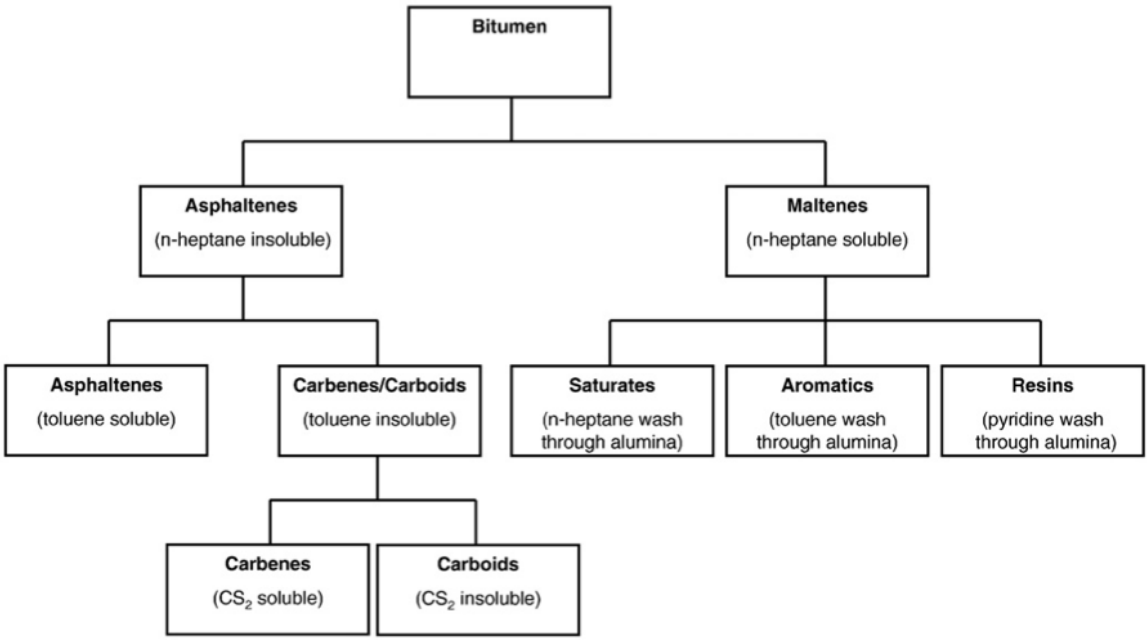

Figure 4: Bitumen separation into various fractions [4]

Bitumen can be separated into fractions. The number of fractions depends on the separation methods [4], which can result into 17 fractions (Figure 4 represents the common fractions). A common first separation is the separation into asphaltenes and maltenes by the solubility in solvent with low carbon number (5 to 7). The maltenes can further be separated by adsorption liquid column chromatography into saturates, aromatics and resins (increasing polarity; Figure 5) [4]. The aspahltenes can be dissolved with methylbenzene. If insoluble compounds remain, these are carbenes or carboids [4]. Asphaltenes, one of the most investigated fractions of bitumen, can be separated into additionally fractions by various methods, depending on the desired interest. The repeated dissolution and precipitation with defined solvent mixtures to obtain heavy, middle and light soluble asphaltenes is common.

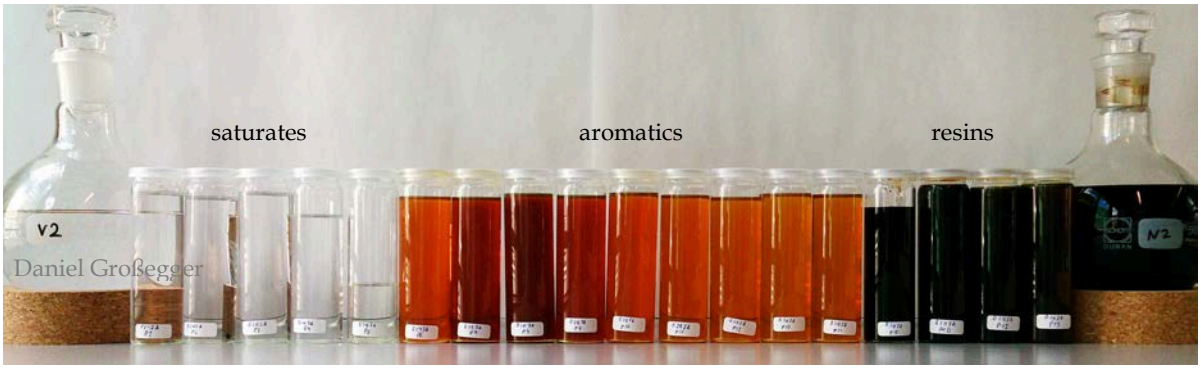

Figure 5: Chromatographic column separation of maltenes obtained from B

The separation into fractions helps to investigate and understand the interaction of fractions among each other and the properties of bitumen. One occurring problem is that fractions obtained with different methods are same labelled. General chemical and physical properties can be the same, but a comparison is hardly possible.

The structures presented in the following described fractions are core structures, which represent the prime chemical molecule structure found in these fractions. When referred to side chains, hydrocarbon chains with different length and different substitution groups are meant.

2.2.3.1. Asphaltenes

Asphaltenes are defined generally as the insoluble part of bitumen in n-heptane and soluble in methylbenzene. This definition is in account with the applied method to obtain asphaltenes (see subsection 4.3.4). Other definitions exist, like the insolubility in n-pentane or n-hexane, which leads to different weight percentages – the lower the carbon number, the higher the content obtained from bitumen [4]. By the definition of insoluble in n-heptane and soluble in toluene also long-chained hydrocarbons (with more than 40 carbons) will count as asphaltenes, due to their solubility [19]. Also asphaltene extraction methods, especially the used filter, and extraction temperature have an impact on the amount of asphaltenes and their properties [20].

At room temperature asphaltenes form a black powder (Figure 6) and constitute 5 to 31wt% of bitumen [1]. The density of asphaltenes is about 1,15 $g \cdot cm^{-3}$ [4]. Isolated dry asphaltenes

do not melt in oxygen atmosphere, but in inert atmosphere they form a liquid-like product with no clear melting point and start to decompose at about 350 °C, leaving carbonaceous residue (coke) [6,19].

Figure 6: Asphaltenes obtained from B_F282

The molecular weight of asphaltenes is estimated to be 250 to 3500 g·mol^{-1}. Asphaltenes have a H/C ratio between 0,98 and 1,56 and have a higher content of hetero elements (nitrogen and oxygen). An average molecule consists of 4 to 10 fused aromatic rings and aliphatic chains (Figure 7a) [4]. Some aliphatic chains are assumed to link multiple groups of rings (archipelago type, Figure 7b) [21]. Asphaltenes contain more condensed rings and polar groups compared to the fractions from maltenes. The condensed rings form almost planar sections of the asphaltene molecule, which can associate through π-π bonding to stacks. These stacks (nanoaggregates) are assumed to be the reason for structural formation and for short-range order. The stacking of asphaltenes also occurs in solution (above 100 mg·l^{-1}) [19,21]. Additional almost all metals from bitumen are present in the asphaltenes. Usually the total amount of metals is below 0,1wt%, which leads to a content of metalorganic molecules (like porphyrines, Figure 7c) of about 1 to 2wt% of asphaltenes [19]. Three classes of compounds can be identified in asphaltenes: polyaromatics with relatively few saturated substituents, porphyrines (insoluble in n-heptane) and other metal organic compounds and n-alkanes with more than 40 carbons [19].

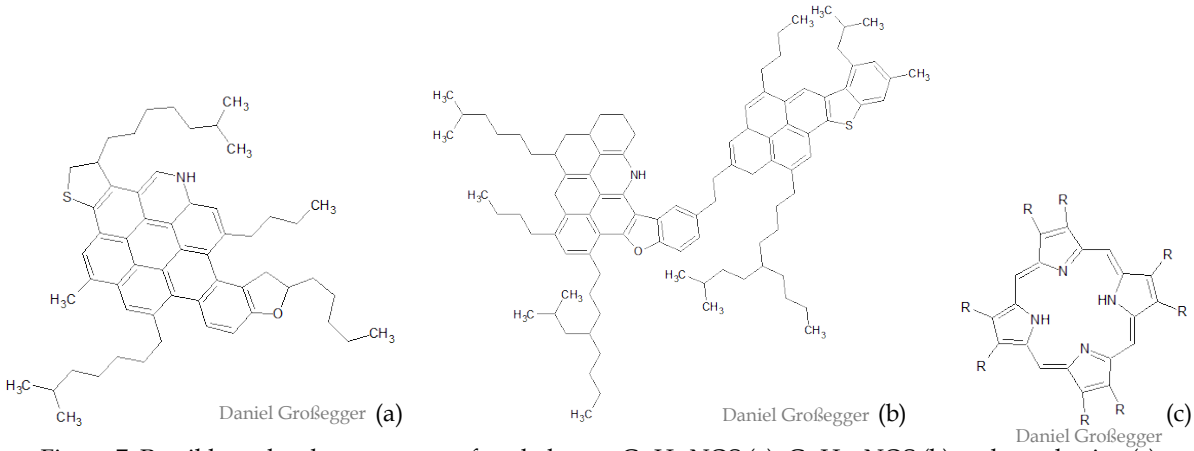

Figure 7: Possible molecular structures of asphaltenes: $C_{57}H_{71}NOS$ (a), $C_{97}H_{129}NOS$ (b) and porphyrine (c)

Asphaltenes have a large contribution to all physical properties. Viscosity and density increase with increasing asphaltene content.

2.2.3.2. Maltenes

As the n-heptane soluble part of bitumen, maltenes are sometimes called deasphaltened bitumen [4]. Maltenes can be further separated into the fractions saturates, aromatics and resins (Figure 5).

Maltenes are a less viscous than bitumen and still black. The structural formation does not occur within pure maltenes (no catana phase observed by atomic force microscopy, no fluorescence centres observed by confocal laser scanning microscopy and disappearing diffusion pattern (indications for ordered features) in small angle X-ray scattering and small angle neutrons scattering), which indicates that asphaltenes play a main part in initialising structural formations [4], but time dependent effects, like steric hardening, still remain [9,22]. The density of maltenes is about 1 g·cm^{-3}.

2.2.3.3. Saturates

Saturates occur at room temperature as a colourless or lightly coloured (white to faint yellow) liquid (Figure 8a) with a density of about 0,9 g·cm^{-3}. With a H/C ratio close to 2 and an average molecular weight of about 600 g·mol^{-1} saturates are mainly straight and branched-chain aliphatic hydrocarbons with few heteroatoms or aromatic rings (Figure 8b, Figure 8c). The content of saturates is between 5 to 20wt% [1,4].

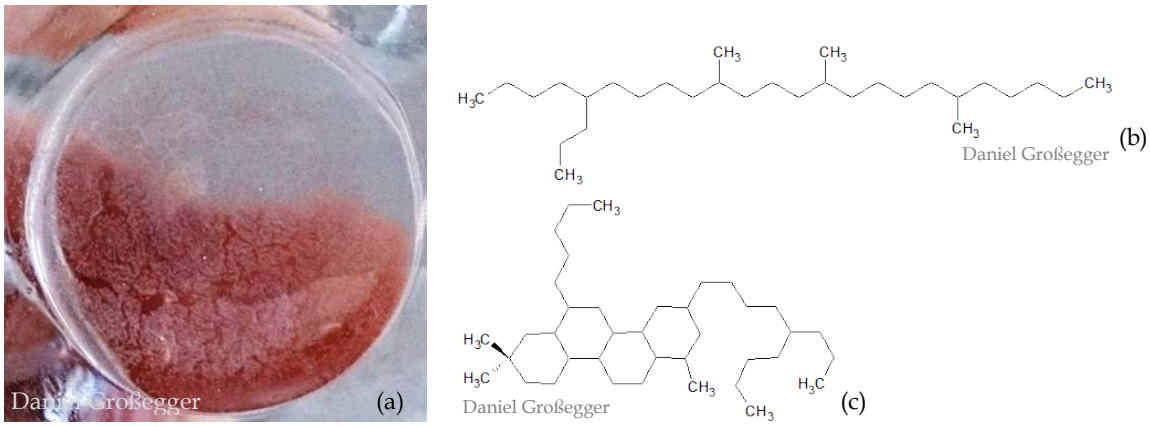

Figure 8: Saturates obtain from B (a) and possible molecular structure: $C_{30}H_{62}$ (b) and $C_{38}H_{70}$ (c)

2.2.3.4. Aromatics

Aromatics or naphthene aromatics appear yellow to orange dissolved from chromatic column (Figure 5) and turn to dark red when merged and inspissated with a density about 1 g·cm^{-3}. Aromatics are more viscous than saturates and constitute 30 to 60wt% of bitumen. The average molecular weight is 800 g·mol^{-1} and they compose of lightly condensed aromatic and naphthenic rings with side chains (Figure 9) [1,4].

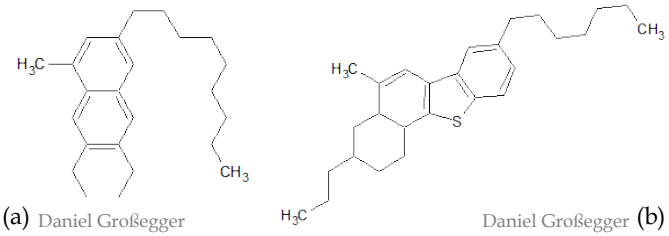

Figure 9: Possible molecular structure of aromatics: $C_{24}H_{34}$ (a) and $C_{27}H_{38}S$ (b)

2.2.3.5. Resins

Resins or polar aromatics are black in solution and inspissated. At room temperature they are solid or semi-solid and liquefy at higher temperature. The density is about 1,07 $g \cdot cm^{-3}$ and resins constitute 15 to 55wt% of bitumen. With similarities between asphaltenes and aromatics there average molecular weight is 1100 $g \cdot mol^{-1}$ with a wide molecular distribution. The H/C ratio is between 1,38 and 1,69. They consist of 2 to 4 fused aromatic rings and probably with side chains (Figure 10) [1,4]. Resins can be more polar than asphaltenes and govern with asphaltenes the rheological properties [12].

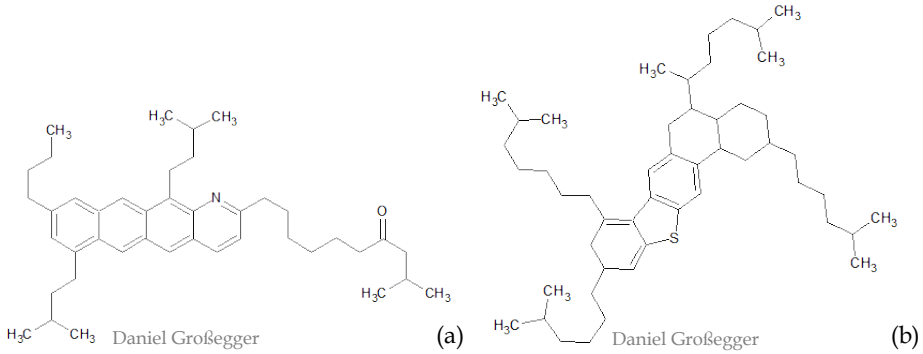

Figure 10: Possible molecular structure of resins: $C_{42}H_{59}NO$ (a) and $C_{50}H_{82}S$ (b)

2.3. Asphalt

Asphalt is a mixture of bitumen and mineral aggregates (filler, sand and gravel, Figure 11). The bitumen content is between 4 and 8,5wt% and functions as a binder. The mineral aggregates (91,5 to 96wt%) are composed accordingly to the asphalt concept and function generally as load bearing support and in the wearing course additionally provides the grip and abrasion resistance. The void content starts with 0vol% for mastic asphalt, is around 4vol% for asphalt concrete, to match the thermal expansion of bitumen, and up to maximum 25vol% for porous asphalt for sonic absorption and water draining [3].

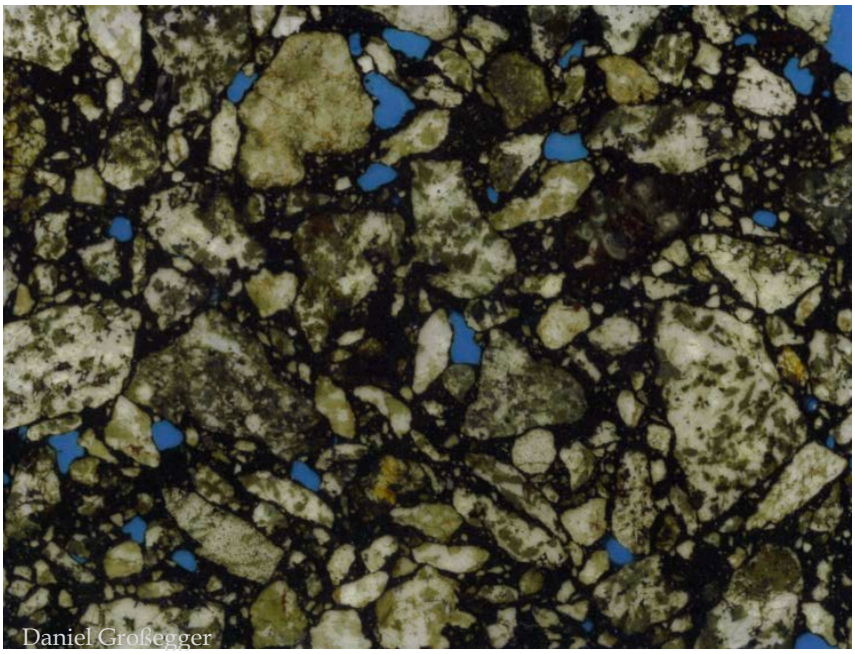

Figure 11: Asphalt microsection; the voids are filled with a polymer (blue) to provide stability during preparation

The mixing can be classified by temperature and process (not characterised). For hot mix asphalt concrete bitumen is heated for lowering its viscosity and the mineral aggregates are dried (for better bitumen adsorption). Mixing takes place at temperature above 130 °C, for polymer modified asphalt at 200 °C. To reduce the temperature, energy and exhaust gas additives (zeolites, waxes, emulsions, etc.) are blended into bitumen, resulting in a mixing temperature of 40 to 130 °C and is termed warm mix asphalt concrete. Cold (temperature below 30 °C) mix asphalt concrete is produced by mixing bitumen emulsion (bitumen-water-emulsion) with mineral aggregates. And other processes, for example, include natural asphalt and recycling asphalt. Temperature limits for bitumen 70/100 are 140 to 180 °C [3].

The production of asphalt usually takes place at a stationary mixing plant (mix in plant). Possible are also mixing at construction side with a moveable mixer (mix in place) and spraying processes (in place recycling or surface treatment). Further only mixing plants are described [3].

The cold aggregates exclusive filler are dried, due to their water content, which consumes a lot of energy. Filler (particle size <63 µm) is stored dry and is added during or after adding bitumen. Bitumen is stored in different heated tanks according to its needle penetration value. Different bitumen can be combined to achieve intermediate grades. The dried aggregates are stocked in hot bins proportional to its particle size. To regulate the correct composition each bin releases a determined quantity into a weight hopper. The weight hopper empties into the mixing drum, where bitumen via bitumen dosing and filler via filler weight hopper are added. The mixing drum can be heated for easier stirring. After mixing the asphalt is stored inside a heated asphalt silo, from there transporters are loaded [3].

The placement is done with a paver filled with asphalt by transporters and compacted through rollers. The placement temperature of asphalt has to be for 70/100 higher than 140 °C [3].

When cooled down, the surface can be deblocked for traffic.

2.4. Sample origin

The base material used was bitumen with a needle penetration value (see subsection 4.3.1) of 70 to 100 10^{-1} mm (B70/100), noted as B. This material was used to produce asphaltic test pieces for the test field and the laboratory/liquid aged bitumen. The bitumen extracted from the road sample had an original penetration value of 70 to 100 10^{-1} mm and a second base material (B2) was included for comparison also with a penetration value of 70 to 100 10^{-1} mm originated from a different charge.

Table 2 shows the codes of the studied bitumen samples, a short description and the (heating) treatments preformed on these samples.

Table 2: Code, description and treatment

Code	description	treatment
B	base	none
B2	base	none
B_LRTFOT	laboratory aged bitumen	RTFOT
B_LPAV	laboratory aged bitumen	RTFOT + PAV
B_LH2O2	laboratory aged bitumen	liquid ageing with H_2O_2
B_F000_A	test field: extraction from asphalt mixture bag	mixing plant and extraction
B_F000_B	test field: extraction of asphalt plate created from asphalt mixture bag by IVW	mixing plant, plate production and extraction
B_F000_C	test field: extraction of asphalt plate created at mixing plant	mixing plant and extraction
B_F0YY_SZ example: B_F012_S1	test field: extraction of layer Z of asphalt plate created at mixing plant after YY months	mixing plant, YY months exposure and extraction
B_F282	road sample from B223 Flötzersteig, wearing course	mixing plant, 282 months exposure and extraction

Due to the expenditure of time for one separation not all samples from the test field were chromatographically analysed. The selection was based on the first results from the chromatographic separation and the diploma thesis of Marina Stoyanova [23]. As abstract from the thesis the needle penetration value and dynamic shear rheometer (methods described in section 3) was chosen (Figure 12, Figure 13). After manufacturing the test pieces, the penetration value ranged between short-term ageing (B_LRTFOT) and long-term ageing (B_LPAV), which indicates an advanced ageing state. The different extracted bitumen samples at the beginning revealed, that the mixture bag (B_F000_A) was stronger aged (lower penetration value) than the bitumen extracted from the comparative test piece made out of the mixture bag filling (B_F000_B). This seems not to be coherent, due to two heating steps in the presence of air for producing the test piece. The first heat treatment occurred during the manufacturing of the asphalt and the second heat treatment was the production of the test piece. Further bitumen of the first layer aged stronger (indicated by needle penetration and phase angle), due to the direct exposure to environmental conditions. Also the fourth layer tended to higher oxidation (only indicated by needle penetration) and only the layer inside the plates seemed lesser aged (identical graphs of phase angle for the second, third and fourth layer). Maybe the higher exposition to air, due to the embedment into gravel, is the reason for this.

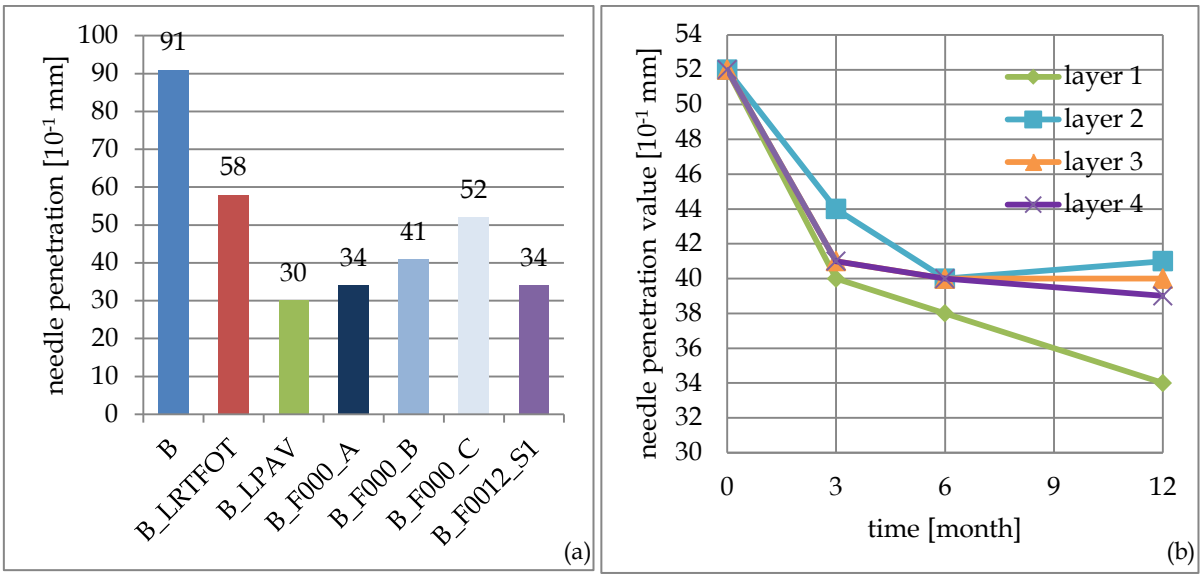

Figure 12: Needle penetration: probed samples (a) and development over time for the layer of the test field (b) (generated with data from [23])

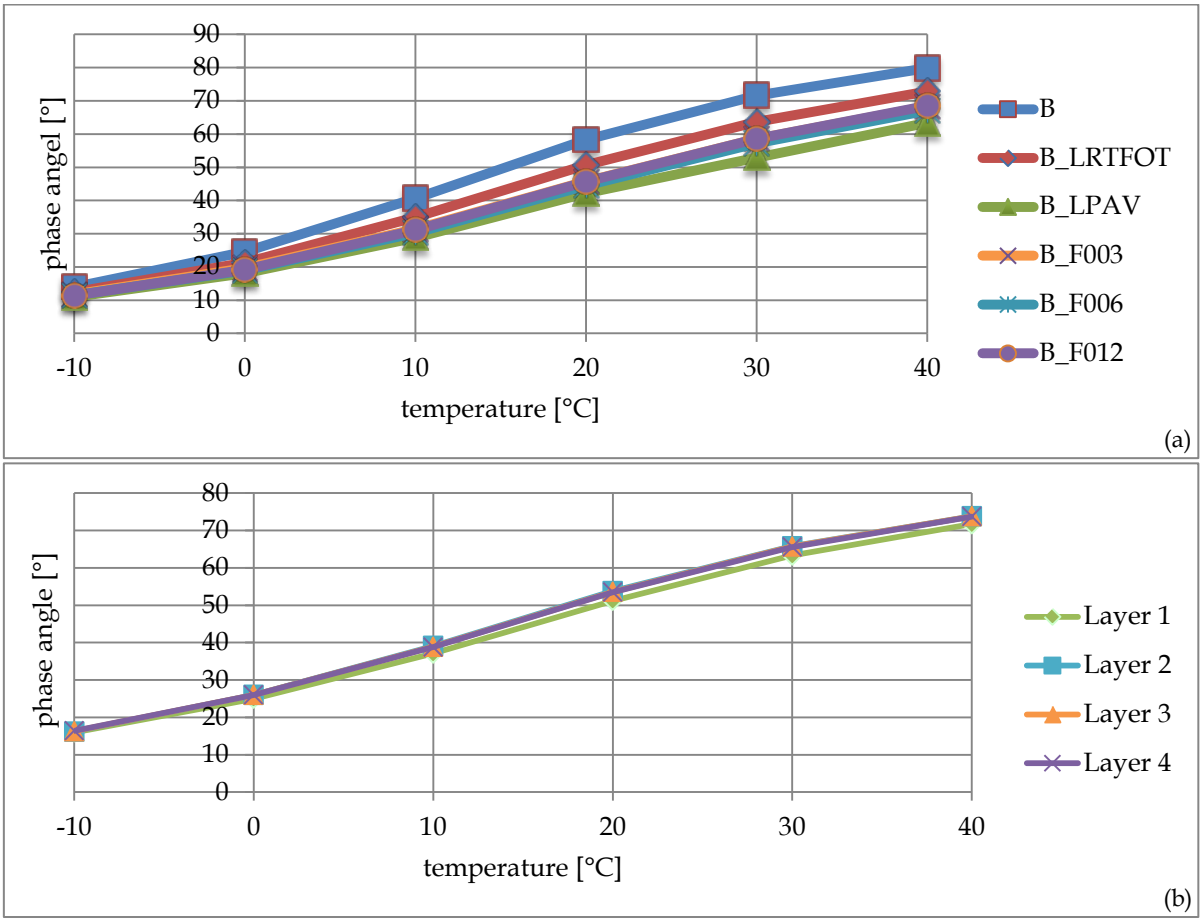

Figure 13: Phase angle: base bitumen, laboratory aged and first layer of test pieces at different time steps (a), layer of the 12 months test piece (b) (generated with data from [23])

On the basis of these results only one bitumen from test field, the first layer of the 12 months, was chromatographically separated.

3. Bitumen ageing

3.1. Introduction

The process of bitumen ageing is not yet fully understood, due to the complexity of bitumen's chemical composition, the interaction with radical spices in the environment and solar radiation.

The ageing process involves chemical changes, which affects the physical properties. This results for example in an increase in viscosity and a decrease of endurable stress at lower temperature. The exact chemical mechanism for ageing is still unknown, but on the level of fractions it can be stated that aromatics decrease while asphaltenes increase. Further the oxygen content increases, indicated by increasing ketone and anhydride formation [14].

Atmospheric oxygen may play an important part during asphalt production, but during service atmospheric radicals have a greater potential for oxidation hence an excerpt of radical generation at tropospheric level is dispensed.

3.2. Excerpt of atmospheric chemistry

Environmental chemistry in general deals with origins, transport, chemical reactions and fates of chemical species in the environment (air, water and earth) and the influence of human activities thereon [24,25]. This subsection deals with the relevant photochemical processes and reaction paths that might have an influence on ageing of asphalt/bitumen.

The earth is encapsulated in a thin layer of gases (approximately 11 km altitude troposphere, thereon stratosphere to approximately 50 km, mesosphere about 85 km and thermosphere up to approximately 500 km), consisting of (excluding H_2O) about 78,1vol% nitrogen (N_2), 21,0vol% oxygen (O_2), 0,9vol% argon (Ar), and 0,04vol% carbon dioxide (CO_2). Water vapour varies from 0,1 to 5vol% and trace gases (neon, helium, methane, nitrous oxide, hydrogen, ozone, etc.) are below 0,002vol% (a selection is given in Table 3) [24–26].

The photochemical reactions are of interest, which are source and sink of different species in the atmosphere. Photochemical reactions are triggered by the radiation energy from the sun, predominantly in the ultraviolet region. The incoming radiation, especially short wavelength radiation, from the sun is reduced by the higher spheres, especially through oxygen and nitrogen bands [24,26]. The relevant incoming radiation onto the earth surface is again reduced by ozone in the stratosphere, which has a strong band between about 220 and 310 nm, known as Hartley bands. With the Hartley and Huggins bands the ultraviolet (UV) light is below 350 nm largely and below 300 nm nearly extinguished. Ozone shows a weak absorption band (Chappuis bands) within the visible range (green part of the spectrum) [26].

To determine the participating species in the aging process, the atmospheric lifetime τ is of great importance. The atmospheric lifetime is the time, when a primary concentration is reduced to the fraction of 1/e (about 0,37). Short living radicals, like $OH^{\bullet}$ or $NO_3^{\bullet}$, have an atmospheric lifetime of seconds to minutes. For trace gases, such as $NO_2^{\bullet}$, with middle living ranges from hours to days, atmospheric mixing-through specifies the spread range.

Vertical boundary layer mixing takes minutes to hours, days to weeks for the distance between two latitudes and one to two months for the distance between two longitudes [26].

Table 3: Snippet of atmospheric trace gases in dry air near ground level [24]

gas or species	volume per cent in the absence of gross pollution	major source	removal process from atmosphere
N_2O	$3 \cdot 10^{-5}$	biogenic	photochemical
NO, NO_2, NO_3	10^{-10} – 10^{-6}	photochemical, lightning, anthropogenic	photochemical
HNO_3	10^{-9} – 10^{-7}	photochemical	washed out by precipitation
H_2O_2	10^{-8} – 10^{-6}	photochemical	washed out by precipitation
$HO^{\bullet}$	10^{-13} – 10^{-10}	photochemical	photochemical
$HO_2^{\bullet}$	10^{-11} – 10^{-9}	photochemical	photochemical
H_2CO	10^{-8} – 10^{-7}	photochemical	photochemical
SO_2	about $2 \cdot 10^{-8}$	anthropogenic, photochemical, volcanic	photochemical

Due to high activation energy (502 kJ·mol^{-1}) of diatomic oxygen molecules at atmospheric temperature and pressure, it is not directly involved as an oxidant in oxidation processes and to break the bond by radiation energy the wavelength regions 135 to 176 nm and 240 to 260 nm are most effective. Instead free radicals function as a good oxidising agent. The radical chains play a fundamental role in atmospheric chemistry, they act as catalysts for the destruction or formation of other species. At tropospheric level the hydroxyl radical ($OH^{\bullet}$), often referred to as "detergent", is the most important and has on average a constant remaining concentration. The production of hydroxyl radicals starts with the photochemical decomposition of ozone (O_3) (1, 2). Tropospheric ozone may be provided by partly mixing with the stratosphere or through photochemical reactions. Ozone concentration varies between 10 and 100 ppb [24–26].

$$O_3 + h\nu \left(308\, nm < \lambda < 1200\, nm\right) \rightarrow O\left(^3P\right) + O_2 \quad (1)$$

$$O_3 + h\nu \left(\lambda < 308\, nm\right) \rightarrow O\left(^1D\right) + O_2 \quad (2)$$

For wavelengths between 308 and 1200 nm oxygen is decomposed in its ground state (^{3}P) (1), which recombinant through impulse reaction instant to ozone again (3). In the near ultraviolet region (UV-B) the ozone photolysis produces oxygen in an energetically excited state (^{1}D) (2). Most excited oxygen transition into the ground state by quenching with

molecular nitrogen or oxygen (M matrix molecule, collision partner for the conservation of momentum) and recombinants to ozone (3) [24].

A small part (about 10%) reacts with gaseous water to hydroxyl radicals (4).

$$O(\,^3P) + O_2 + M \rightarrow O_3 + M \tag{3}$$

$$O(\,^1D) + H_2O \rightarrow 2\,OH^\bullet \tag{4}$$

Due to an average lifetime from about one second and the requirement of sunlight, the concentration drops quickly over night-time [25].

Hydroxyl radicals form lager transient free radicals ($HOCO^\bullet$) by addition reaction with carbon monoxide (CO) (5). This free radical reacts swiftly with molecular oxygen in an oxidation process (6), fully oxidizing to carbon dioxide (CO_2) and forming hydroperoxy radicals ($HOO^\bullet$). The hydroperoxy radical is converted back to hydroxyl radical by oxidation of nitric oxide (NO) to nitrogen dioxide (NO_2) (7). Nitrogen dioxide is photochemically decomposed with a wavelength below 420 nm, more sufficient below 394 nm (UV-A), to nitric oxide and atomic oxygen (^3P) (8). Ozone is formed by the reaction of atomic oxygen and molecular oxygen (3) [24,25].

$$OH^\bullet + CO \rightarrow HOCO^\bullet \tag{5}$$

$$HOCO^\bullet + O_2 \rightarrow HOO^\bullet + CO_2 \tag{6}$$

$$HOO^\bullet + NO^\bullet \rightarrow OH^\bullet + {NO_2}^\bullet \tag{7}$$

$${NO_2}^\bullet + h\nu\,(290\,nm < \lambda < 420\,nm) \rightarrow NO^\bullet + O(\,^3P) \tag{8}$$

These reactions are the source of tropospheric ozone. Unburned hydrocarbons and nitric oxide (photochemical smog), emitted to a great amount by vehicles, are the origin of urban ozone (Figure 14). The emission of volatile organic compounds (VOCs) also leads to an increase in radical concentration, since aldehydes are among the intermediate product of degradation processes, which photochemically decompose through UV-A (wavelength < 338 nm) radiation producing additional free radicals. Nitric oxides are produced during fuel combustion. On part is due to the nitrogen release from the fuel itself. Another part is from the direct reaction of molecular nitrogen and oxygen at high combustion temperatures. This is the reason for the increase of ozone in smog areas, due to the synergy of VOCs and NO_2 [25].

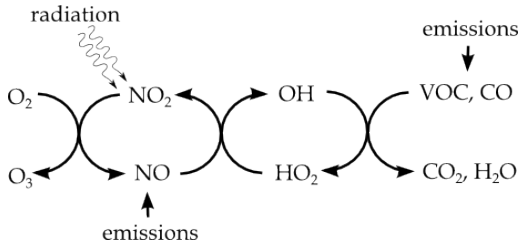

Figure 14: Schematic concept of tropospheric ozone generation [27]

Important hydroxyl radical sinks are the reaction with carbon monoxide (dominant) (5), the reaction with ozone (9), the reaction with VOCs and the formation of hydrogen peroxide (H_2O_2) (10) or nitric acid (HNO_3) (11), which are washed out in the presence of water. By photochemical decomposition nitric acid is fragmented back into its components. The same applies to nitrous acid (HONO or HNO_2) (12) [24,25].

$$OH^\bullet + O_3 \rightarrow HOO^\bullet + O_2 \quad (9)$$

$$OH^\bullet + OH^\bullet \rightarrow H_2O_2 + O_2 \quad (10)$$

$$OH^\bullet + NO_2 + M \rightarrow HNO_3 + M \quad (11)$$

$$OH^\bullet + NO^\bullet \rightarrow HONO \quad (12)$$

Without radiation nitric acid and nitrous acid are stable and their concentration increases over the night. Analogous conclusions are stated for nitrate radicals ($NO_3^\bullet$) (13), which rapidly dissociate photochemically during daytime and at night acts similar to hydroxyl radicals by initiating the oxidation of unsaturated hydrocarbons and certain VOCs (14) [24,25].

$$NO_2{}^\bullet + O_3 \rightarrow NO_3{}^\bullet + O_2 \quad (13)$$

$$NO_3{}^\bullet + RH \rightarrow HNO_3 + R^\bullet \quad (14)$$

Due to desulphurisation, lesser anthropogenic sulphur dioxide is released (acid rain and forest decline). The conversion of sulphur dioxide into sulphuric acid occurs by several sequential steps in areas with high radical concentration, whereas in relatively clean air dry deposition removes the main content. Dissolved sulphur dioxide is oxidized to sulphate ion (SO_4^{2-}) by hydrogen peroxide and ozone (main oxidation pathway) [24,25].

Two main pathways for radical interaction with asphalt surfaces can be identified. The first is direct contact with radicals in gaseous state. The second is that radicals dissolve in water droplets and precipitate. Beside radicals the water droplets contain acids like nitric acid, nitrous acid or sulphuric acid generated by radical reactions.

3.3. Chemical ageing and evaporation

Chemical ageing involves oxidative reactions, fragmentation and polymerisation, and in addition new structural organizations, due to the chemical changes of bitumen content and loss of fragmentised compounds. Therefore bitumen ageing is an irreversible mechanism

[4,28]. During the reaction with oxidative species the molecules increase in size (by uptake of oxygen) and additionally the polarity increases. This leads in general to a hardening and embrittlement of bitumen. During the manufacturing chemical ageing is specifically used to produce harder grades of bitumen (oxidised bitumen, see subsection 2.2.1). The condition for oxidation is not quite the same as during manufacturing asphalt and is very different from those that occur under service [4].

Two ageing conditions can be distinguished: short-term ageing and long-term ageing (see subsection 3.5) [3,4,11,23,28].

The largest contribution to short-term ageing is in the production of asphalt. During the intermixing of bitumen and mineral compounds two loss flows can be identified. One flow is a material loss by particle emission as aerosols. These particles consist nearly to 100% of organic hydrocarbons. The other flow is the evaporation of oxidised and decomposed compounds. Saturates and aromatics evaporate at a temperature of 100 to 350 °C under nitrogen atmosphere. Resins have an initial weight loss from 50 to 150 °C and continue till 350 °C. Mass loss of bitumen occurs in the temperature range from 100 to 350 °C under nitrogen atmosphere and above 350 °C cracking of heavy fractions of bitumen or bitumen fractions begins [6]. Temperatures above 100 °C are typical for hot and partially for warm mix asphalt concrete [3]. Additionally the higher temperature until placement is concluded might be responsible for evaporation. Particles (PM10 – particulate matter with diameter of 10 µm or less) measured during a laboratory mixing experiment revealed that the emitted particles consisted to a high part of organic carbon, which decreases with increasing distance to the blender. Analysed volatile organic compounds from hot bitumen identified ketones, alkenes, aldehydes and aromatics to be the main functional groups in emitted volatile compounds [29].

Under service the surface of asphalt roads rarely exceeds 75 °C (Austria) [3], therefore evaporation of compounds is less favoured until they are fragmented by chemical reactions or radiation.

The sensitivity to chemical ageing varies widely with the bitumen origin (chemical composition). Oxidation introduces polar, oxygen-containing functionalities and may cause aromatization. Often the assessment of chemical ageing is done on fraction level or by studying the increase of functionalities. So it is generally accepted that the aromatic content decreases and the aphaltene content increases, thereby the asphaltene content can give hints of the state of ageing. The resin content varies, depending on formation of asphaltenes out of resins or aromatics and formation of resins out of aromatics. The saturate content remains essentially constant, due to low chemical reactivity [4,14]. However, this is an interpretation in the case of a polarity and solubility concept and may not be understood from a chemical and structural point of view. The “new” formed asphaltenes during ageing may differ from the “original” asphaltenes in their chemical structure. Isolated asphaltenes are fairly unreactive to atmospheric oxygen at ambient temperature, but when melted or in solution

they are highly reactive [14]. The state in which asphaltenes occur in bitumen can be notable. The same applies for structural features, which change during ageing.

The major chemical functional groups containing oxygen, which increase and form through ageing, are ketones, anhydrides, carboxylic acids and sulphur oxides. Ketones and sulphur oxides are rapidly formed during the shot-term ageing with sulphur oxides as the easiest formed oxidation products. During long-term ageing their formation proceeds at a much slower rate (oxidation of bitumen films showed that the oxygen uptake rate decreases until the rate becomes linear) and the oxidation reaction usually stops with ketone formation. The good correlation between ketone formation and viscosity implies that ketones are responsible for the formation of additional asphaltenes. Sulphur oxides generally reach a steady state, depending on sulphur content and oxygen diffusion [4,14,15].

The mineral aggregates in asphalt can act as a catalyst, especially to oxidise the more non-polar fractions, but it was proposed that polar functional groups of the more polar fractions can be adsorbed onto the catalytically active sites and so prevent further activity. Thus the catalytic effect of mineral aggregates on bitumen oxidation is negligible, relative to the amount of oxidation that occurs in the bitumen bulk. The same applies to metals, metal salts and some metal-organic complexes, which can have catalytic effects [14].

Core samples from road constructions showed that general bitumen from the wearing course (upper part) is oxidised stronger than bitumen from the base course (lower part). The development of the oxidation gradient over the vertical cross section depends on the variability in permeability, which itself depends on void content, peroxidation of bitumen until paved and environmental conditions. The gradient within bitumen is limited to a significant degree by the diffusion rate of oxygen from the surface into the bulk, where in asphalt the mineral aggregation matrix presents a hindrance [14,30].

The effect of radiation on bitumen becomes important during service life, dropping the life span of road construction. High energy radiation (γ-radiation) penetrates through bitumen and introduces bond breaking in the main chain or in side chains (scission; even for polymeric modifier) and crosslinking through polymerization (enhancing elasticity). Ultra violet radiation (UV radiation) affects mainly the surface, causing lesser scission and polymerisation reaction. Radiation increases the concentration of carbonyl compounds (like ketones or carboxylic acids) and sulphur oxides. Scission produces small molecular fragments, which cause a decrease in creep compliance and increased compliance [28,31,32].

With increasing dose of γ-radiation saturates decrease, due to scission. The radiation leads to unsaturation, which favours the formation of aromatic rings. Hence aromatics and resins increase. Asphaltenes remain constant [31].

The majority of publications worked with artificially aged bitumen, aged at higher temperature (like RTFOT and PAV, see subsection 4.2.1.1 and 4.2.1.2), to reduce time effort. This is not a problem for the investigation of short-term aged bitumen, but for long-term aged bitumen under the exposure of environmental condition it can lead to interpretations, which are only correct for the investigated method. As an example: The rolling thin film

oven method reproduces the rheological values of short-termed aged bitumen well, the same values can be produced with γ-radiation, but both artificially aged bitumen differ in their chemical composition.

3.4. Steric hardening

Steric hardening describes the phenomenon that viscosity (increasing) or any mechanical property at temperatures lower than 80 °C changes over time without the influence of chemical changes, on account of its reversible nature (heat-reversible). In a simple manner steric hardening results from molecular restructuring [4].

The fastest rate of viscosity increase was found to occur at 50 °C. This temperature correlates with crystallisation kinetics for most bitumens with less than 5wt% paraffin-like crystalline content (measured by differential scanning calorimeter - DSC). Wax crystallisation is additionally referred to as physical hardening and occasionally counted as an independent phenomenon [4].

A further approach is the correlation of steric hardening and the ordering of aspahltenes. This approach is supported by the increase in steric hardening upon oxidation (increasing asphaltene ratio). Asphaltenes form an ordered amorphous phase (mesophase), which grows over up to two 2 weeks and contributes most to steric hardening. The mesophase possible results from nucleation and growth of asphaltenes. Additionally maltenes show time dependent behaviour and thus contribute, as the original bitumen displayed hardening only during 2 to 3 days [9,22].

Images gathered by atomic force microscopy showed that reliefs are detectable after a relaxation time and disappear with higher temperature (starting above 90 °C), which can be seen as an indicator for steric hardening and its connection to structural formation. But the exact mechanisms that lead to steric hardening remain still uncertain[4].

3.5. Ageing stages

Three stages of ageing can be distinguished defined by the applied conditions over time [3,11].

The first stage is non-aged, which occurs after bitumen production [3,11].

The second stage is short-term aged, which encompasses hot storage, asphalt production, asphalt transportation and placement on construction side. Asphalt production has the highest potential of oxidation, due to high temperatures (2.3 Asphalt), high surface area and air contact as a consequence of the mixing process. Asphalt transportation and placement still occur at higher temperature, but have a lower significance ascribed to the lower agitation[3,4,11].

The third and last stage is long-term aged. It includes short-term aging, due to the conditions that an asphalt concrete road layer sustains during the production steps, which accord with short-term ageing. This stage lasts until the end of lifetime of the construction (from 5 up to 30 years) and hence is the longest stage. Over the constructions lifetime ambient temperatures (location depending) can be found in the range of -30 to +60 °C. The

air contact is limited by a compacted construction and so oxidative species have to diffuse into the bulk. The wearing course is more exposed than the base course, which leads to a chemical ageing gradient over the cross section (higher aged at the top and lower aged at the bottom) [3,4,11]. The dissemination is enhanced by crack formation. Embrittlement, leading to cracks, can be postponed by structural changes occurring within bitumen. Oxidative created, more polar molecules diffuse to regions that have the potential to keep them dissolved or form clusters and become encapsulated. At the end of lifetime bitumen ageing is one contributor among others that causes pavement distress.

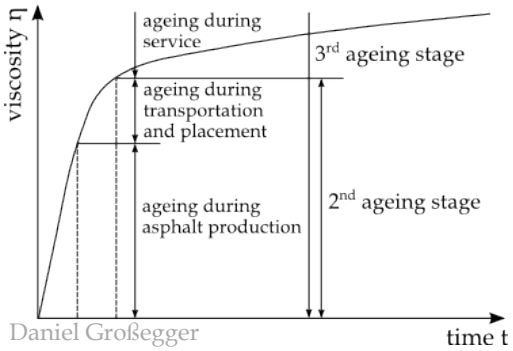

Figure 15: Trend of ageing

4. Methods

4.1. Introduction

This section introduces the main techniques that were used in this study or were related to it.

With the description of each method an understanding for the properties of bitumen will be built. The reader should be able to recognise the presented results as coherent.

In general the fractions obtained in this thesis cannot be directly compared to results from other publication, due to the significantly affection of the relative ratio of each fraction through experimental setup, but they feature comprehensive properties (see subsections 2.2.3).

4.2. Ageing methods

The two contemplated ageing methods can be divided into laboratory ageing and field ageing. As standard laboratory ageing refers to artificially aged bitumen, usually at higher temperature (163 °C), generated in a laboratory. Liquid ageing was an attempt to find a method that simulates field ageing at an accelerated speed. Bitumen extracted from asphalt concrete, which has been aged under environmental exposure over time, will be denoted as field ageing.

4.2.1. Laboratory ageing

The objective of laboratory ageing is to represent the effects of the occurring changes inside the bitumen during the manufacturing of asphalt, transport, placement – known as short-term ageing – and over the lifetime of the road – known as long-term ageing, in a shortened timeframe. Different test methods are then applied on the received aged samples to characterise it and conclude on its behaviour over lifetime.

There exist different methods to age bitumen. The following two are the most common used in Austria and were also used in this study.

4.2.1.1. Rolling Thin Film Oven Test (RTFOT)

The aim of the Rolling Thin Film Oven Test is to represent the short-term ageing, which occurs during the admix process in the asphaltic mixture plant and occasionally during transport and placement.

35,0 g ± 0,5 g homogenised, water-free bitumen samples are filled into glass tubes. These filled tubes are placed horizontally into a rotator (Figure 16). The rotator itself is inside a preheated chamber and moves with 15 min^{-1} ± 0,2 min^{-1} number of revolutions. A constant air stream (4,0 $l \cdot min^{-1}$ ± 0,2 $l \cdot min^{-1}$) is applied onto the tubes for 75 min ± 1 min after reaching the test temperature of 163 °C ± 1 °C. Due to the high surface area, high temperature and constant airflow the main ageing processes are volatilization and oxidation. The asphaltenes typically increase by 1 to 4wt% [4,11,33].

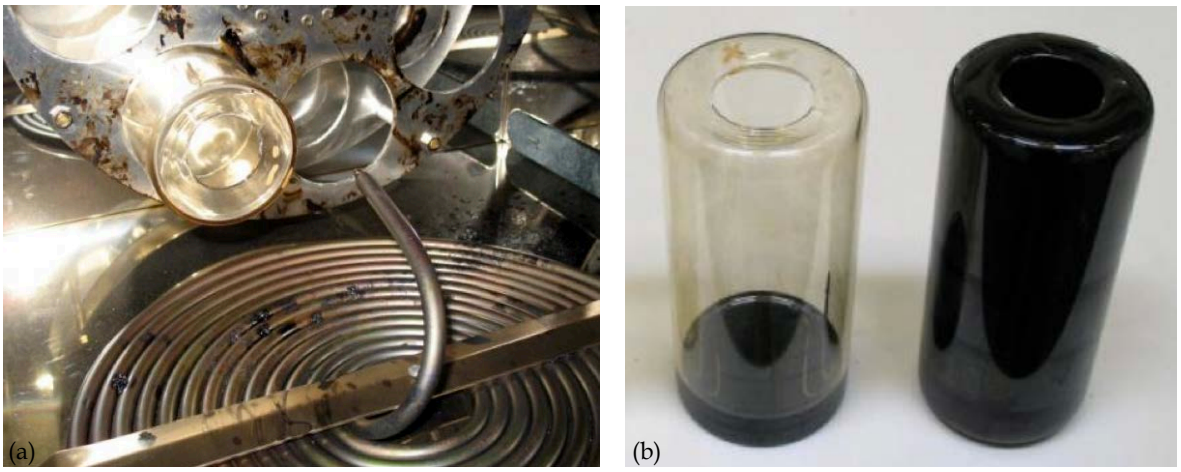

Figure 16: Rolling Thins Film Oven Test: heating chamber with rotator, glass tube and air injection lance (a), filled glass tubes before (left) and after (right) treatment (b) [11]

4.2.1.2. Pressure Ageing Vessel (PAV)

The Pressure Ageing Vessel method is used to represent the ageing process during a life span of 5 to 10 years in the surface parts of asphaltic road constructions. It is not a simulation of in situ ageing of bitumen because environmental effects cannot be exactly reproduced, but a good approximation to the effects can be achieved.

Short-term aged samples from the RTFOT are united and decanted into a stainless steel pan. The film thickness should be 3,2 mm. The filled pans are put into a frame and the frame is put into a preheated (110 °C) pressure vessel. Temperature and pressure inside the vessel are regulated to 20,7 bar and 110 °C over the time of 20 h ± 10 min. Those conditions were used for sample treatment, likewise 90 °C or 100 °C for 20 h ± 10 min and 85 °C for 65 h ± 30 min are also possible. The standard refers to the proceeded temperature that has to be as low as possible, because at higher temperature the result is not any longer representative for field ageing [11,34]. Through high temperature and pressure oxygen can diffuse into the film and begin to oxidize the compounds of bitumen. The pressure is likely to prohibit volatilization and fractional compounds evaporate after treatment.

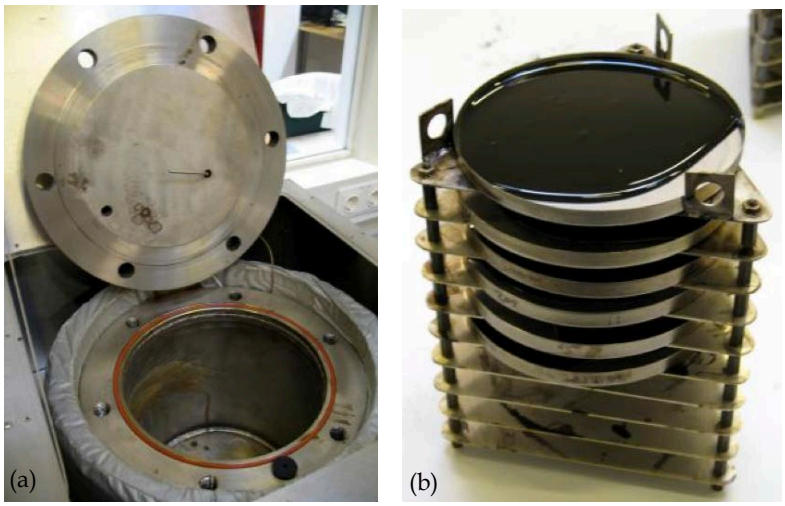

Figure 17: Pressure Ageing Vessel: pressure vessel (a), frame with filled stainless steel pans (b) [11]

4.2.1.3. Liquid ageing

Due to the fact that in reality aging after placement does not occur under higher temperatures and pressure a method was sought that could simulate the ageing process. The approach was to specify the substances, which are in charge for reaction inside bitumen.

UV radiation can affect the first nm of the surface layer of asphalt. Reactive substances in gaseous form in the atmosphere (NO_x, SO_2, O_3 and $OH^{\bullet}$, see subsection 3.2) can diffuse into the bulk and affect deeper layers, likewise if those substances are dissolved in water.

Due to the lack of equipment for reactive gas production and UV radiation generation a liquid approach was performed. Hydrogen peroxide (H_2O_2) was chosen as promising agent of all species that occur in the environment.

The first investigation was to verify if spectroscopic methods could detect changes on bitumen films. Therefore with a heated spatula a bitumen sample was taken and smeared onto a microscope slide. To receive a flat surface the sample was heated with a hot air gun. The samples were measured with a fluorescence spectrometer (see subsection 4.3.6.2) and then treated with different liquids and light conditions and reference samples were stored without further treatments.

After different storage times under these conditions the surface was cleaned with pure water and dried with pressurised air and then the samples were measured again.

For chromatographic separation one liquid treated sample were prepared. In two crystallising dishes (diameter 19 cm) 6,33 g respectively 8,25 g bitumen were heated until less viscose, so that to a certain extent whole bottom was covered with a thin film. After cooling a solution of 30% H_2O_2 (stabilised) in water was added until approximately 2 cm fill depth was reached. Both dishes were covered with glass plates to eliminate dust pollution and were put near the window to ensure exposure to sunlight on the surfaces. After the duration of 21 days left under this condition the liquid was removed and the surface was cleaned with pure water to ensure that no dust or stabiliser was left on the surface. When the thin film was dried (Figure 18), it was scraped off and stored in an 1 l round bottom flask for the next analytical steps. The yield collected in the round bottom flask was 14,38 g.

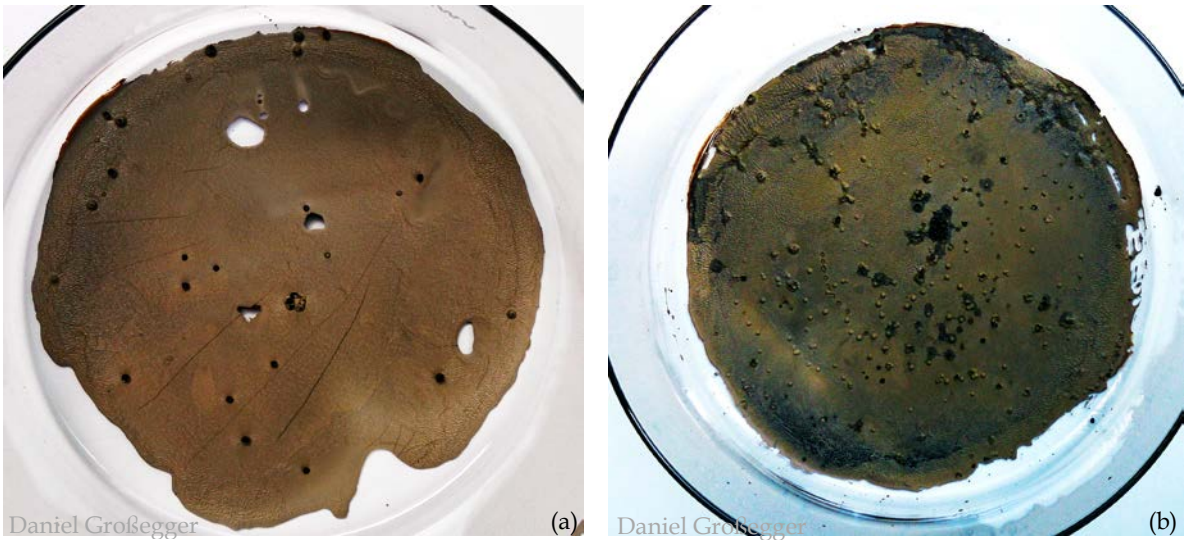

Figure 18: Liquid aged samples for chromatographic separation: 6,33 g (a) and 8,25 g (b)

4.2.2. Field ageing

Field ageing refers to a natural ageing of bitumen in its environment.

To obtain bitumen from asphalt, bitumen has to be separated from the mineral aggregates. Therefore asphalt segments were heated and fragmented into smaller pieces. These pieces were put into a rotary sieve and were washed with hot solvent. The main solvents used are methylbenzene, trichloroethene and tetrachloroethene. The extraction was conducted with tetrachloroethene. The dissolved bitumen with part of the filler component was conveyed to a beaker centrifuge to acquire filler-free solution. The solvent was removed by a rotary evaporator. The remaining solvent within the bitumen should be less than 1wt%, according to weighed and collected solvent removed [23]. Remaining solvent within the bitumen sample have an influence on the rheological and physical properties. Sometimes mineral aggregates were found inside the filter of the maltene extraction process, when the asphaltenes were obtained by Soxhlet extraction with methylbenzene (see subsection 4.3.4).

4.2.2.1. Test field

To investigate the effects of in situ ageing a test field was built on 18th September, 2012 initiated and conducted by Bernhard Hofko. 72 asphaltic test pieces were created (Figure 19). To reduce the influence of different bitumen types, production processes or production days, the same fresh bitumen (70/100) was used for all test pieces. 36 pieces were unmodified, the other 36 pieces were modified with 4,3% styrene-butadiene-styrene (PmB 45/80-65). To see the changes over the thickness, the test pieces were cut into four slices [23]. Studying the effect of snow service some test pieces were treated in a regular and uniform way with a defined amount of sprinkled salt (~15 g·m²). Snow was removed from all test pieces [35]. In this study only selected unmodified test pieces are investigated as noted in section 2.4.

Figure 19: Test field: with snow service (right) and without snow service (left) of unmodified (back) and modified (front) test pieces [23]

4.2.2.2. Road sample

The road sample was taken from B223 Flötzersteig. Unfortunately, there do not exist any adjourned bitumen from the placement or data, so comparison is not really possible. But it was the only sample that had not been modified and still showed good performance at the end of a lifetime of 282 months (23,5 years).

4.3. Analytical methods

4.3.1. Needle penetration

This method is used for determining the consistence of bitumen and belongs to the conventional testing methods. A clean tube, made of metal or glass, with flat bottom and dimension according to the penetration depth is filled with heated bitumen with a temperature of 100 °C over the softening temperature to ensure good results. The filled tube has to be covered with a cup while it will cool to room temperature, so that no air bubbles are created and the sample is protected from dust. A stainless steel needle with the specification as given by the standard is placed into the penetrometer and the cooled sample is put inside a water bath at a temperature of 25 °C. After an initial time, when the sample has reached the temperature of 25 °C, the needle is placed in a short distance above the bitumen surface and the measurement starts. The needle will be loaded with 100 g for 5 s and the penetration depth of the needle will be measured (Figure 20). More than one measurement can be made with one filled tube under following conditions: All penetration points must have a distance of 10 mm to the brim and to the previous points and a clean needle has to be used for each new measurement. As a test result the penetration value is given in 1/10 mm (10^{-1} mm) as the arithmetic mean of at least 3 tests [4,11,36].

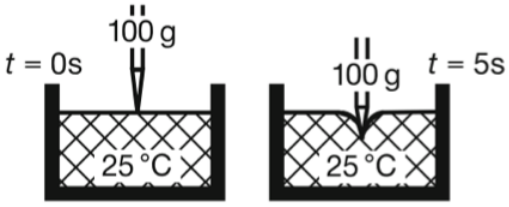

Figure 20: Measurement principles for needle penetration [23]

The higher the penetration value, the softer the bitumen. For 70/100 the penetration value at 25 °C ranges between 7 and 10 mm and it is considered as an intermediate bitumen.

4.3.2. Dynamic Shear Rheometer (DSR)

The dynamic shear rheometer counts to the SUPERPAVE (superior performing asphalt pavement) binder specification and is used to characterize the viscoelastic behaviour of bitumen [3].

Bitumen is heated until sufficiently fluid and poured into a mould. The dimension of the mould should be correlated to the used circular plate. Temperature, plate diameter and sample thickness depend on the bitumen type. If the complex modulus is in a range from 1 kPa to 100 kPa (soft bitumen, short-term aged bitumen or bitumen at higher temperature) a plate with a diameter of 25 mm and a sample thickness of 1 mm is used. When the complex modulus increases up to 10 MPa (long-term aged bitumen or bitumen at lower temperature) a plate with a diameter of 8 mm and a sample thickness of 2 mm is used. The sample thickness given is a suggestion from the standard. Other values are possible, but are not in use. The cooled sample is placed between two plates. The lower plate is fixed and can be heated with a Peltier-element. The upper plate has the according diameter and can oscillate. When the sample is placed, the heated plates are moved together until the gap between them is equal to 1,05 mm for the 25 mm plate or 2,05 mm for the 8 mm plate. The jut is cut away and the plate distance is adjusted to the final distance (±0,01 mm) only when the sample covers the entire upper plate. The slight bulge is to negate boundary effects from cutting. The test cell is regulated to the starting temperature. The measurement can start after the cell has reached the starting temperature and has held it for 10 to 20 min. Variable parameters are temperature, amplitude and oscillation frequency. The temperature range was from -10 °C to +80 °C in steps of 10 °C and the frequencies were 0,1 Hz, 1 Hz, 3 Hz, 5 Hz and 10 Hz. The output parameters are complex shear modulus (Pa) and phase angle (°). The phase angle is the phase shift between the applied oscillating force and the measured resulting displacement. For pure viscous materials the phase angle has maximum value of 90° ($\pi/2$). Elastic materials response without delay to applied forces and hence the phase angle is 0°. Viscoelastic materials, like bitumen, exhibit both behaviours. The same is valid for the complex shear modulus, which can be separated into a real part and an imaginary part. The real part represents the elastic behaviour of stored energy and is regarded as shear storage modulus and the imaginary part represents the viscous behaviour of energy dissipation, which is referred to as shear loss modulus [11,37,38]. The correlation between complex shear modulus and phase angle can be visualized as *Black* diagram (Figure 21). With increasing complex shear modulus phase angle decreases (decreasing viscous behaviour) [38].

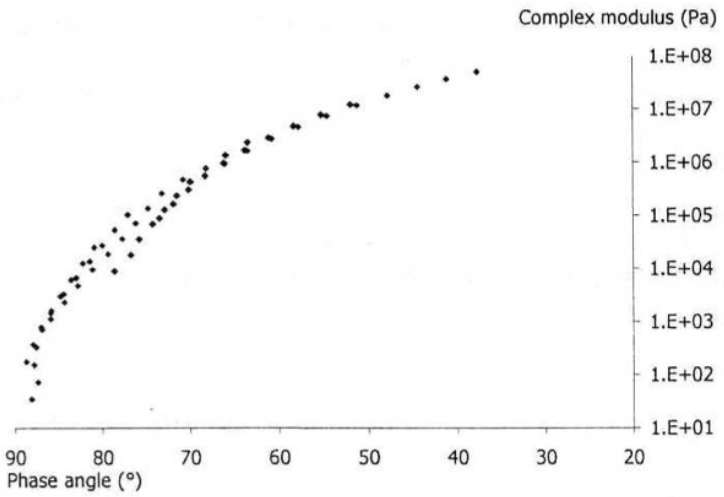

Figure 21: Correlation between complex modulus and phase angle (*Black* diagram) [38]

Additionally creep tests and creep recovery tests can be conducted with a dynamic shear rheometer (Figure 22). The sample is prepared as described. Then a constant shear stress is applied immediately and the resulting deformation is measured over time (creep test). In addition after stress removal the deformation measurements can be continued (creep recovery test). To eliminate the influence of different shear stresses, the creep yield, strain to stress ratio, can be displayed [38].

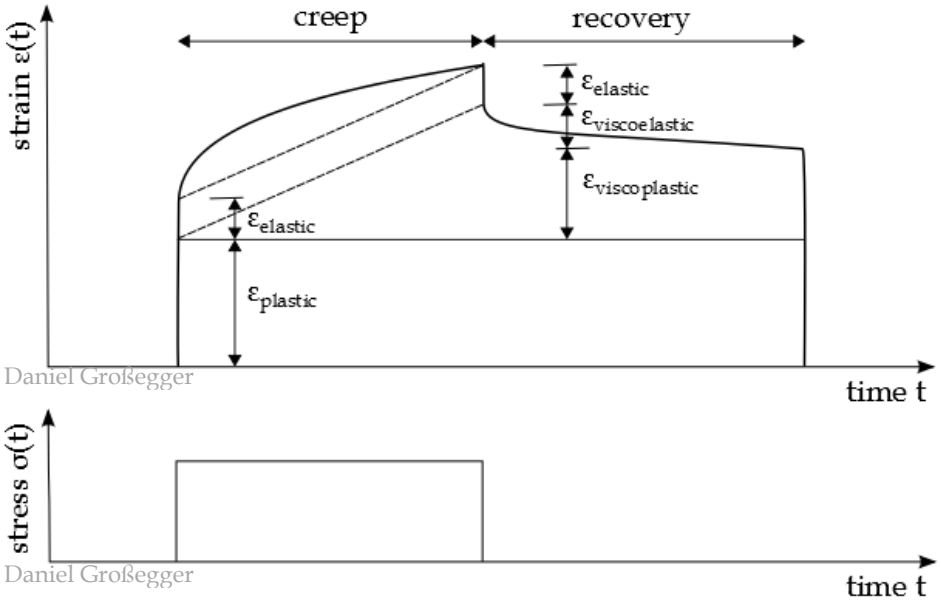

Figure 22: Creep behaviour of viscoelastic materials

Creep and creep recovery tests were conducted at the laboratory of the Institute of Transportation, Research Centre of Road Engineering with a HAAKE MARS II Modular Rheometer (Thermo Scientific) at +5 °C; operated by Markus Hospodka. The 25 mm plate was used. A shear force of 14400 Pa was applied for 1800 s (30 minutes), except for the resins the shear force was increased to 28800 Pa.

4.3.3. Classical liquid column chromatography

Chromatographic methods are used for the separation, identification and determination of chemical components in elaborate mixtures [39–41]. From the various types of chromatographic methods only liquid column chromatography will be described in detail, but all are based on the same common general principles.

In general chromatography is the separation of a mixture into its components by passing as a solution, suspension or as vapour through the stationary phase, in which the components move at different migration rates due to their different interactions with the stationary phase. The stationary phase (adsorbant) is fixed in place inside a column or on a planar surface and can be either solid or liquid. The mobile phase (eluent), which carries the analyte mixture, moves through the stationary phase and may be a gas, a liquid or a supercritical fluid. The two basic types are column chromatography and planar chromatography. All aggregation states mentioned are possible for column chromatography. Hence it can be subdivided into three general categories based on the nature of the mobile phase (gas chromatography – GC, liquid chromatography – LC and supercritical fluid chromatography – SFC). Further classification is done by the type of the interaction in preference to the stationary phase. Five types ensue for liquid chromatography: partition, adsorption, ion exchange, size exclusion and affinity [39–41].

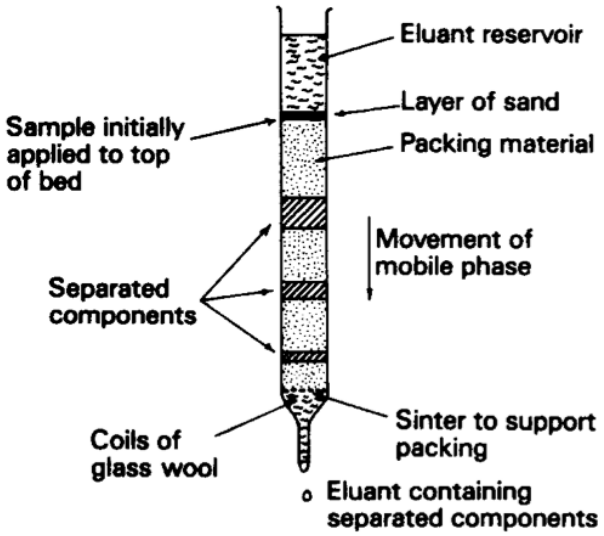

Figure 23: Basic experimental set-up for column chromatography [39]

The executed column chromatography with a liquid mobile phase and a solid stationary phase is adsorption chromatography. The separation mechanism is, as implied by its name, adsorption. The stationary phase consists of fine solid particles, which are packed densely inside narrow-bore tubing, or gels. For a surface increase the stationary phase can be microporous. The space between the particles is occupied by the mobile phase. If pores exist in the stationary phase, wettability and pressure will determine the degree of filling. The solution of an analyte mixture is inserted at the head of the column as a narrow cover. Elution occurs through adding mobile phase to the column. Thereby the different

components interact with the stationary and mobile phase. The distribution between them depends on the degree of adsorption and discharge rate. Adsorption involves the interaction of polar molecules or of molecules with polar groups with a polar stationary phase, which is typically silica gel or alumina (sometimes problematic due to catalytic active). This process of partitioning happens along the column. The migration rate depends on the fraction of time the component is retained by the stationary phase. The resulting difference in migration rates between components should be in such a way, that the separation along the column appears in bands or zones. The selection of the mobile phase has to be in such a way, that the compound will be separated effectively [39–41].

The classical open-column chromatography consists of a vertical glass tube with an inner diameter from 5 mm to 50 mm and a height of 50 mm to 1000 mm. The height is in accordance with the degree of separation and depends on the interaction with the stationary phase chosen. The upper end is open and has typically a ground joint. The lower end has a valve and some kind of filter. The filter can be a glass frit or a glass wool plug and hinders the stationary phase to wash out. The column can be prepared dry or wet. Dry means that the column is filled with a dry stationary phase, like a powder. The densification is done by gently tapping the column and/or generating a low pressure. After packing the mobile phase is added until the whole stationary phase is wetted. In contrast a slurry is generated for the wet preparation consisting of stationary phase and mobile phase. The slurry is poured into the column avoiding air bubbles to form. After the stationary phase is filled inside it is given some time to sediment. A layer of sand or a glass wool plug is placed on top of the stationary phase, independent of the way of preparation, to protect the bed from dispersing while adding additional eluent [39,40].

The classical chromatography is displaced in most ranges of applications by modern instrumental techniques. Yet it is still used when more sample volume is needed or the regeneration of the stationary phase is inefficient [40].

4.3.4. Bitumen separation into four fractions

The separation was conducted according to ASTM D 4124 – 01 standard test methods for separation of asphalt into four fractions [42]. Deviations to the standard are noted.

Balances used:

PCE-BT 2000 (manufacturer: PCE instruments; type: PCE-BT 2000; weighing range (max.): 2100 g; instrument read out: 0,01 g; linearity: ±0,03 g; repeatability: ±0,03 g; last calibration: unknown)

Sartorius AW-224 (manufacturer: Sartorius AG; type: AW-224; weighing range (max.): 220 g; instrument read out: 0,0001 g; linearity: ±0,0002 g; repeatability: ±0,0001 g (calculated repeatability from 15 measurements: ±0,0009 g); last calibration: unknown)

Chemicals applied:

n-heptane (purity: ≥99%, for residue analysis)

methylbenzene; trivial name: toluene (purity: ≥99,9%, for HPLC)

methanol (purity: ≥99,9%, for HPLC)

trichloroethene (purity: ≥98%, for synthesis, stabilized)

aluminium oxide 90 acidic (particle size 0,063 – 0,2 mm (70%), filtration rate: ≥0,3 ml·min^{-1})

Bitumen separation into maltenes and asphaltenes:

In order to take a representative sample, the top layer exposed to air is removed and the sample is taken from a more vertical line forward the bulk centre. For an easier removal and sample extraction the metal spatula and knife are heated by a hot air gun. The obtained bitumen sample is placed into a 1 l round bottom flask and weighed to the nearest 0,01 g. The used scale was the PCE-BT 2000. The standard suggests that the yield of maltenes should be about 10 g [42]. With a known asphaltene ratio, equation 1 can be obtained (also mentioned by the standard [42]).

$$s = \frac{10}{1-a} \tag{1}$$

s: sample mass [g]

a: asphaltene ratio [-]

This results in an initial weight of 11 to 12,5 g of bitumen [42].

About 500 ml n-heptane solvent is added (an approximated ratio of 53 ml solvent per 1 g bitumen compared to the standard with a ratio of 100 ml of solvent per 1 g of sample). Due to adding a Soxhlet extraction step and to avoid high filtrate volumes less solvent is used. Also the Erlenmeyer flask is exchanged for a round bottom flask.

A magnetic stir bar is added to the flask and placed on an oil bath on a magnetic stirrer. To reduce the solvent evaporation a Dimroth condenser is placed on top of the flask. The stirring is started and additionally the heat is increased until the boiling point is reached. After reaching the boiling point the temperature and number of revolutions are held unchanged for 1 h. Then the heat is turned off and the oil bath is lowered so that the flask no longer remains inside, the stirring still continues. When the flask is cooled to a temperature, that allows handling, the condenser is replaced by a ground glass joint, which seals it off. The remaining oil on the flask from the oil bath is carefully removed, so that the content does not swash over the joint. The flask is set aside overnight and shielded from light. During this time the asphaltenes can sediment at the bottom of the flask [42]. Slightly adjustments were made by replacing the air-powered stirrer by a magnetic stirrer and for safety precautions the foil-covered rubber stopper which seals the flask while stirring is replaced by the condenser.

On the following day a Büchner funnel (Buchner funnel) with a diameter of 125 mm, a (2 l) suction flask and a rubber bung are set up. The appropriate fitting qualitative grade filter paper with a slow to medium filter speed is placed inside the Büchner funnel. A qualitative filter paper (410) with slow filtration rate, particle retention of 2 µm and a diameter of 110 mm is used. Before placing the filter paper it is weighed on Sartorius AW-224. For the provision of low-pressure a diaphragm pump is coupled with the suction flask. When the

low-pressure is installed the filter paper is fully wetted with n-heptane, so that the filter abuts tight on the Büchner funnel. The content of the round bottom flask is added slowly and controlled onto the filter. As guidance a glass rod is used and the main part of the filtration should happen in the centre of the filter paper. Periodically the filter especially the rim should be wetted with n-heptane to ensure a tight seal with the funnel. Caution is demanded when little solution is left in the flask. This is typical when about a ¼ is left. At no time asphaltenes should creep over the edge of the filter, this gets more difficult with the increase of the filter cake. And the magnetic stir bar is still inside the flask. With a magnetic stirrer the magnetic stir bar is animated to rotate and then carefully the flask should be moved and rotated above to loosen the asphaltenes, which are sticking to the glass. If nearly free of sticking asphaltenes the magnetic stir bar is rinsed of and placed aside. It is recommended to rinse off the walls of the flask as well and then add the content onto the filter paper. During the loosening of the asphaltenes the filter paper should not dry out. This requires the continuing of the periodical wetting. When the whole content of the round bottom flask is poured onto the filter, but the n-heptane solution of the rinse cycle is not clear or still asphaltenes stick to the glass wall, the magnetic stir bar is placed again inside the flask, n-heptane is added and the process starts anew. Is the n-heptane solution of the rinse cycle clear, the flask is weighed to confirm that almost all is removed. The asphaltene cake inside the Büchner funnel is to be washed with n-heptane until the filtrate becomes colourless [42]. The low-pressure is then stopped and the filter cack is given time to dry a little. The filter with the filter cake is removed from the Büchner funnel without losing material especially when the funnel is still in place over the suction flask. If the operator is not skilled enough, it is recommended to move the Büchner funnel onto a new suction flask and then remove the filter paper with filter cake. The filter paper is folded so that the filter cake remains inside and then a second weighed filter paper is to be folded around the first one. To ensure leak tightness a third filter paper can be applied, which was the case in an extraction and then a thin uninsulated wire is twined around the last paper. The geometric dimension should be chosen to secure fitting trough the ground joint of the Soxhlet extractor. If there is residue on the Büchner funnel tip, it is washed into the suction flask. Now the main soluble bitumen part will be inside the suction flask. The content of the suction flask is poured into a weighed 2 l round bottom flask and rinsed until clean. Here monitoring of how careful the process has been carried out is possible. When the emptying of the suction flask is done slowly, larger particles have time to settle and will be visible on the bottom of the flask.

Soxhlet extraction (solid-liquid extraction)**:**

This step is not part of the standard, but it was integrated to ensure that the asphaltenes gained are pure (removal of trapped maltenes in the asphaltene filter cake).

The folded and tightened filter papers with the filter cake consisting of asphaltenes are placed inside the Soxhlet extractor. The Soxhlet extractor is placed onto the round bottom flask filled with the maltenes dissolved in n-heptane and an additional magnetic stir bar.

Then a Dimroth condenser and a dry tube with indicating silica gel as desiccant are mounted on the extractor. The dry tube is necessary to avoid condense water inserting from the condenser. New n-heptane is poured into the chamber containing the filter papers until it is half filled. The chamber of the used extractor had a filling volume of 500 ml. With about 250 ml from the chamber and about 700 ml from the round bottom flask it is enough to keep the apparatus from running dry. The apparatus is placed above an oil bath. The temperature is increased to a constant reflux. After three days [20] the temperature is turned off. Testing if the liquid in the extractor chamber is pure solvent, a drop is placed onto a glass plate and evaporated. If there are any stains, the extraction continued for another day otherwise the remaining liquid of the chamber is added to the round bottom flask. In most cases three days of Soxhlet extraction had been enough to obtain pure aspahltenes.

The bundle of filter papers is removed from the Soxhlet extractor and is dried inside a drying oven at 120 °C over night. After drying and cooling to room temperature the wire is removed as are the not weighed filter papers. The removed filter papers changed in colour from white to light ochre. The second applied filter paper can have some dark spots, asphalenes and is weighed and the filter paper containing the main part of the asphaltenes is also weighed. From the weight difference the asphaltene mass is obtained. The fact that also recovered bitumen from asphalt is used which still can contain methylbenzene insoluble parts like mineral fragments (filler) can be neglected. In the first executed separations for this thesis the solvent was exchanged after three days to toluene. After another three days of extraction the filter paper was removed and weighed. The base bitumen and the laboratory aged bitumen showed no residuum and only one sample obtained from asphalt concrete showed a maximum residuum of 0,3wt% (identified as mineral aggregates). The detailed results can be found in subsection 5.1. The standard records the mass of the asphaltenes from the filter paper of the Büchner funnel after drying in a 104 °C oven until a constant mass is achieved [42].

The Soxhlet method leads to a decreased asphaltene yield (about 0,5wt%), density (about 0,023 $g \cdot cm^{-3}$) and molar mass (about 100 $g \cdot mol^{-1}$), compared to the standard [20].

The dissolved maltenes are concentrated to a smaller volume via a rotary evaporator. Then another filtration step is executed. The remaining filter cake is dried and counted to the asphaltene fraction. The filtrate is inspissated until no solvent remains in the maltene fraction. The maltenes are weighed and dissolved in 50 ml n-heptane. In order to determine mass changes in the separation process (remaining of solvents or lose of fractions), the sum of asphaltene and maltene weight is compared to the original sample initial weight. Additional the weight of the maltenes can be used to calculate the column hold-up of the chromatographic column.

Liquid column chromatography:

With the liquid column chromatography the maltene fraction is unravelled into three further fractions.

The geometry of the glass column is 997 mm in length, 30 mm as inner diameter and an integrated glass frit with 3 mm height at the bottom of the column. The closing-off is a valve made of polytetrafluoroethylene. Due to the slight bending of the glass column adjusting was done for the middle part.

The column is installed vertical inside a fume hood. A glass wool plug (chemically pure, fibre size: ~11 µm) typically 25 mm height is placed at the bottom to assure that the frit is not clogged by the stationary phase and then the column is filled with aluminium oxide as stationary phase. The amount of aluminium oxide used is in a range from 450 (standard) to 503 g. The variation is sometimes problematic causing retention of the packed column. The used amount is mentioned in the results for each separation. While adding aluminium oxide the column is gently tapped with a rubber tube to ensure dense packing. This task is done more easily by two people. For personal safety a dusk mask should be worn while handling aluminium oxide. When the column is filled, the tapping should continue for at least 10 min, with paying attention to the intersection from discrete adding (one person handling). At the end, another glass wool plug is placed on top of the horizontal aluminium bed to stabilise the bed during adding dissolved maltenes and constant dropping of eluent from the dripping funnel [42]. The column is sealed by placing a glass joint on top and closing the valve. This is the case because the column is packed the day before the separation is conducted. The slow flow rate was about 1,7 $ml \cdot min^{-1}$ the standard gives a dripping rate of about 5 $ml \cdot min^{-1}$ and an eluate collecting rate of 5 ±1 $ml \cdot min^{-1}$ [42]. The prepared columns were two to three times slower than the standard recommends. The separation lasted longer than twelve hours and so it was chosen to pack the column in advance.

Typically failure, which lead to poorer separation, are that the column is not vertical, the interface between glass wool and stationary phase are not plane and horizontal (main problem when using glass wool) or air bubbles are present inside the stationary phase. Also column diameter and length should be chosen in a sensible way and complementary to the amount of substance applied.

The next day the vertical position of the column is audited. The glass joint is removed and it is very important to open the valve. The column is pre-wetted with n-heptane until the aluminium oxide powder is saturated (typically about 300 ml). Proceeding this step faster pressure is applied on top of the column. Redensification will take place inside the column. For adding new solvent the pressure is to be diminished slowly and at no time the solvent level should be lower than the alumina bed. Typically gaps appear when the pressure is cut-off too quickly and the compressed air expands at once. The forerunnings are also collected, since there is no exact cut off point between saturates and forerunnings. When the column is pre-wetted (Figure 24a) and the solvent level is at the height of the upper glass wool plug the dissolved maltenes are transferred to the column using a minimum amount of additional n-heptane to transfer everything (Figure 24b) and leave a light darkened bottle behind. A dropping funnel is placed on top of the column filled with 200 ml n-heptane. The dropping rate is adjusted so that the liquid level never falls below the alumina bed. When the forerunnings are collected, the amount is equal to the amount of pre-wetting, the bottle

is replaced by 50 ml snap-cap vials. The snap-cap vials are used instead of an additional funnel (dropping funnel) and a tared receiver (beaker or flask) to document a weight distribution and see if another peak appears in this distribution beside those of the three fractions. Whenever the eluent in the dripping funnel is nearly empty, the valve is opened to discharge the rest onto the column and new eluent is filled inside. The used eluents and their amount are listed in Table 4.

Table 4: Order of used eluents

eluent solvent	volume
n-heptane	200 ml
methylbenzene	400 ml
methanol/methylbenzene (50/50)	300 ml
trichloroethene	500 ml

The standard notes 600 ml of trichloroethene [42], but after 400 ml the eluent colour becomes anew colourless.

The snap-cap vials are additionally exchanged when a new fraction starts to drop into the vial. The cut point between saturates and aromatics is from colourless to yellow. The aromatics alter from yellow to deep red. The resins are black. The cut point between aromatics and resins is better detectable then the cut point between saturates and aromatics (Figure 24c) [42].

Once the resins are being collected, after four snap-cap vials, the receiver is changed to a round bottle flask capable to contain 500 ml to collect the tailings. The snap-cap vails are sealed with the corresponding snap-on lids.

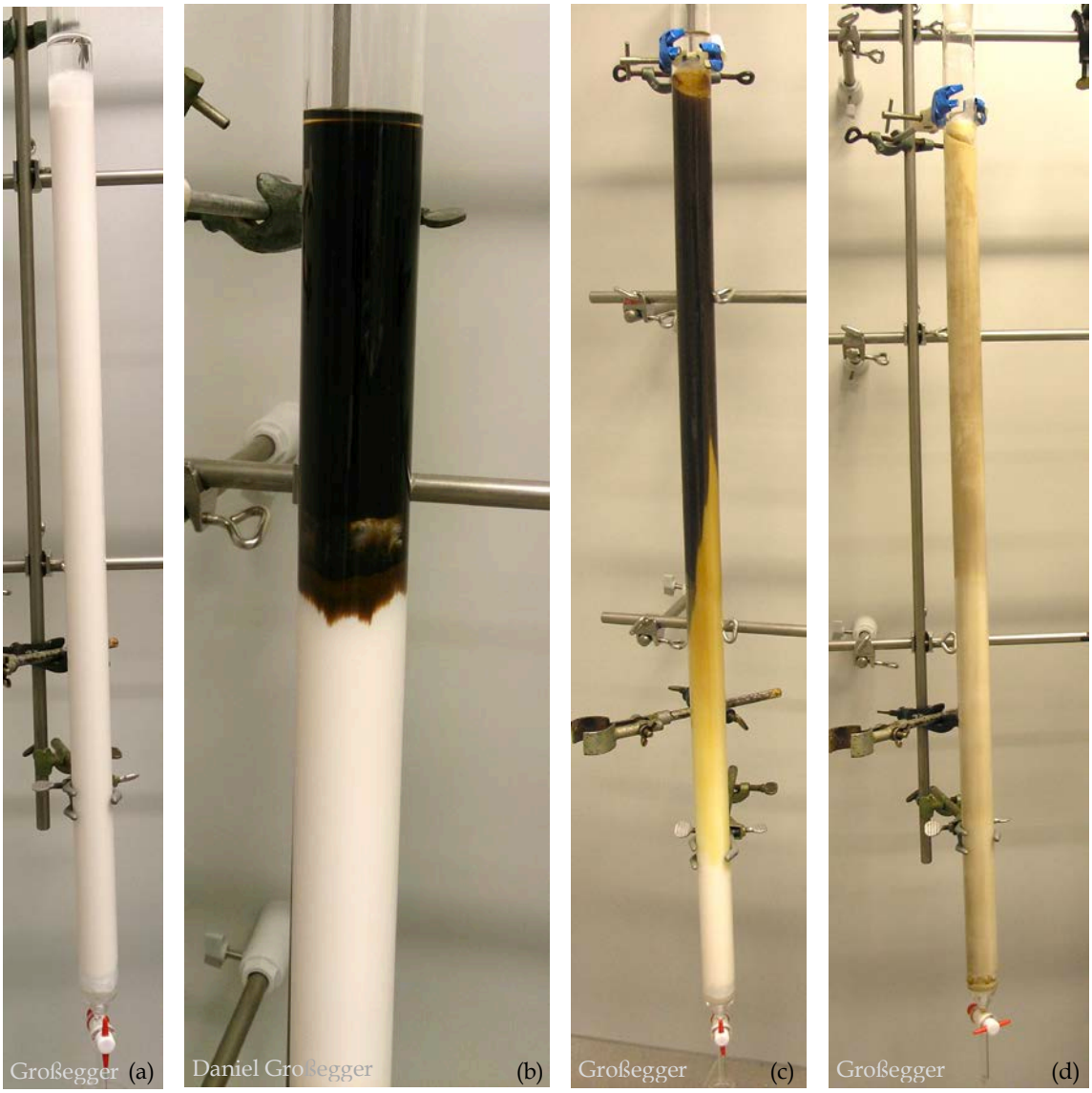

Figure 24: Development of chromatographic separation: pre-wetted (a), start of separation (b), advanced separation stage with no horizontal interface between the fractions (c) and column after separation (d)

Solvent removal:

The content of a snap-cap vial is transferred to a tared round bottom flask. For the removal of solvents a rotary evaporator is used. The oil bath is heated to 110 °C and a vacuum of 500 mbar is applied. After an initial waiting time for an equilibrium the pressure is further reduced until solvent condenses on the condenser. The rate of decreasing has to be slow to avoid boiling retardation. Before the solvent starts to evaporate from the solvent receiver the sample is to be moved out from the oil bath (giving it enough time to cool down), the pressure is to be restored to ambient conditions and the solvent receiver is to be emptied. For saturates the bath temperature is left at 110 °C and the vacuum is reduced to 10 mbar. For aromatic, resins and also the maltenes the bath temperature is increased to 160 °C and the vacuum is reduced to 10 mbar. Under this condition no solvent remained in the sample.

The oil is removed from the flasks and after cooling the samples are weighed.

4.3.5. Liquid-liquid extraction

Liquid-liquid extraction or solvent extraction is a selective dissolving method. The analyte is removed from the original solvent and subsequently dissolved in a different solvent, while most of the residuum of the sample remains in the original solvent. The two important criteria are that the two liquids are immiscible and that the analyte is more soluble in the extracting solvent than in the original solvent [40].

Bitumen respectively maltenes were placed inside a separation funnel and dissolved within methylbenzene. Water (purity: ≥99%, for residue analysis) was added as second solvent to the separation funnel. The stoppered separation funnel was shaken and vented repeatedly. To vent the stopcock was opened, while inverted. After shaking the separation funnel was positioned vertical with a stage clamp and left undisturbed for a period of time to allow the two immiscible layers to separate once again [40]. The separation of the two liquids took two weeks, did not form a defined interface and bitumen stuck to the glass wall. Water, as the denser liquid, was the bottom layer. A round bottom flask and a filter were placed under the separation funnel. The stopper was removed and the stopcock was opened. The bottom layer was drained through the filter into the round bottom flask and the stopcock was closed when the interface between the layers was a little above the stopcock. Since there was no interest in quantity the process was not repeated. The water was removed from the round bottom flask (see solvent removal in subsection 4.3.4). The analyte was dissolved in methanol and prepared for spectrochemical analyses.

4.3.6. Optical and spectrochemical methods

Spectrochemical methods involve the absorption or emission of electromagnetic radiation. The methods can be classified according to the used or produced region of the electromagnetic spectrum. The spectrochemical methods applied were used in first-line to verify the separation of the chromatographic column. The fluorescence spectroscopy was further used to detect changes on prepared bitumen surfaces to investigate the effect of natural occurring (in higher concentration) reactance on bitumen.

4.3.6.1. Optical methods

For verification and documentation pictures were taken with my mobile phone camera (Sony Xperia™ Z; model number: C6603; 13 megapixel camera with Exmor RS and autofocus) and additionally a microscope (Olympus BX51) with a microscope CCD camera (Hengtech MDC320) were used to document the surface changes during liquid ageing and other curiousness.

4.3.6.2. Fluorescence spectroscopy

Fluorescence is a photoluminescence process. Some substances have the property to absorb light at a particular wavelength (excitation wavelength) and emit light of a longer wavelength (lower energy; emission or fluorescence wavelength) after a brief interval (fluorescence lifetime). With absorption of a photon atoms or molecules transits into an excited state, these excited electronic energy states, as the ground state are further

subdivided into several vibrational or rotational energy levels. Two important processes that causes loss in excess energy are non-radiative relaxation (loss of excess energy in the absence of light emission) and fluorescence emission. Non-radiative relaxation involves vibrational relaxation and internal conversion, which compete with fluorescence emission. Vibrational relaxation leaves the molecules in the lowest vibrational state of an electronic excited state by transferring excess energy to other molecules. The same applies for internal conversion with the pass of energy difference from the lowest vibrational level of an excited electronic state to a lower electronic state and higher vibrational level. Both mechanisms result in an increase of temperature. Fluorescence is nearly almost always observed from the lowest excited electronic state to various vibrational levels of the ground state, producing a range of photon energies during emission (closed band). The shift to longer wavelength is called the Stokes shift. If intersystem crossing occurs and a photon is emitted when it transits into the ground state, this is regarded as phosphorescence (sometimes called delayed fluorescence) [41,43,44].

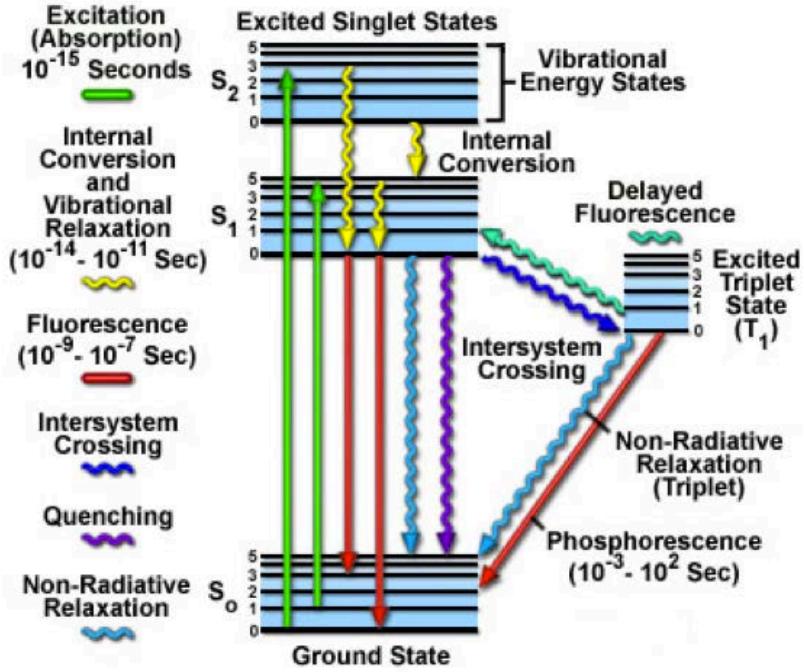

Figure 25: Jablonski energy diagram [44]

Fluorescent compounds containing aromatic rings, certain aliphatic and alicyclic carbonyls and/or highly conjugated double-bonded structures. Aromatic rings grand intense fluorescence emission and with increasing number of rings the intensity increases and shifts to higher wavenumbers. Substitution on an aromatic ring causes additional shifts in absorption and emission maxima and affects the fluorescence efficiency. Carboxylic acid or carbonyl groups on aromatic rings significantly reduces or inhibits fluorescence. Additional fluorescence is favoured in rigid molecules. If measured in solution, also temperature and the used solvent have an influence on fluorescence (for example quenching) [41].

The equipment used was produced by Edinburgh Instruments Ltd. The whole setup consisted of different power supplies (xenon lamp supply, model XE900 for the xenon lamp;

power hub, model PH 1 for the two monochromators and the sample chamber; PMT cooler, model CO 1 for the detector), a XE900 xenon arc lamp, two TMS300 monochromators, an UC920 sample chamber and a S900 single photon photomultiplier detection system. The last calibration was carried out in February 2009. A lamp exchange showed that the incoming lamp spectrum shifts 1 nm to lower wavelength. If something similar occurs on the detector side is unknown. Over the duration of this thesis the xenon arc lamp was exchanged three times. The second lamp had a defect, not recognisable at the beginning, but after the short service life. The obtained spectra had lesser intensity and some peaks shifted in the range of 20 nm. These spectra were not used further (exceptions mentioned in the text) and thus not for all bitumen or fractions spectra are available.

It was important for this thesis to visualise the change of the spectrum. This was accomplished by emission scans and excitation scans. For the emission scans the excitation wavelength was fixed at 280 nm and the emission wavelength was detected from 300 to 750 nm. The spectrum was obtained by two scans. The first scan range was from 300 to 540 nm and the second scan range was from 480 to 750 nm with an inserted 340 nm filter between sample and detector to avoid the reflection peak at 560 nm (twice the excitation wavelength). The two obtained scans were merged at 510 nm with an overlap of 30 nm on each side to match the scans intensity. For the excitation scans the detected/emission wavelength was fixed at 515 nm and the excitation wavelength was ranged from 250 to 500 nm. The parameters were obtained by an overview 3D scan and as an additional cause the confocal laser scanning microscope (not part of this thesis) had a detection wavelength of 525 nm ±10 nm. The scan steps were 1 nm and the dwell time was 1 s for each step. The emission/excitation wavelength was ±0,5 nm per step. The spectra were post-processed by normalising them.

For sample preparation bitumen or inspissated fractions were smeared onto a microscope slide to cover an area across the entire width of the slide as opaque as possible (Figure 26). To ensure an even surface the sample was slightly heated by a hot air gun until flat. After cooling (about 1 min) the sample was placed inside the sample chamber. The position of the sample was adjusted for optimal intensity output and the measurements were started.

Figure 26: Two prepared samples of saturates, aromatics, resins and asphaltenes (right to left)

Photobleaching (loss of fluorescence, due to high repetition of excitation and emission cycles) did not occur at the parameter used, only after a mapping scan a slit appeared on the bitumen surface.

With the applied scanning parameters, not only fluorescence signals are measured, due to the long dwell time it is also possible that phosphorescence signals are measured. So it would be more precise to call it photoluminescence spectroscopy instead.

4.3.6.3. Infrared spectroscopy

Infrared light can excite only vibrational and rotational transitions, resulting in defined peaks from transitions among the various vibrational quantum levels (in solids or liquids rotational levels are often hindered or prevented) [41].

For the interpretation of such a spectrum, often positions of characteristic maxima for common functional groups are used. To identify functional groups comparison with a spectrum of known compounds is done or as well a mathematical approach is possible (complicated with increasing number of atoms) [40,41].

For attenuated total reflection (ATR) the transparent material have a high refractive index. The infrared light beam passes through the transparent material and is reflected from the sample. Through the reflection on the sample the intensity of the infrared light beam is reduced and detected [40].

The location, shape and relative intensity of a peak is used to identify the particular type of bond. The region of the spectrum spans from 4000 to about 600 cm^{-1} (2,5 to about 17 µm). The region from 4000 to 1500 cm^{-1} is especially useful for correlating peak location with bonds. The region from 1500 to 400 cm^{-1} is referred as fingerprint region, which gives clues about the compounds [40].

The used spectrometer was a VECTOR 22 (Fourier transformation infrared spectrometer – FTIR), produced by Bruker (warranty expired 1997) with a deuteriated triglycine sulphate (DTGS) detector. It was measured in attenuated total reflection (ATR) with a single reflection attenuated total reflection microsampler (3 mirrors), which was flushed with dried air; optical comparts produced by Harrick (SplitPea™ ATR Microsampler). The attenuated total reflection window was a Germanium crystal. The control program was OPUS 5.5. The spectra were recorded by adding up 512 or 1024 scans at a resolution of 4 cm^{-1} in the spectral range between 4000 to 400 cm^{-1}. The first conducted scans were background measurements, then the sample was placed on the crystal and the sample was measured. The background was automatically subtracted from the measurement with sample. The resulting spectrum was cut to a range from 4000 to 450 cm^{-1} to avoid artefacts from the closing in crystal transparency. Then a baseline correction was applied (concave rubberband correction with 7 iterations and 64 baseline points) and the spectrum was normalised.

5. Results and discussion

5.1. Bitumen separation

5.1.1. Gravimetrical analyses

The process was started with the separation into maltenes (n-heptane soluble compound) and asphaltenes (n-heptane insoluble compound). The weight per cent of the obtained asphaltenes varied not only for the ageing stages, but also for repeated separations of the same sample. The mean asphaltene fraction is for the base bitumen, excluding spikes, 9,36wt% with a corrected sample standard deviation of 0,26wt%. The uncertainty calculated with corrected sample standard deviation is 0,09, compared to the uncertainty of about 0,06wt% (Sartorius AW-224) to 0,51wt% (PCE-BT 2000), calculated from the reproducibility of the used scales. When the obtained fraction was measured with the scale PCE-BT 2000 the uncertainty is higher than the acceptability criteria of standard deviation (0,32wt% [42]) of the standard (ASTM D 4124 - 01 [42]). The second investigated base bitumen has a mean asphaltene fraction of 12,58wt% with a corrected sample standard deviation of 0,27wt%.

Figure 27 shows the mean asphaltene fraction of non-aged and aged bitumen. The increase of asphaltenes from base bitumen (B) to laboratory short-term aged bitumen (B_LRTFOT) is about 15,5% and the increase from laboratory short-term aged to laboratory long-term aged bitumen (B_LPAV) is about 40,2%. Bitumen extracted from the first layer of the 12 months test piece of the test field (B_F012_S1) had an high asphaltene ratio and is closer to laboratory long-term aged (B_LPAV), as needle penetration already indicated [23]. The laboratory liquid aged bitumen (B_LH2O2) is between laboratory short-term (B_LRTFOT) and long-term aged bitumen (B_LPAV). Since only one separation for laboratory liquid aged bitumen with known H_2O_2 concentration and exposure time was conducted, no further statements on the influence of H_2O_2 to the asphaltene generation can be made. The road sample (B_F282) has the highest asphaltene ratio, which is most likely due to the long service lifetime of 23,5 years.

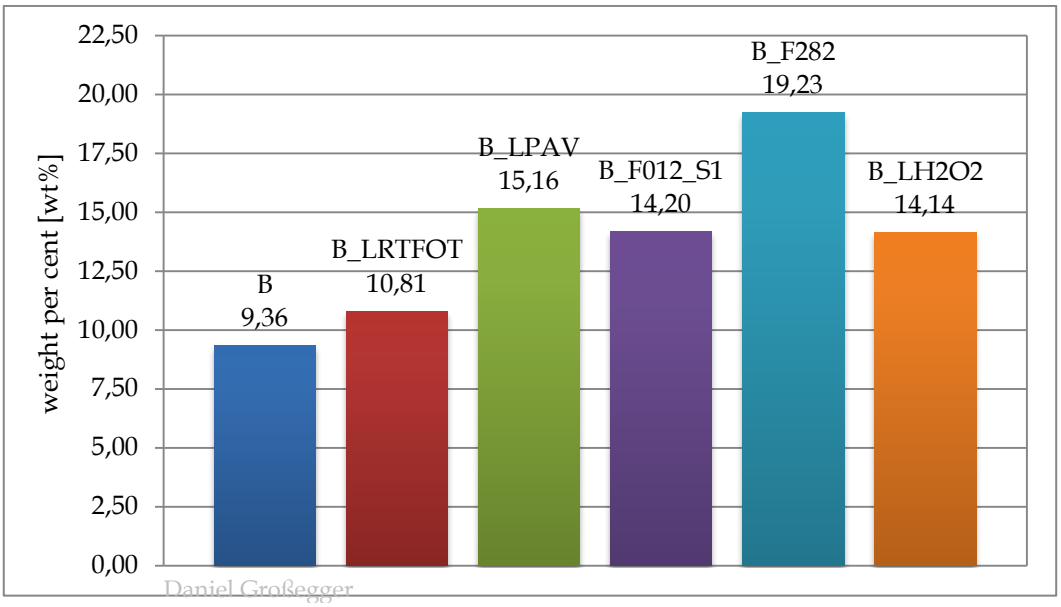

Figure 27: Mean asphaltene fraction for different bitumen ageing stages

The separation of maltenes into three additional fractions was sometimes difficult. Not fully separated fractions were obtained when the retention of the column was too short. Especially the cut point between aromatics and resins was not defined. In order to verify that additional 50 g aluminium oxide for pour packed column did not have a significant influence on column chromatography, two additional columns with about 50 g and 100 g were conducted using base bitumen B and one additional column with about 50 g were conducted using base bitumen B2. The results are shown in Figure 28. There are minor changes in the fractions between the 450 g-packed and the 500 g-packed columns for base bitumen B. The deviation is in the range of the calculated uncertainty. A significant difference shows the 565 g-packed column. An influence on the distribution of the saturate, aromatic and resin fractions is due to the higher amount of asphaltenes and hence a minor amount of maltenes was used for the chromatographic column. Still the difference of about 10% in aromatics and resins is significant. The second base bitumen B2 exhibited similar behaviour, except that the quantity of saturates increased with additional aluminium oxide.

It is important to keep in mind that variation in conducting the separation have an influence on the obtained fraction and that the difference in the results by adding 50 g more aluminium oxide where regarded as minor.

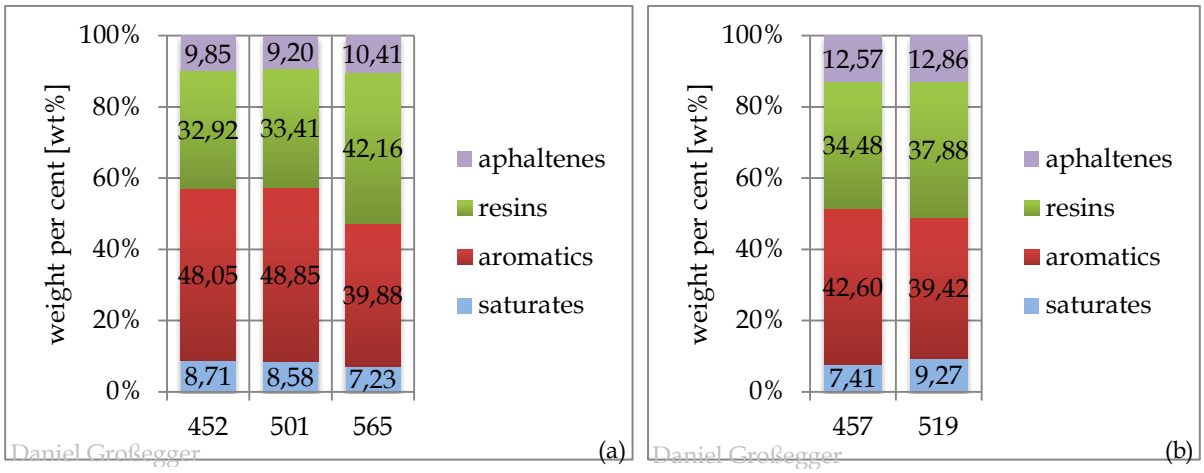

Figure 28: Weight per cent distribution of base bitumen fractions for different amount of used aluminium oxide: B (a) and B2 (b)

The individual measurements (Figure 29) confirm the trend measured by other analytical methods. Saturates are unchanged in concentration (average uncertainty about 0,12wt%) except B_F000_C, which is identified as outlier. This is expected, due to the inert nature of saturates against oxidation. Aromatics decrease as the resins and aphaltenes increase. It is commonly assumed that aromatics form resins and/or aphaltenes (see section 3.3). With the increase in resins and asphaltenes (more solid fraction) and the decrease in aromatics (viscous fraction) bitumen gets "harder" and favours a more elastic/brittle behaviour. The investigated bitumen from the produced test pieces already had a high quantity of asphaltenes and resins, and aromatics are reduced, which is similar to laboratory long-term aged bitumen. It is assumed (due to a lack of references or proof) that during the production higher temperature, longer mixing duration or usage of bitumen with a trend to poorer ageing behaviour, then indicated by laboratory tests (not favoured), led to the provided results. The contribution of the bitumen extraction process from asphalt to the fractional distribution is unknown. The differences between bitumen from the asphalte mixture bag (B_F000_A) and bitumen from an asphalt plate (B_F000_C) could be due to the loose aggregation inside the mixture bag, where oxygen had an easier access to a greater bitumen surface as it occurs for a plate. During the first year the first layer of the test piece (B_F012_S1) approaches the same distribution as the laboratory long-term aged bitumen (B_LPAV), with an increase of 12% in asphaltenes and a decrease of 3% in resins and 4,6% in aromatics from B_F000_A to B_F012_S1.

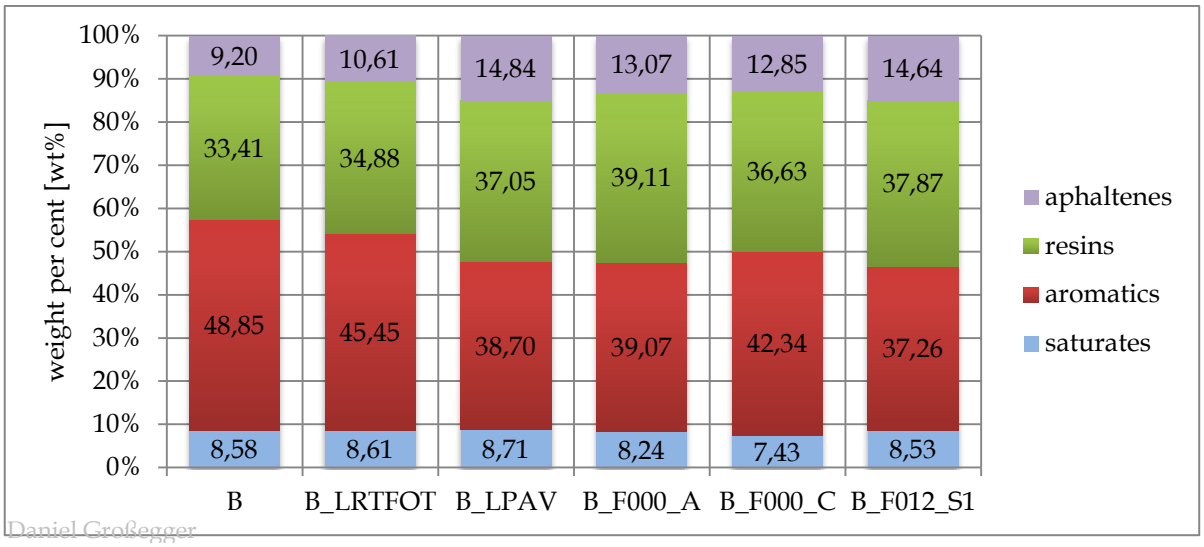

Figure 29: Fractional distribution related to test field

The laboratory liquid aged bitumen (B_LH2O2) is in its fractional composition similar to laboratory long-term aged bitumen (B_LPAV) with a lower asphaltene and aromatic content and higher resin content (counting the 2,48wt% of column hold-up as resins, given a resin content of 39,94wt%; Figure 30). The fact that the two laboratory aged bitumen are nearly alike is mere coincidence. Yet, it shows that liquid ageing affects aromatics a bit stronger than ageing with air and produces resins and little less asphaltenes. It can even have an influence on saturates, but further studies would be necessary to confirm the mechanism of ageing with hydrogen peroxide.

The road wearing course sample (B_F282; Figure 30) has less aromatics and resins, compared to artificially aged bitumen and an increased amount of asphaltenes. A comparison is not really possible, due to the fact that not the same bitumen was used for asphalt production and no adjourned samples were available.

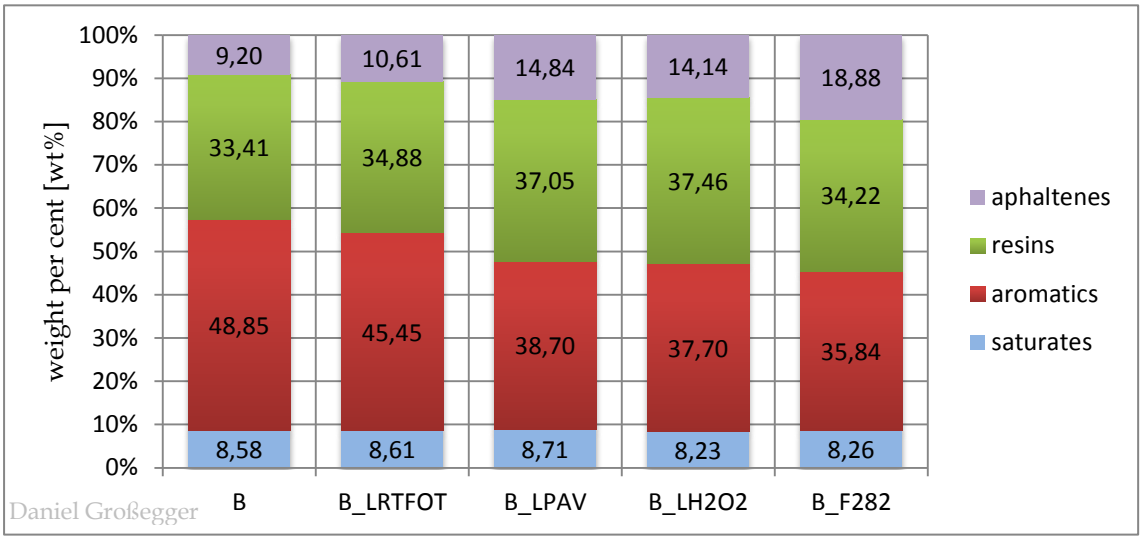

Figure 30: Fractional distribution of artificially aged bitumen

The eluate from the chromatographic column was collected in 50 ml snap-cap vials (Figure 5), and the volume was condensed and weighed, resulting in a weight per cent distribution

(Figure 31). Saturates 1 include the forerunnings, while the last of the resins (usually resins 5 or resins 6) was collected into a round bottom flask and thus held more resins.

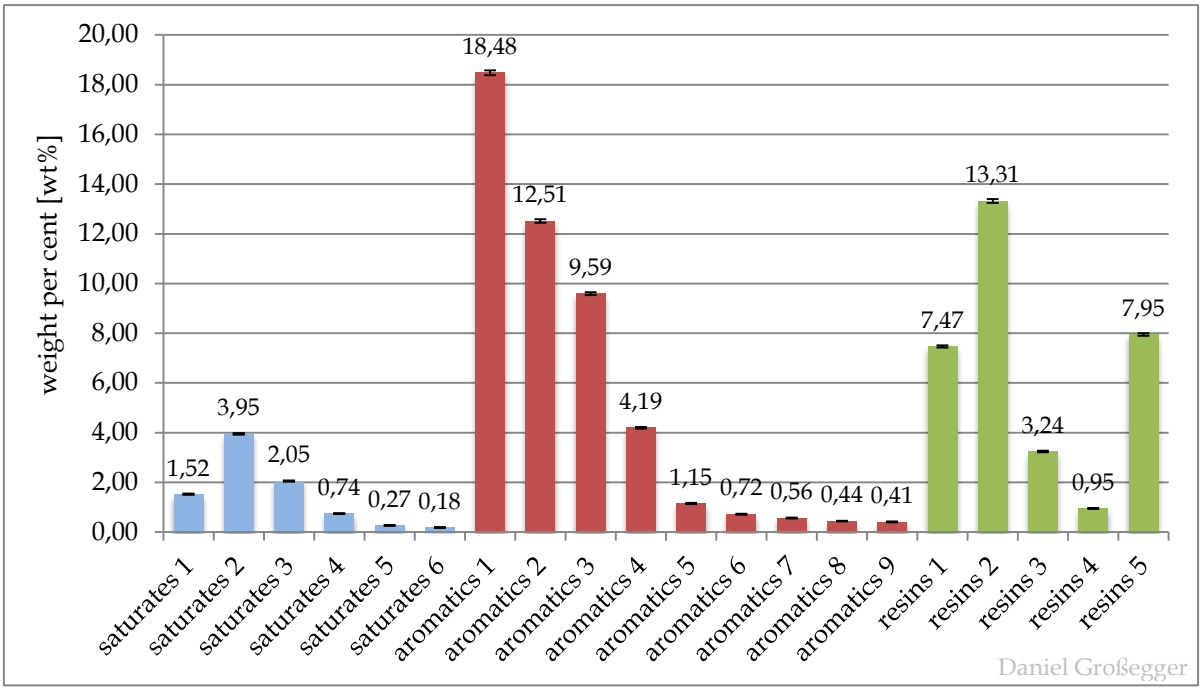

Figure 31: Weight per cent distribution of B (452 g aluminium oxide)

The exemplified weight per cent for each snap-cap vials from the chromatographic separation of the bitumen B (451,86 g aluminium oxide) with a column hold-up of 0,47wt% (Figure 31) shows that the main part of the collected fractions were two and three for saturates and one to two for aromatics and one to three for resins with an additional main part from the tailings. Similar distributions were obtained for the other bitumen separations.

An adapted liquid column chromatography was performed to verify (basics see subsection 4.3.3 and 4.3.4), that asphaltenes are not the most polar fraction [12]. The length of the column was shortened to 510 mm and 150 g aluminium oxide was used. The applied solvents were reduced to 135 ml methylbenzene, 100 ml methanol/methylbenzene (50/50) and 200 ml trichloroethene [42]. The amount of asphaltenes used for the separation was about 2 g. The first try was with asphaltenes as powder and included 65 ml n-heptane as solvent. The asphaltenes clustered and did not dissolve completely in the following solvents, resulting in a visible residue on the top of the column and a column hold-up of about 3wt%. Yet it showed nearly the same distribution as the second attempt. For the second try, asphaltenes were dissolved in 20 ml methylbenzene. Due to the definition of asphaltenes as insoluble in n-heptane, no fraction corresponding to saturates was obtained. It could be possible that asphaltenes have non-polar compounds like long-chained hydrocarbons [19], but the methods applied were not capable to reveal these compounds. Through the crude collection with 50 ml snap-cap vials and that no visible cup point could be identified, it is not possible to divide directly into fractions, which correspond to aromatics or resins. From the experience with maltene separation the cut point should be

within asphaltenes 3, which results in about 42wt% corresponding aromatics (including asphaltenes 3) and 58wt% corresponding resins.

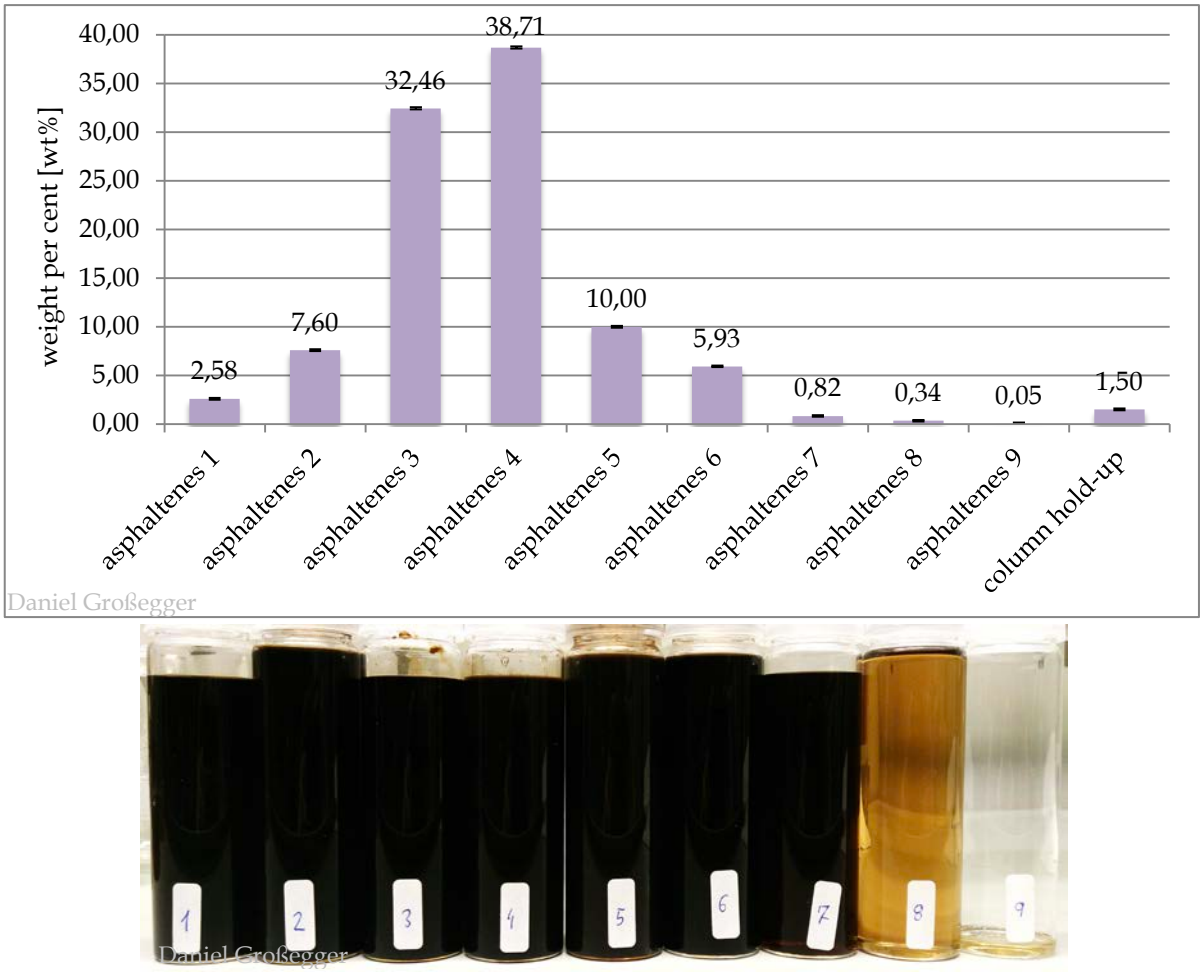

Figure 32: Weight per cent distribution and snap-cap vials of asphaltenes (obtained from B) separated by liquid column chromatography

5.1.2. Fluorescence analyses

Fluorescence spectra were obtained from handpicked snap-cap vials (depending on the amount of fraction and lamp assignment for fluorescence spectroscopy, see subsection 4.3.6.2). The following fluorescence spectra are correlated to the weight per cent distribution shown in Figure 31.

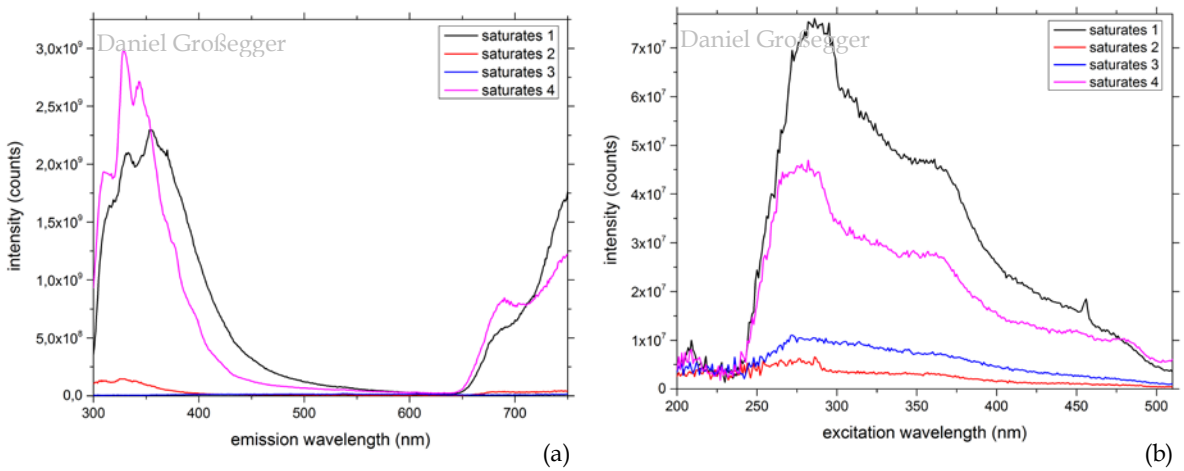

Figure 33: Fluorescence spectra of saturates: emission (a) and excitation (b)

The main part of saturates exhibit less intensity than the first and last obtained saturates. The last obtained saturates always occurred faint yellow when inspissated, meaning a little bit of aromatic content is found in these saturates (cut point see subsection 4.3.4). The range from about 450 to 650 nm in the emission spectra had less intensity and the main part of saturates shows no intensity. The increase of intensity starting with 650 nm could be phosphorescence. The peak at 456 nm in the excitation spectrum of saturates 1 is regarded as artefact.

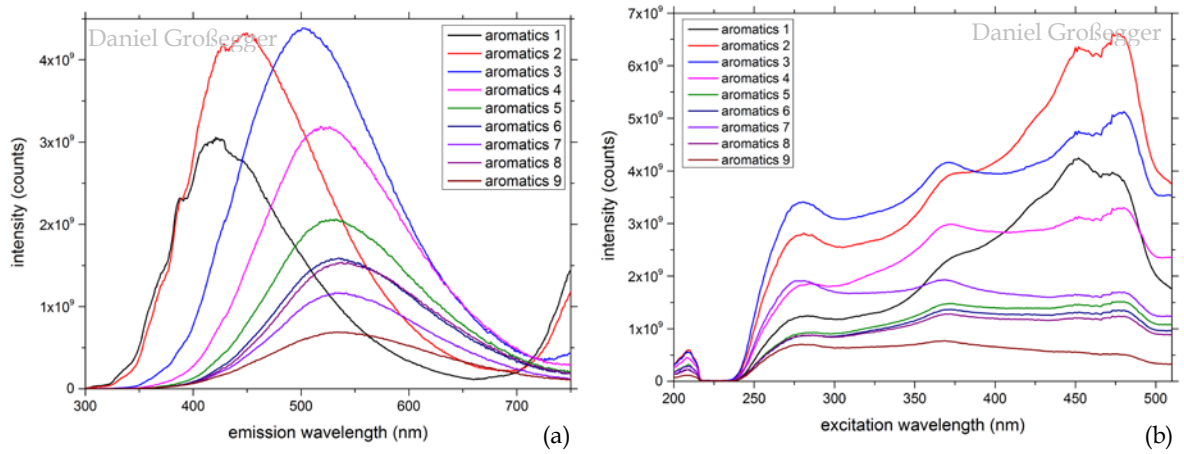

Figure 34: Fluorescence spectra of aromatics: emission (a) and excitation (b)

Aromatics exhibit the highest intensity with a decrease in intensity forwards resins. Additionally, a shift in maxima happens as the content approaches the resins, clearly visible in the emission spectra. Aromatics 2 and aromatics 3 show the highest intensity. They happen to be in all measured fractions the ones with the highest intensity.

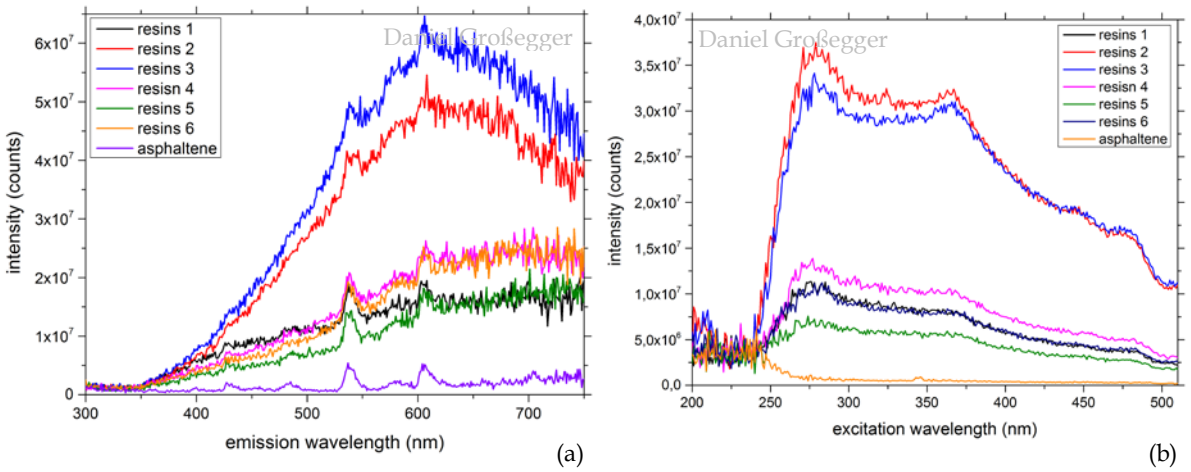

Figure 35: Fluorescence spectra of resins and asphaltenes: emission (a) and excitation (b)

Resins exhibit less intensity and asphaltenes in solid state do not show fluorescence in the measured region. Like aromatics, resins 2 and resins 3 display more intensity. The noticeable peaks within the emission spectra at about 536 nm and 605 nm are also present in the spectra of saturates (not clearly visible, due to the intensity of the other peaks). The asphaltenes spectrum is identical with a spectrum obtained by measuring only a microscope slide. Even though asphaltenes and resins are opaque these two peaks appear. They are not artefacts introduced by the detector, because an empty spectrum was measured for the detector itself (no sample or light source). Less favoured causes are that the microscope slide is responsible or that the mirrors are not clean. This would have also influenced other measurements, which was not the case. A cuvette with resins, dissolved in trichloroethene, was measured in L-geometry (without mirrors), same for the dissolved aspahltenes (see below). The resin concentration was high and the obtained spectrum is identical with an asphaltene spectrum. These peaks are of further interest, since base bitumen does not always feature them and aged bitumen often features them. Maybe they only occur at lower intensity and can be used as an indicator for the increase of resins and asphaltenes and the decrease of aromatics during ageing, which affects intensity.

A comparison between the three spectra reveals that each fraction has its unique spectroscopic features. Aromatic ring groups (aromatics) exhibit intense fluorescence and to the second aromatic snap-cap vial the number of rings increases (increased intensity). Further through substitution the spectrum maxima shifts (see subsection 4.3.6.2). From aromatics 2 to aromatics 3 this shift is approximately 50 nm. It is suspected that with increasing substitution and occurrence of heteroatoms the intensity decreases and the maximum shifts to a higher wavelength.

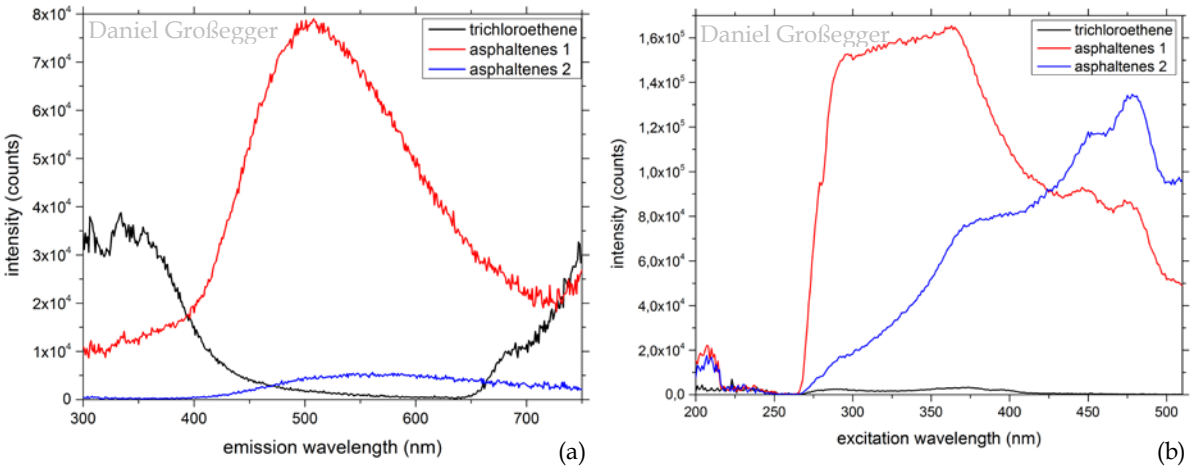

Figure 36: Fluorescence spectra of asphaltenes dissolved in trichloroethene: emission (a) and excitation (b)

Asphaltenes were dissolved in trichloroethene, the only solvent available with little intensity and no major peaks (Figure 36, black line). The dissolved asphaltenes exhibit fluorescence in the observed region and with increasing asphaltene concentration (from asphaltenes 1 to asphaltenes 2) the intensity decreases, due to Beer's law, and the maxima shifts forward to a higher wavelength (Figure 36).

5.1.3. Infrared analyses

The change in infrared spectra was studied on the separation of base bitumen B2 (weight per cent distribution see Figure 37). The separation conducted with 519,33 g aluminium oxide (see subsection 5.1.1) was chosen, because separation was clearer and the spectra were better (less background noise). The described developments in the spectra are also found in base bitumen B and laboratory long-term aged bitumen (B_LPAV).

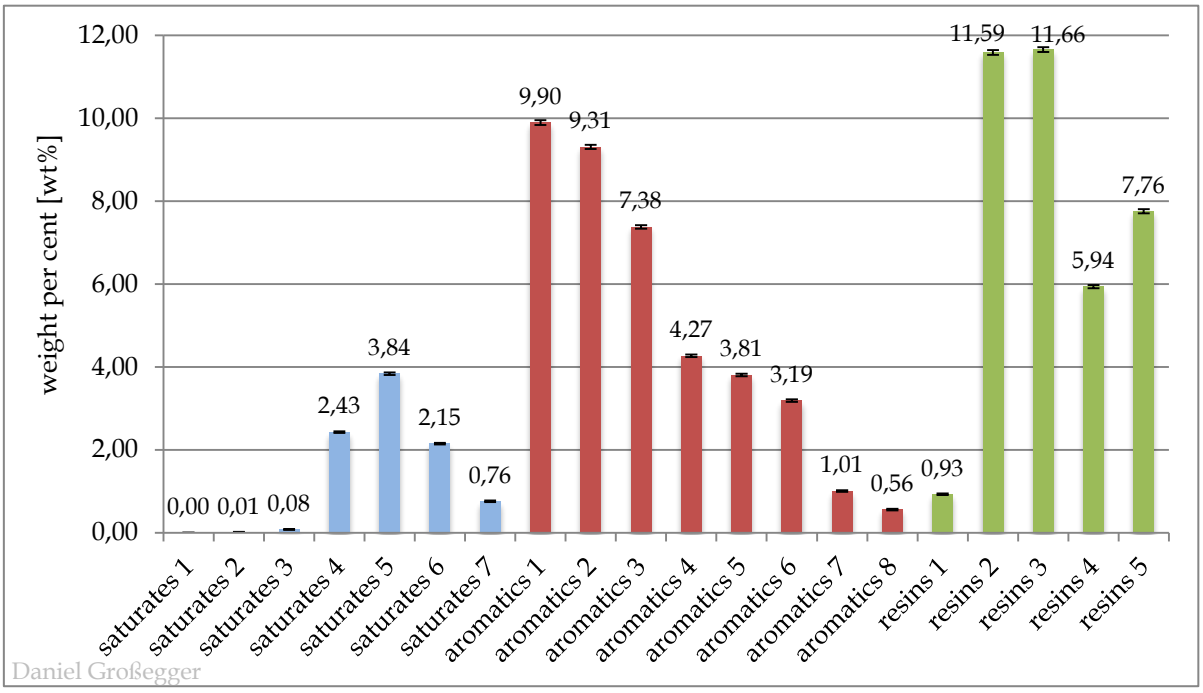

Figure 37: Weight per cent distribution of B2 (519 g aluminium oxide)

The missing spectra of saturates 1 and saturates 2 are due to the lesser amount of saturates obtained from these snap-cap vials.

The main peak at 2922 cm^{-1} and the peak at 2852 cm^{-1} are referred to as CH_3-strech vibration (asymmetric and symmetric) and the two shoulders at 2953 cm^{-1} and 2870 cm^{-1} are referred to as CH_2-strech vibration (asymmetric and symmetric) [31,41]. The double peak, clearly visible for resins 5 and adumbrate in some other spectra, at 2349 cm^{-1} (centre), is due to gaseous CO_2, which was not fully reduced by the auto background correction (fluctuations in the flushing gas and in the laboratory room). The same applies for the gaseous water at about 1600 cm^{-1} (centre; H-O-H scissor vibration) and its overtone at about 3788 cm^{-1} (centre with a broad band; O-H stretch vibration).

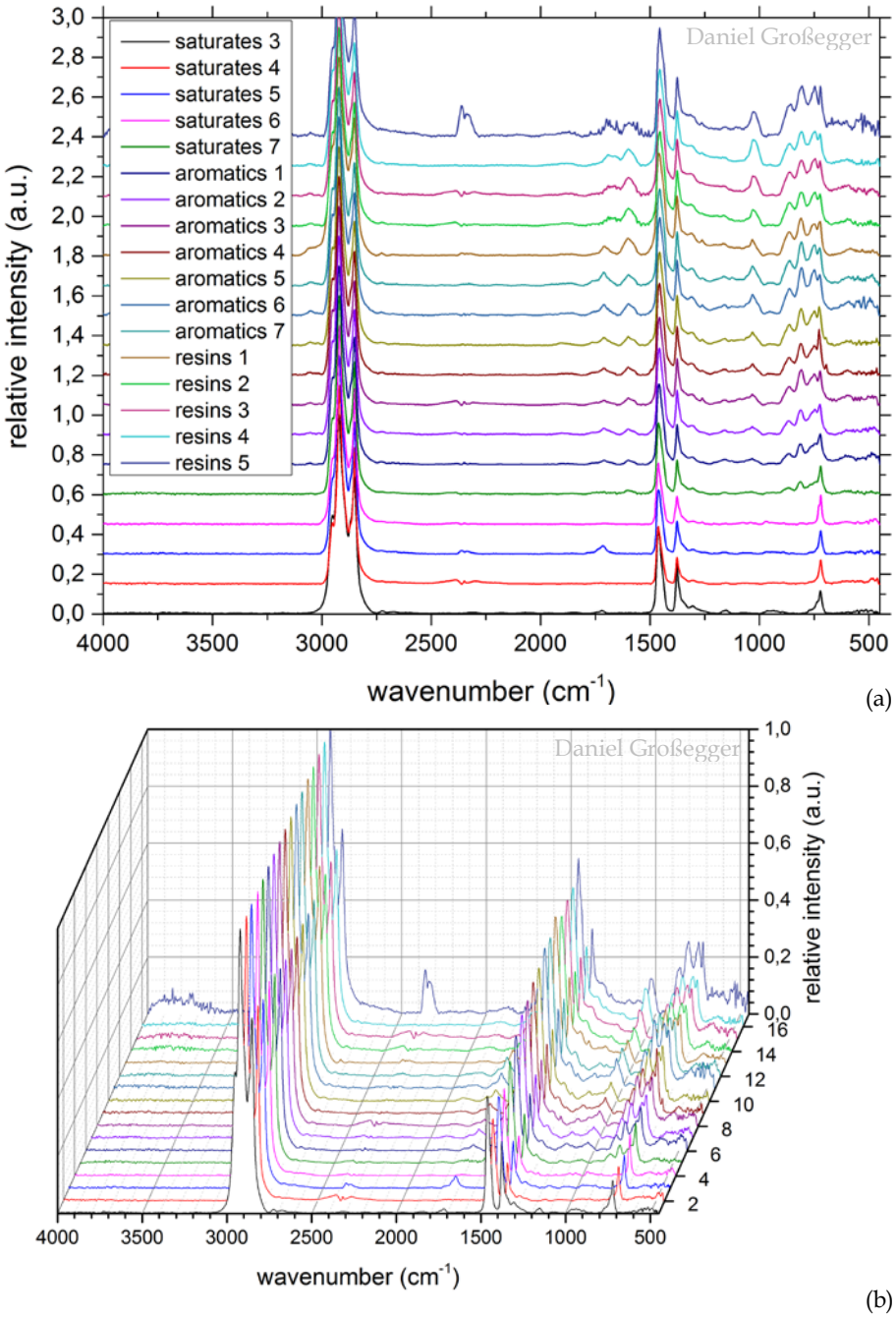

Figure 38: Infrared spectra of separated maltenes B2: staggered plot (a) and waterfall-development (b)

More details and visible changes from one fraction to the next can be found in the fingerprint region (Figure 40 and Figure 40).

Saturates have three distinct peaks in the fingerprint region. The peak at 721 cm^{-1} corresponds with $(CH_2)_n$ with n greater 3, indicating 8 to 38 $(CH)_2$ units (with increasing methylene content the absorbance peak shifts closely to 720 cm^{-1}) [45]. The CH_2 band has a peak at 1375 cm^{-1} and the CH_3 band has a peak at 1459 cm^{-1}. This means that saturates consist mainly of alkanes. Saturates 7 is similar to aromatics, which can be the first aromatic structure present in saturates, due to the chosen cut point and marked by the faint yellow colour when inspissated.

Aromatics and resins are similar in their infrared spectra with no additional appearing bands, just increasing absorption. The region from 900 to 700 cm^{-1} and the peak at 1599cm^{-1} indicates aromatic hydrocarbons [31,46], which increase as the aromatic content increases. The ketone absorption band (including carboxylic acids, both bands are indistinguishable) is at 1713 cm^{-1} [14,15,31,46]. This absorption band is also present in saturates 5, which can insinuate an oxidised state. At 1031 cm^{-1} the sulphur oxide (SO) absorption peak [14,31,46] increases towards the resins, indicating higher sulphur content for resins. Two weak peaks at about 1307 and 1157 cm^{-1} also represent sulphur oxide (SO_2).

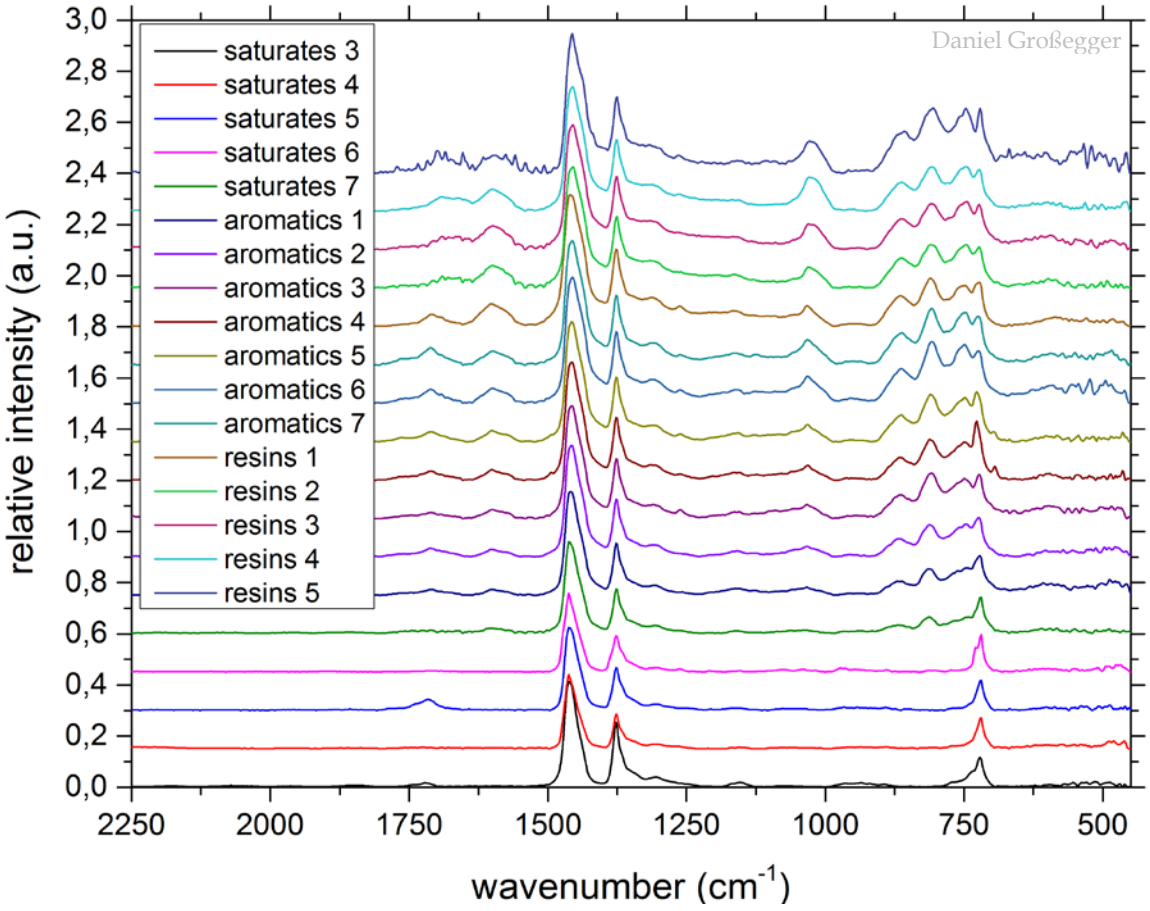

Figure 39: Infrared spectra fingerprint region of separated maltenes B2

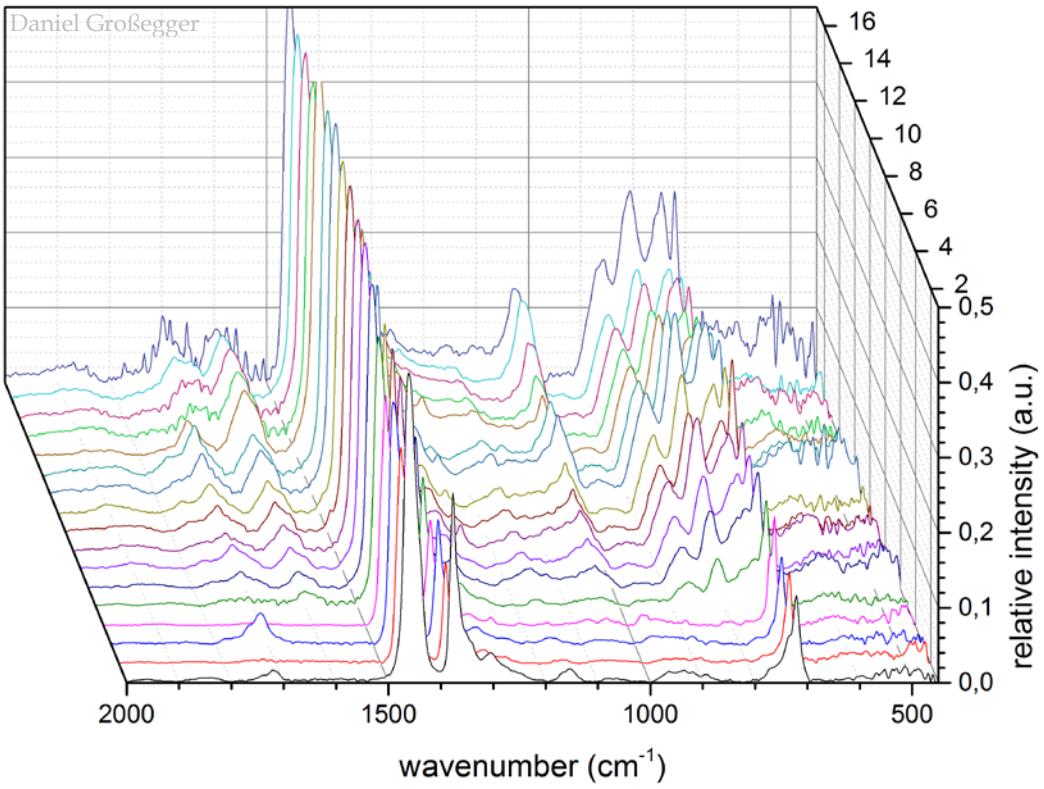

Figure 40: Infrared spectra fingerprint region of separated maltenes B2 as waterfall-development

More functional groups contribute to the spectra, but the above described are the main with dominant peaks. Especially for the region from 900 to 700 cm^{-1}, which was referred to as aromatic, different functionalities can be assigned (e.g.: alkene, cycloalkane). And some minor peaks with a broad band could have been erased by the rubberband correction.

The example of laboratory long-term aged bitumen (B_LPAV) is used to demonstrate that the spectra are in generally the same (Figure 41). As one of the first measurements the closing in the transparency of the attenuated total reflection crystal was not considered, a consequence for some spectra the baseline correction resulted in a bevel/slope, starting at about 1000 cm^{-1} to 420 cm^{-1}, where a jump occurs.

The more visible shoulder at 3060 cm^{-1} indicates double bonds and aromatics. The sulphur oxide band at 1030cm^{-1} (SO) is higher and the bands at 1308 cm^{-1} and 1159 cm^{-1} are also better visible. The peak at 1693 cm^{-1}, which is alluded to ketones and carboxylic acids, shifted in comparison to the fractions of B2 20 cm^{-1}. This could be to the cause of oxidation, aromatic structures with carboxylic acid side chains or side chains with a ketone at the first place absorb in this region. The peak at 1263 cm^{-1} could possible be ether group absorption band, which has also other peaks to identify, but they overlap with other functionality bands.

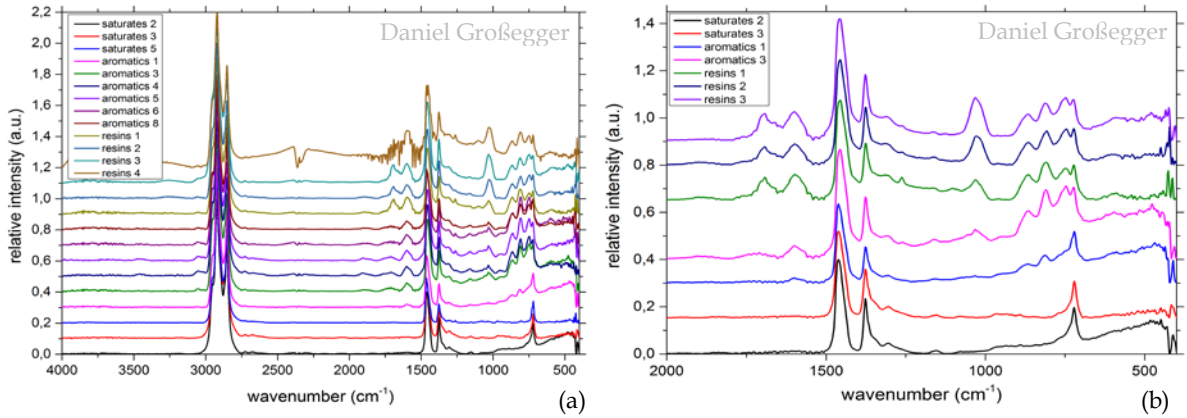

Figure 41: Infrared spectra: overview (a) and fingerprint region (b) of separated maltenes B_LPAV

5.1.4. Fractions analyses

The merged individuals of a fraction have the same common features as the individuals (see subsection 5.1.2 and 5.2.3 for individuals). Aromatics exhibit the highest fluorescence signal with a maximum at about 489 nm (Figure 42a). This maximum is between the maxima of aromatics 2 and aromatics 3. The intensity is one order of magnitude higher compared to the base bitumen. Resins show less signal intensity (Figure 42). Maltenes exhibit more fluorescence than base bitumen. This and the fact that with increasing ageing the fluorescence signal deceases, identifies aromatics as the majority fraction responsible for high signals and asphaltenes maybe quench signals. The infrared spectra for the fractions are the same as for the individuals of the fractions (Figure 43). The maltene spectrum is similar to the aromatic spectrum.

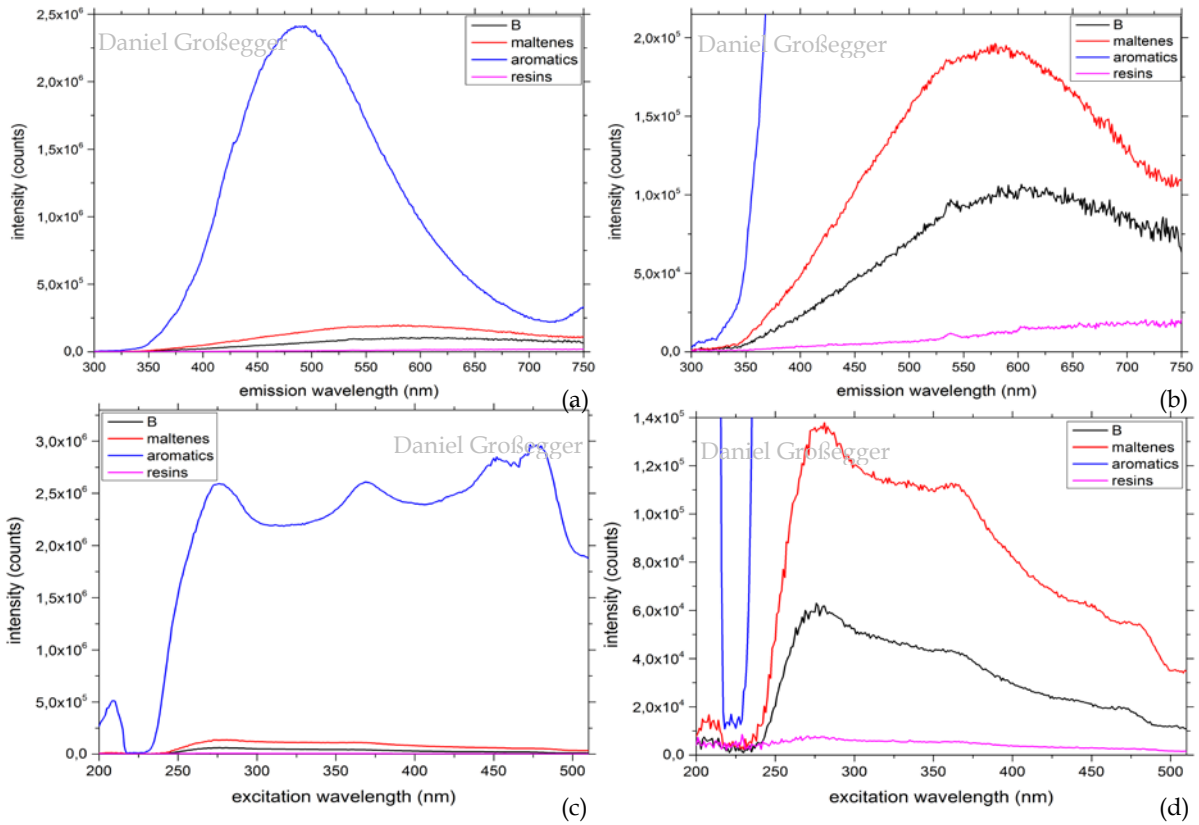

Figure 42: Base bitumen and fractions of base bitumen B: overview emission spectra (a), zoomed emission spectra (b), overview excition spectra (c) and zoomed excitation spectra (d)

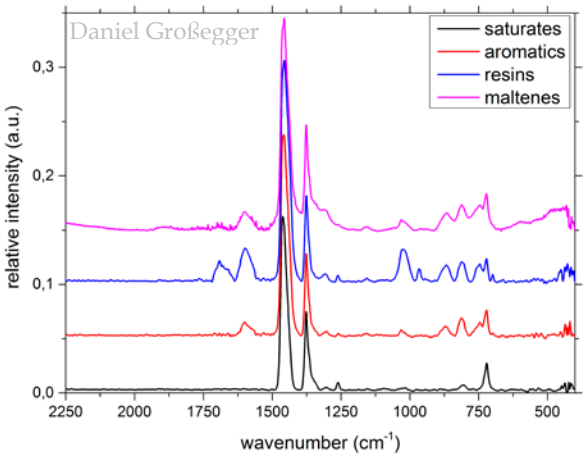

Figure 43: Infrared spectra fingerprint region of base bitumen and fractions of base bitumen B

5.1.5. Viscoelastic analyses

Due to the fact that asphaltenes are solid powders and saturates are less viscos[e], these fractions could not be tested. To include their contribution to the physical and rheological properties of bitumen, in this subsection modified bitumen samples are added to the fractions. All fractions and bitumen presented in this subsection are from base bitumen B.

Aromatics behave purely viscose and have not shown elastic or viscoelastic recovery, they even had a small increasing jump in deformation when the shear force stopped. Resins act mostly elastoplastic with a little contribution of viscoplasticity. Maltenes show viscoelastic behaviour with a small elastic recovery and still great viscoplastic contribution. From base

bitumen (b) to aged bitumen (B_LPAV) the elastic recovery respond increases (Figure 44). The increase of asphaltenes and resins, as the decrease of aromatics makes the bitumen stiffer and less viscous.

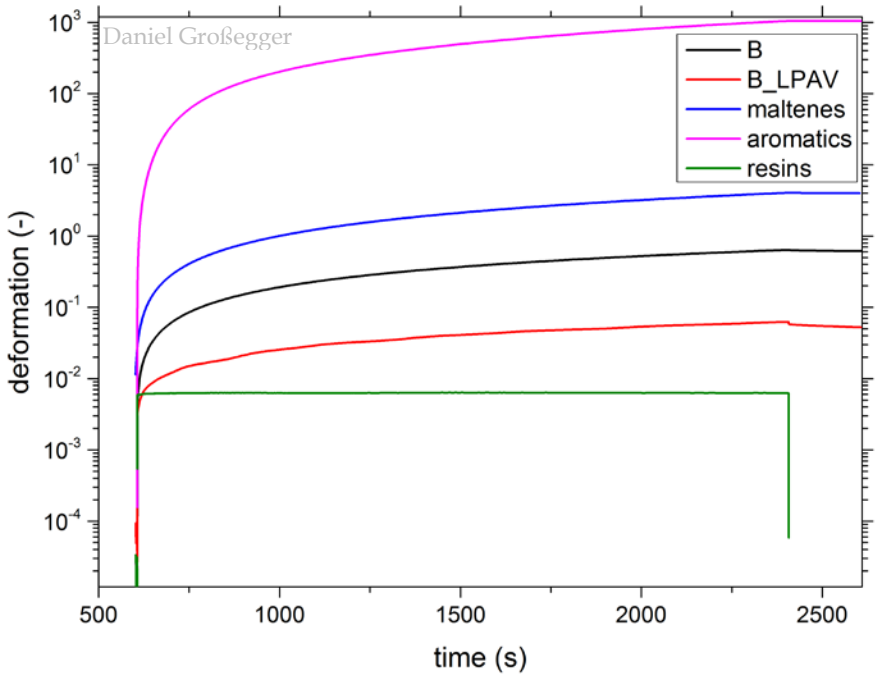

Figure 44: Creep test of base bitumen, aged bitumen and its fractions (data from [35])

On the example of maltenes the variation in the received results is shown (Figure 45). Sometimes the results can be reproduced well (maltenes-1 and maltenes-2) and occasionally it differs (maltenes-3). The variation of one fraction is not in the same range of the difference between fractions.

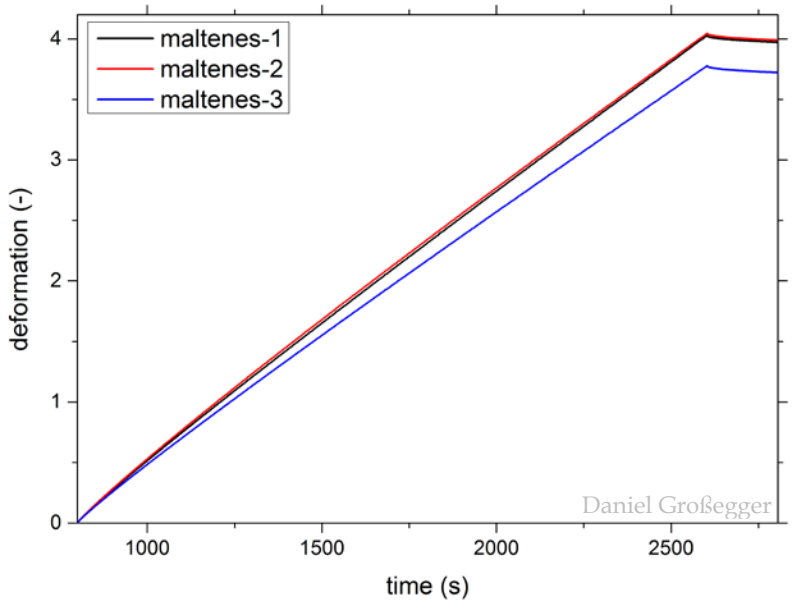

Figure 45: Creep test of maltenes (data from [35])

Bitumen without saturates are more viscous and less elastic (Figure 46a). Bitumen without saturates were generated by mixing a calculated amount of aromatics, resins and

asphaltenes together and remove the solvent afterwards (see subsection 4.3.4 for fraction obtaining and solvent removal).

In order to study the influence of asphaltenes base bitumen was doped with maltenes or asphaltenes. The separation of asphaltenes and maltenes were conducted as described in subsection 4.3.4, but a different filter was used (lesser particle retention, exact particle size unknown). Asphaltenes respectively maltenes dissolved in methylbenzene (known concentration) were added in an amount to result in the desired concentration (in wt%) to weighed base bitumen dissolved in methylbenzene. After stirring the solvent was removed. Due to the filter used, the time span and the heating and cooling steps until the measurement was conducted, asphaltene like compounds were newly formed (visualised by atomic force microscopy [47]) and thus measured maltenes were not pure. Still there is a high stiffness gain from 0% asphaltenes to 5% asphaltenes (Figure 46b). Bitumen gets stiffer as the asphaltene content increases. The 30% asphaltenes sample behaves almost in an elastoplastic way.

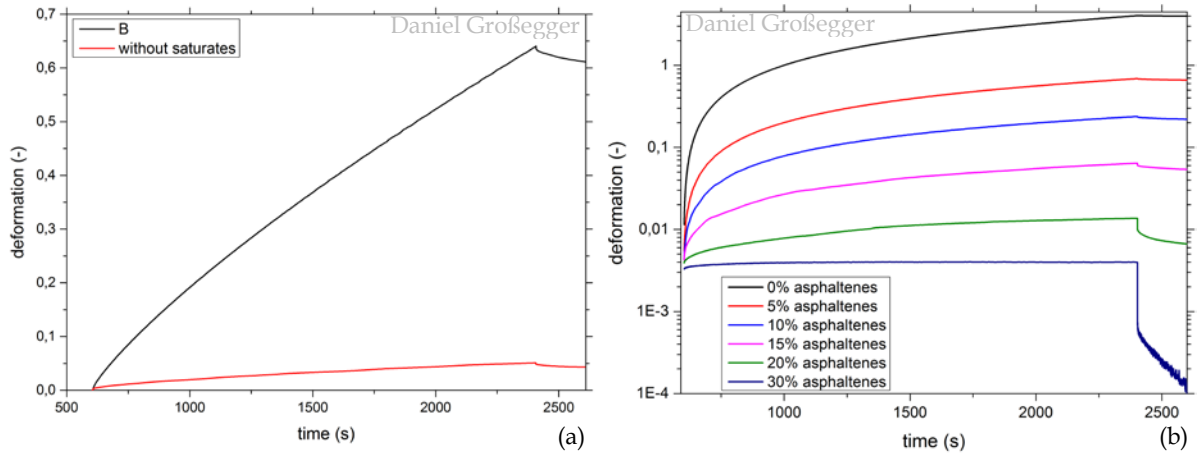

Figure 46: Creep tests of modified bitumen: base bitumen without saturates (a) and base bitumen with different amount of asphaltenes (b) (data from [35])

The same method as doped bitumen was produced was applied to produce aged bitumen. The fractions of base bitumen B were combined in the weight distribution of B_LPAV. The results were in range of the aspired laboratory long-term aged bitumen (B_LPAV). The artificial bitumen shows a little bit more of elastic behaviour, but in the range of variation, which was conformed for single fractions. From a viscoelastic point of view it makes no difference if the change in fractional distribution is due to ageing or by recreation. The sensitivity of the test gear and whether the reverse also applies (creating from fraction of an aged bitumen non-aged bitumen) was not tested.

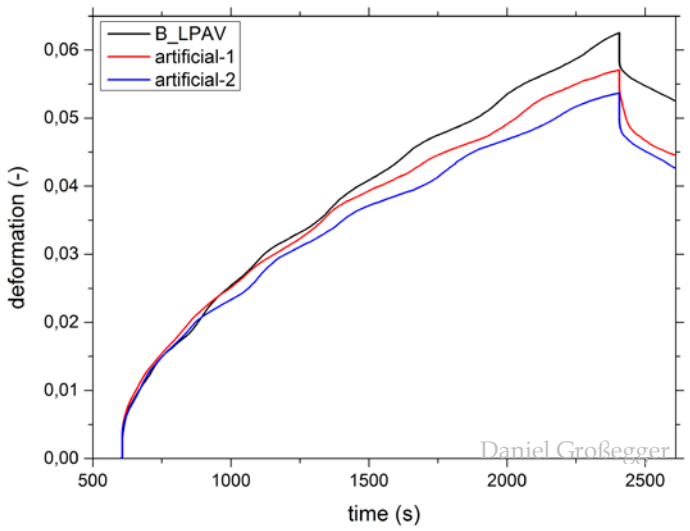

Figure 47: Comparison of aged bitumen and artificially produced bitumen

5.1.6. Water soluble compounds

The solubility of bitumen in water is negligible. Leaching tests showed that most compounds (heavy metals, polycyclic aromatic hydrocarbons and benzene, methylbenzene, ethylbenzene and dimethylbenzene) were below detection limit, except naphthalenes, fluorenes and phenanthrenes [1]. The leachate was not environmentally harmful, due to concentration below regulatory limit for drinking water [1].

No quantitative analysis of the liquid-liquid extraction was done, due to the amount of time for the separation of the two liquids and that the first extracted amount was below the uncertainty of the scales used and resulted in 0 mg recovery.

The water soluble part (analyte) was dissolved in methanol and one part was inspissated on a microscope slide. Both were measured with fluorescence spectroscopy (Figure 48). The analyte exhibits fluorescence signals, indicating compounds that are capable of fluorescence, like naphthalene, fluorene and phenanthrene [41]. The adsorption on a solid surface (microscope slide) provides rigidity and changes the spectrum (Figure 48).

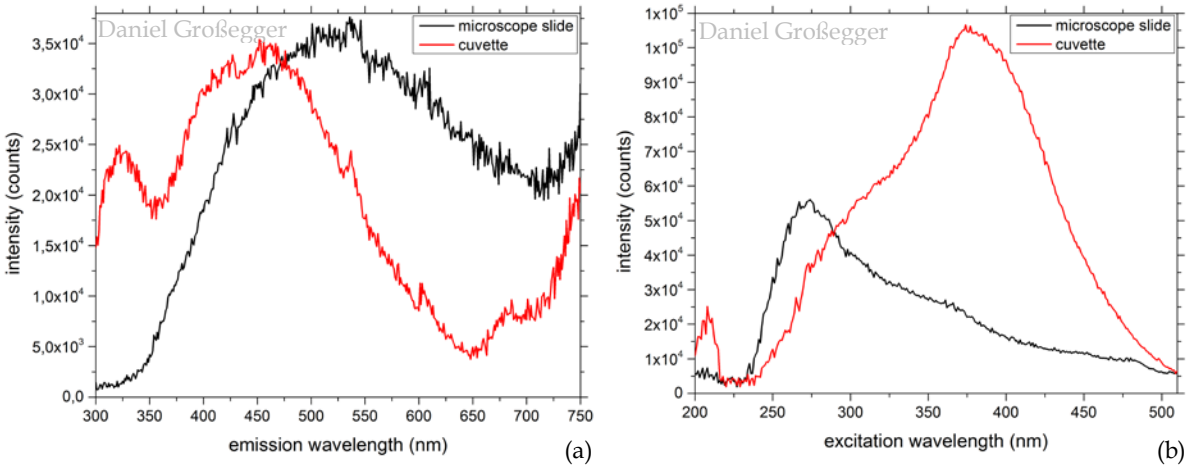

Figure 48: Fluorescence spectra of water soluble compounds, dissolved and non-dissolved: emission spectra (a) and excitation spectra (b)

The excitation measurements were repeated and changes occurred during the repetitions. Due to the vaporising of the solvent the shoulder at about 270 nm started to increase (Figure 49) and deposition on the glass walls occurred.

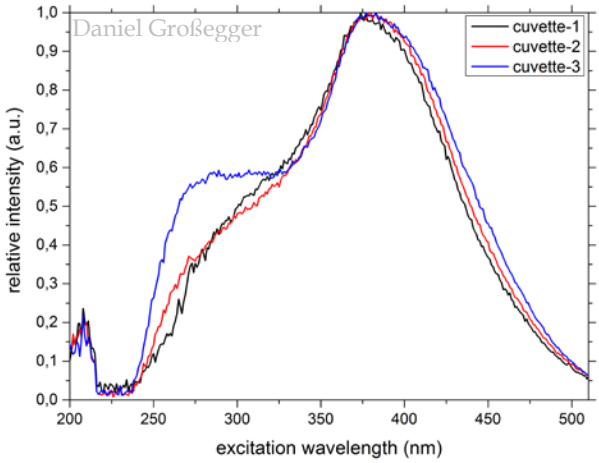

Figure 49: Change in fluorescence excitation spectrum by repeated measurements

The spectra of the water soluble compounds obtained from base bitumen are similar to those of the base bitumen or maltenes (measured on microscope slides). So a liquid-liquid extraction was performed with maltenes obtained from base bitumen B. The spectra are similar to those obtained from leached bitumen (Figure 50). The intensity increased for maltenes and the slight changes in spectra may refer to the difficulties for the microscope slide preparation. The yield was less, but the extraction was better. The better extraction was due to less influence of asphaltenes, which are considered to affect the separation of the two liquids and also affect the formation of a defined interface. Base bitumen needed longer to form this interface, as it was the case for maltenes.

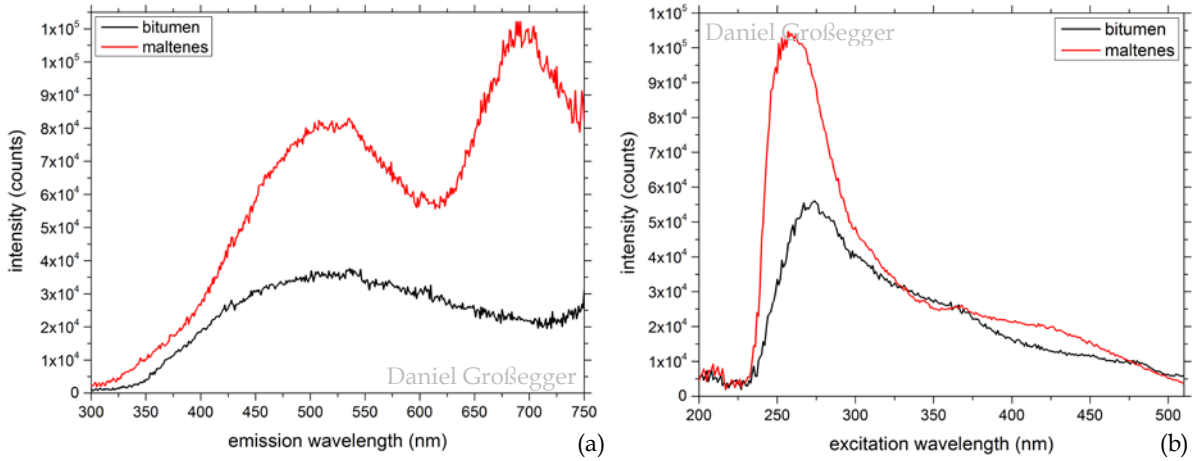

Figure 50: Comparison of analyte obtained form bitumen and maltenes: emission spectra (a) and excitation spectra (b)

In the infrared spectrum the carbon dioxide band and the water band are distinct (Figure 51). The water band was due to an applied droplet of analyte dissolved in a water methanol mixture. The CH_3 and CH_2 bands at 2925, 2852, 1458, 2957, 2872 and 1375 cm^{-1} and the $(CH_2)_n$ peak at 729 cm^{-1} (indicating approximately 3 units [45]) [14,15,31,45,46] indicates that

alkane chains are present (likely as side chains). Aromatic hydrocarbons, as capable structure for fluorescence, are related to the region from 900 to 700 cm^{-1} and the peak at 1599 cm^{-1} (masked by the water band) [14,31,46], which is not very distinct. The peak at 802 cm^{-1} is connected to double bond band or aromatic band, the weaker correlated peaks are masked by the water band. The water band also masks the ketone band. Sulphur oxide could be present as SO_2 indicated by the peak a 1140 cm^{-1} and a shoulder at 1305 cm^{-1} [14]. The region from 993 to 1217 cm^{-1} has many peaks and shoulders. Possible functional groups in this region are aromatics with different substitutions, ether groups, ester groups and alcohols, and methylbenzene as the organic liquid in the extraction [41,48]. Functional groups that allow a molecule to be dissolved in water are favoured.

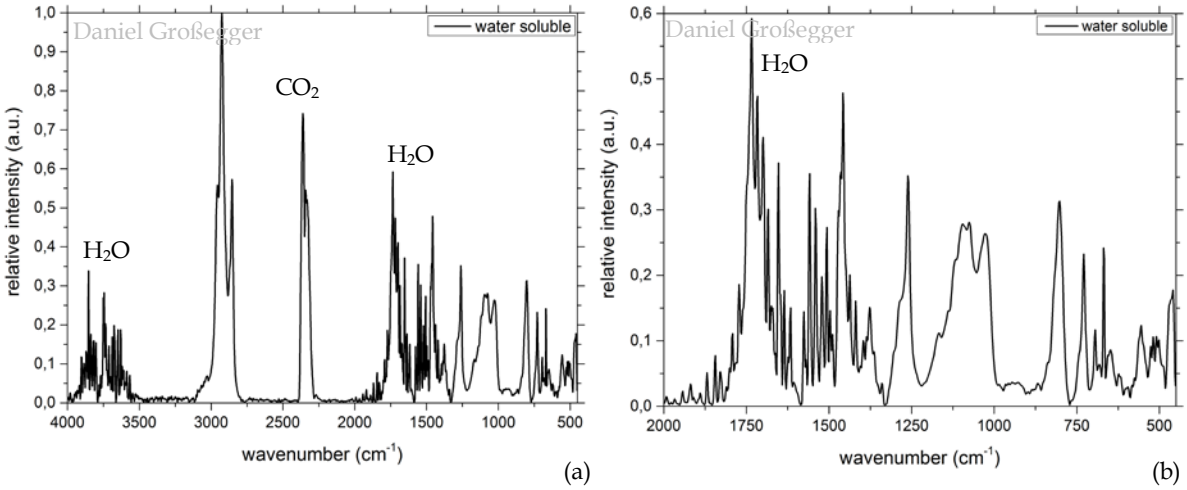

Figure 51: Infrared spectrum of analyte: overview (a) and fingerprint region (b)

An ultraviolet and visible molecular absorption spectrum shows two peaks at 264 and 272 nm and less absorption in the region of higher wavelengths. Solvent, impurities and optics have an influence on the position of the peaks and curvature. The possible chromophores (that part of an molecule consisting of an atom or group of atoms in which the electronic transition responsible for a given spectral band is approximately localized [10]) are carbonyl and aromatic [41], giving aromatic the precedence due to fluorescence.

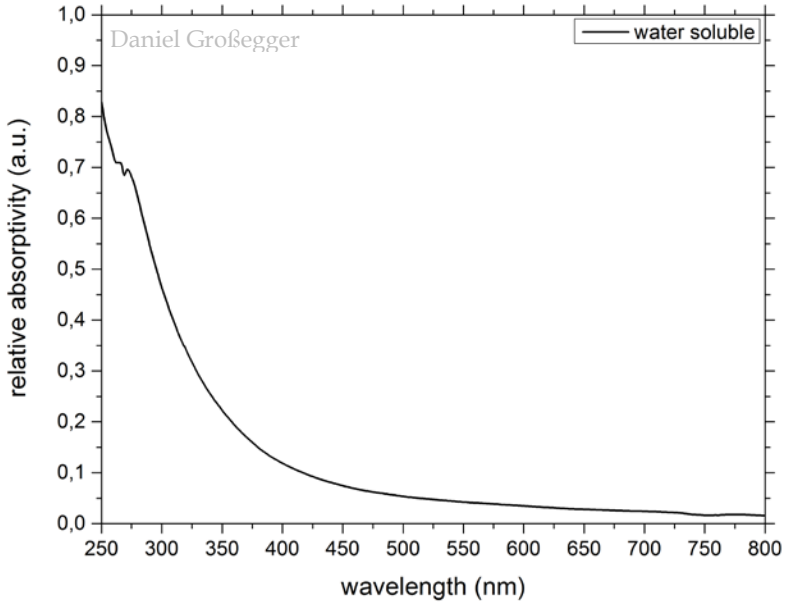

Figure 52: Ultraviolet and visible molecular absorption spectrum of the analyte dissolved in methanol

5.2. Investigation of ageing by optical and spectrochemical methods

5.2.1. Fluorescence spectroscopy

Prepared solid samples are placed inside the sample chamber. The position of the sample was varied with a hand wheel until a maximum signal (not a defined peak, more a plateau) was found in the count window on the display. The position of the sample and hence the measured intensity had an influence on the spectrum (Figure 53). At the optimal position the spectrum had a high intensity and repeated measured spectra were similar (see below). In Figure 53 position A is the spectra obtained at the optimal position region ($2 \cdot 10^7$ counts), position B is further away in the direction of the incoming light ($1 \cdot 10^7$ counts) and for position C the movement was against the direction of the incoming light ($3 \cdot 10^5$ counts). The normalised emission spectra are quite similar, but the noise increases with decreasing intensity. The normalised excitation spectra of position A and position B are also similar, but the spectrum of position C is not comparable, due to a shift in the maxima from 272 nm to 366 nm.

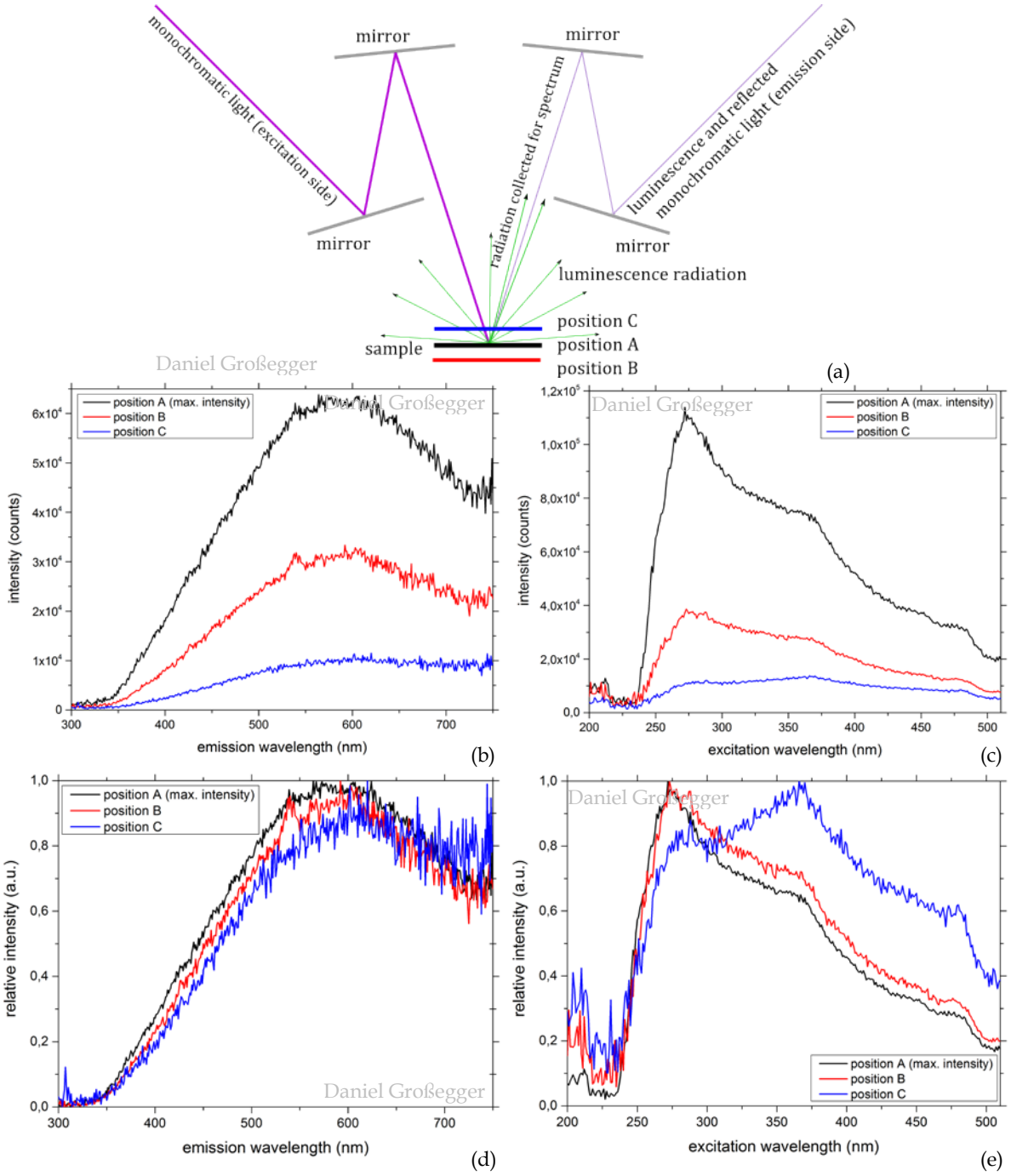

Figure 53: Influence of sample position onto the spectrum: sample chamber geometry (a), emission spectra (b), excitation spectra (c), normalised emission spectra (d) and normalised excitation spectra (e)

In order to verify the change in fluorescence spectra, the spectrum of the base bitumen B was recorded over the course of the thesis several times. This included at different optimal position inside the sample chamber and the use of three arc lamps, due to wear away of xenon arc lamps. The obtained spectra are the basis of a belt, in which 95% of the signals occur (Figure 54). This was only done for the base bitumen B. The broad variation of one sample shows that a comparison is difficult to spectra obtained from one measurement, which are close to the belt. But changes in the spectra from different treatments can be worked out and general trends are identified.

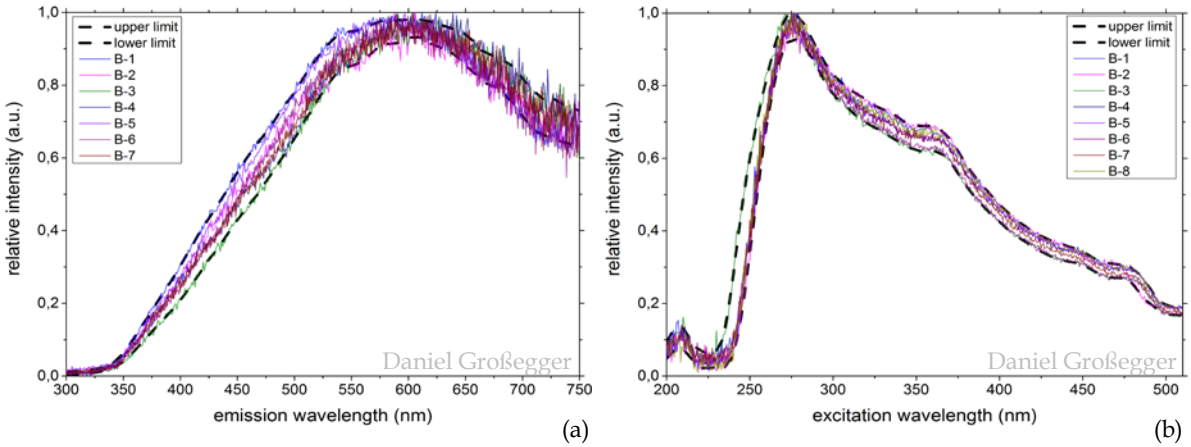

Figure 54: Fluorescence belt of base bitumen B: emission spectra (a) and excitation spectra (b)

A general trend is that with increasing ageing the intensity decreases (Figure 55). Saturates remain constant during ageing and thus their contribution to the spectra remains approximately the same. Aromatics show the highest fluorescence signal and decrease during ageing, while asphaltenes and resins, which exhibit less fluorescence, increase. Hence, the decrease in the aromatic fraction leads to a decrease in the fluorescence signal.

The decrease in intensity is not due to the changed ageing method from short-term ageing to long-term ageing, and thus short-term ageing was conducted for two additional temperatures, 20 °C and 40 °C above the standard temperature (163 °C) and for two additional duration times, two times and three times longer than the standard duration. In both cases intensity decreased while temperature (Figure 55c) or duration increased.

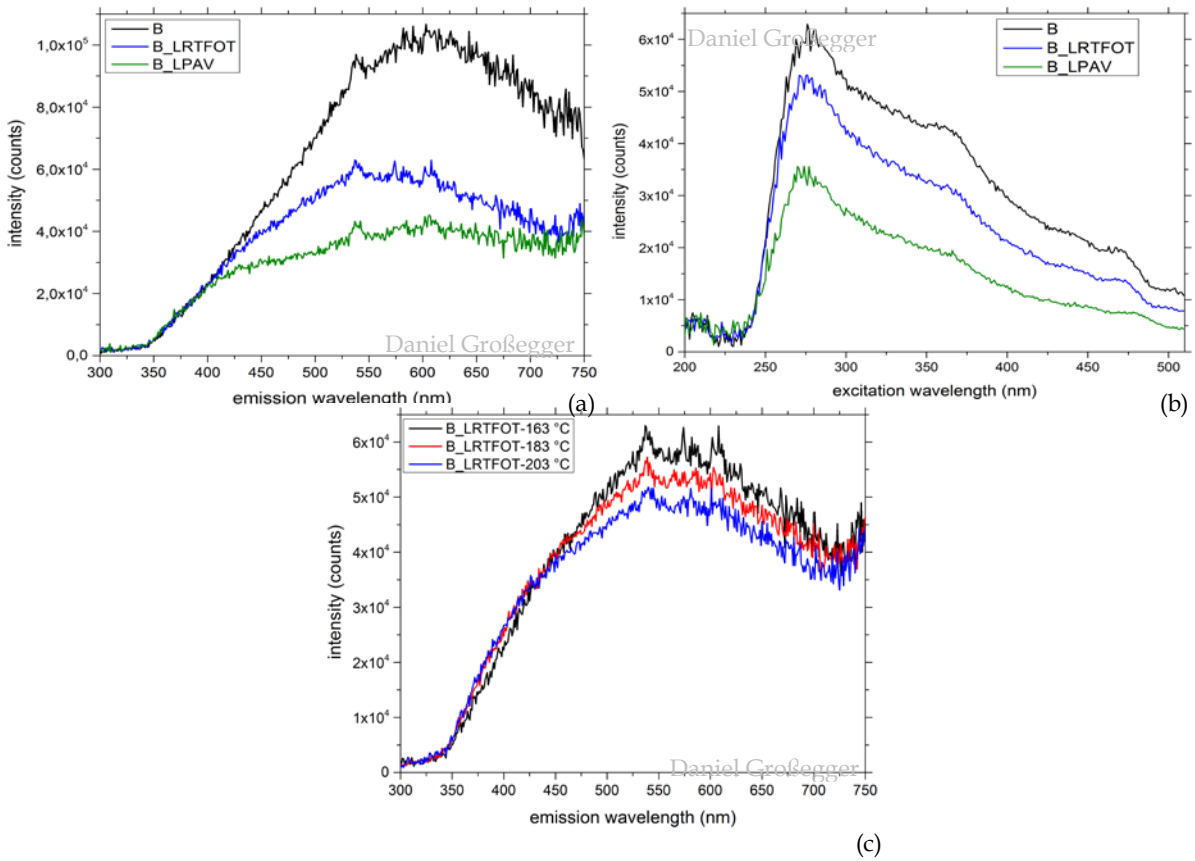

Figure 55: Decreasing intensity during laboratory ageing: emission spectra (a), excitation spectra (b) and emission spectra of laboratory short-term aged bitumen at different temperatures (c)

The problem with comparing intensity is that the position of the sample inside the sample chamber has an influence on the intensity (see above). So the spectra were normalised to avoid this influence. Though position, as the preparation method had an influence on the normalized spectra, resulting in little variation of the spectra of one bitumen and therefore the fluorescence belt was generated. For emission spectra the normalisation resulted in different slopes for different bitumen (Figure 56a). The slope (starting at about 350 nm) is in general the same for same bitumen (aged and non-aged) (Figure 55a and c). With decreasing maxima and alter of the maxima position the slope increases for aged bitumen and increases with increasing ageing period (Figure 56a). The aged bitumen lies above the upper limit of the belt form 350 to about 500 nm. In the excitation spectra the aged bitumen lies below the lower limit of the belt (Figure 56b). As bitumen age the spectrum lies lower and lower in the range from about 280 to 510 nm.

Some acquired spectra of aged bitumen are similar, so it happened that short-term aged bitumen and long-term aged bitumen have nearly the same normalised spectra (Figure 56b B_LRTFOT-1 and B_PAV). They also vary in a range of a belt. Quite unexpected were the spectra obtained from the defect xenon arc lamp. Spectra of base bitumen were similar to long-term aged bitumen and by far outside of the generated belt.

The field aged bitumen B_F282 is spectroscopically considered between long-term and short-term ageing. In the emission spectra it is close to long-term aged bitumen (B_LPAV)

and in the excitation spectra it is in the first part closer to long-term aged (B_LPAV) and than (at about 420 nm) closer to short-term aged bitumen (B_LRTFOT-2).

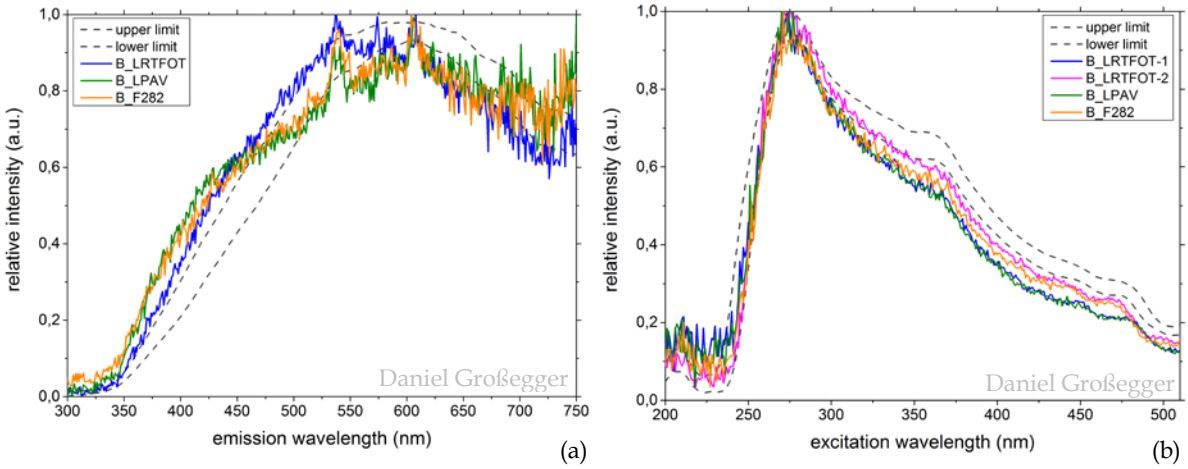

Figure 56: Comparison between laboratory and field aged bitumen: emission spectra (a) and excitation spectra (b)

5.2.2. Investigation of liquid aged bitumen

Fluorescence signals originate from the surface and fewer from the bulk (effected by transparency and self absorption). Hence the changes on the surface can be studied, which occurred during liquid ageing (see subsection 4.2.1.3).

Prepared samples were measured before treatment (data for the generated fluorescence belt) and after treatment. The treatment consisted of different storages. One group was stored light shielded (referred to as dark) and the other group was stored on the windowsill to be exposed to sunlight (referred to as light). The dark group included storage in air, water and hydrogen peroxide (H_2O_2). The light group consisted of storing in air, hydrogen peroxide, citric acid ($C_6H_8O_7$) and nitric acid (HNO_3).

Only one problem occurred: Due to the surface tension between bitumen and water, the water-stored sample minimised its surface area and did not covered the necessary area of the microscope slide (Figure 57a). For the measurement the bitumen was heated until it covered the required area (Figure 57b).

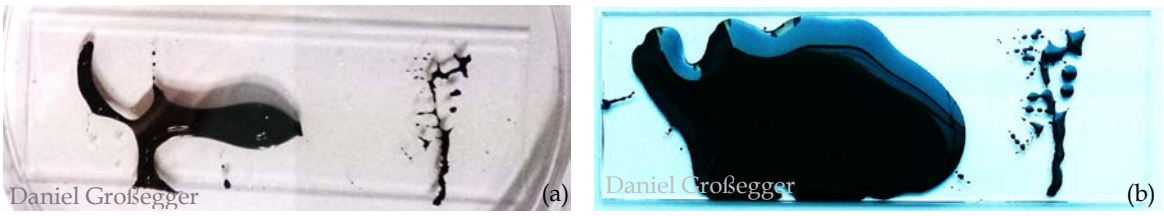

Figure 57: Water-stored sample: after 18 days (a), heat treated for measurements (similar to initial sample) (b)

Air-stored dark, water-stored dark and hydrogen peroxide-stored dark spectra (all from the same base bitumen B) are in the belt for the emission spectra (Figure 58a). The air-stored light is marginal above the upper limit and then below the lower limit, which is an indication for an aged state. Yet in the excitation spectra the air-stored light sample lies within the belt, as does the air-stored dark spectrum (Figure 58b). Air and/or light have an

influence on the surface (Figure 59) and both emission and excitation are to consider for identifying aged or non-aged. It is considered that air stored light exposed bitumen is to a minor extent aged. The water-stored dark spectrum is above the upper limit, indicating to be "younger". This could be due to the polar storage substance (water), which affects the surface and may cause water soluble components [1] to assemble near the interface (water intake of bitumen is very less, most time neglected), which remained partially in the surface layer after heating. In the excitation spectrum the hydrogen peroxide-stored dark sample is aged. The surfaces of the samples remained black after the treatment and nothing unusual, except for the water-stored sample, was visually noticed.

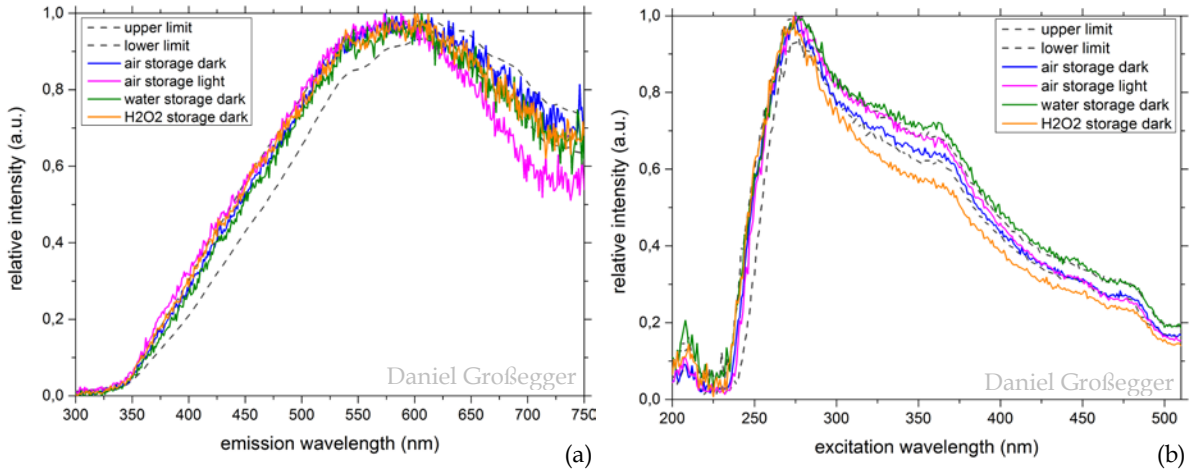

Figure 58: Base bitumen B subjected to different storage conditions over 18 days: emission spectra (a) and excitation spectra (b)

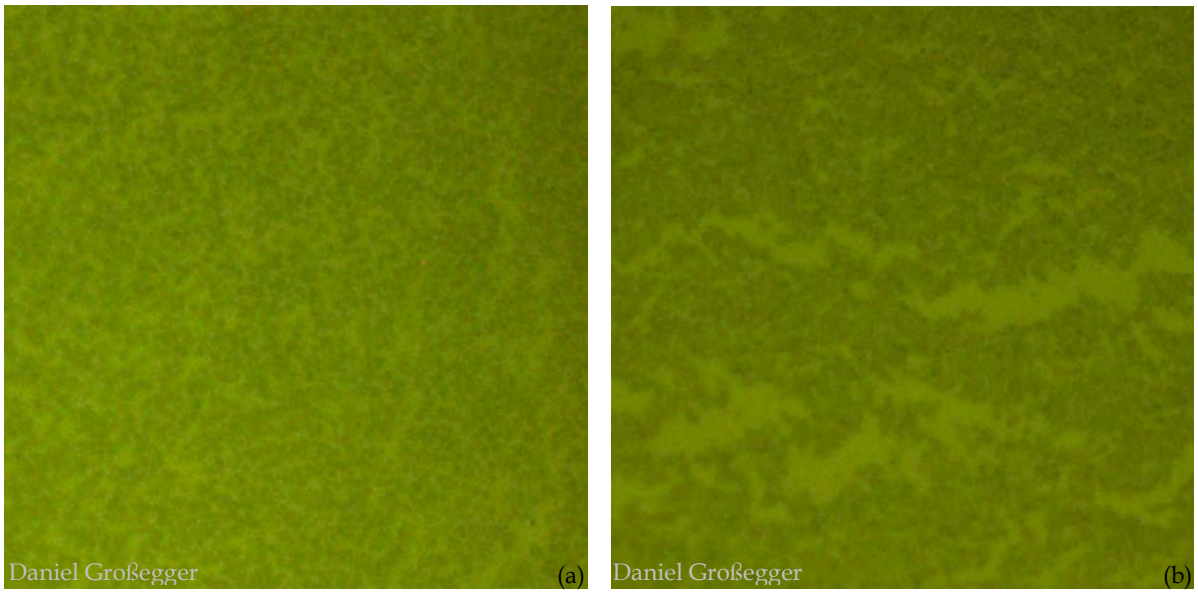

Figure 59: Microscope images: non-aged bitumen (a) and light exposed bitumen (b)

The storage within hydrogen peroxide and the exposer to light had a greater influence on the spectrum as on the visual appearance of the surface. The separation already showed that the laboratory liquid aged bitumen (B_LH2O2) is similar to the laboratory long-term aged bitumen (B_LPAV) (see section 5.1), but the spectra differ. The excitation spectra show that with increasing duration the relative intensity decrease in the back section and are similar to

the standard laboratory ageing methods except that the shoulder at about 470 nm (sometimes at 477 nm) decreases and nearly vanishes (Figure 60b). In the emission spectra there is a shift in the maxima position of about 30 nm for 19 days to 24 days duration and about 7 nm for 24 days to 38 days. For spectrum of the 19 days duration the slope is low. For the two spectra with the longer duration the slope is the same as for laboratory short-term aged bitumen. The appearing shoulder features the same wavelength range as for laboratory long-term aged bitumen (about 460 nm). The reactions for the liquid ageing methods are clearly different from the methods operating with air.

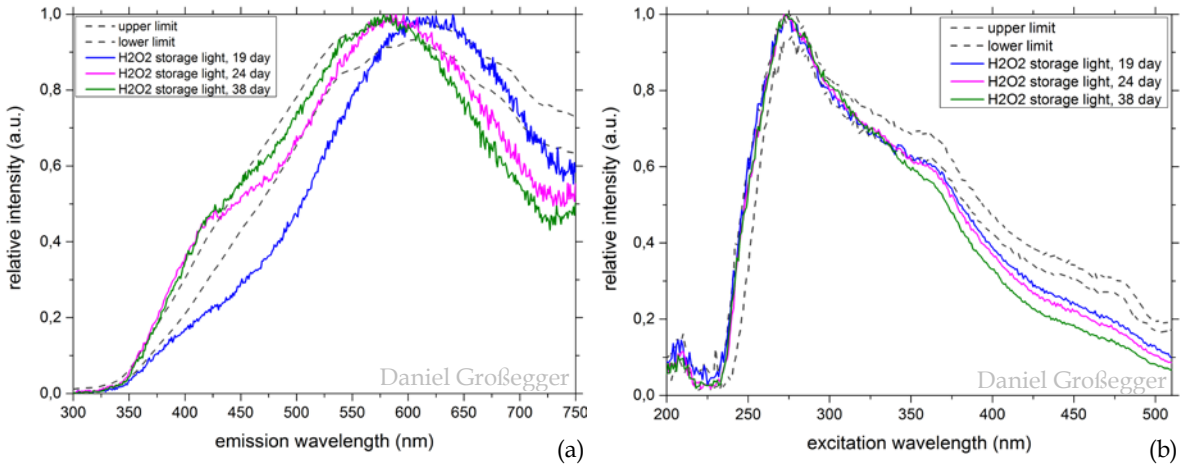

Figure 60: Base bitumen B stored in hydrogen peroxide for different durations: emission spectra (a) and excitation spectra (b)

A visible change happens for the hydrogen peroxide stored and light exposed. The surface changed from black for base bitumen to grey/greenish colour and the texture changed from smooth to curly. Under the microscope in some parts of the surface fine cracks could be seen, which means that the surface gets more brittle (Figure 61). The surface changed back to black, the texture remained, after about a month stored inside a drawer. The same effect was achieved in hours by placing the sample on a heating plate with 50 °C with fewer surface texture remaining.

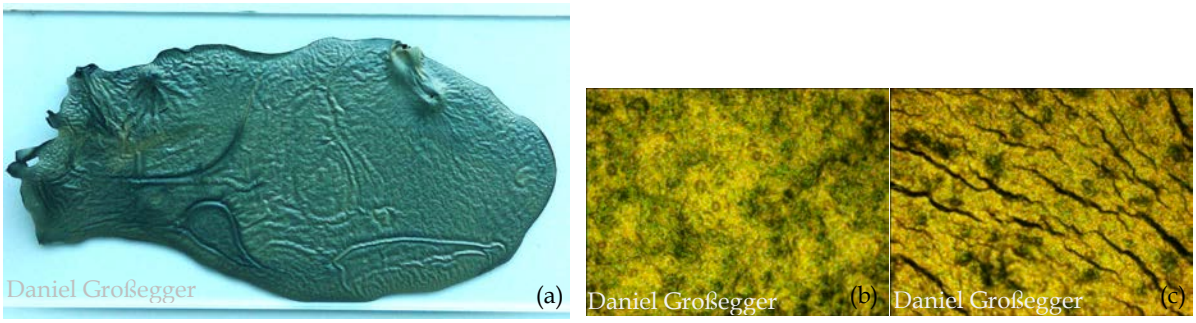

Figure 61: Laboratory liquid aged bitumen: microscope slide (a) and microscope images (b, c)

A section of the liquid aged bitumen sample in Figure 61 was cut out and the cross section was viewed under the microscope. With a comparison measurement of a known length the depth of visible change was calculated to about 13 µm. The depth is in the micrometre range, an exact value cannot be given due to the cutting process. Assuming the chemical

change happens in the layer to a depth of about 15 µm, and deeper layer are not affected by oxidative species. The asphaltene content of the laboratory liquid aged bitumen B_LH2O2 was 14,14wt% relating to the used amount of bitumen. By estimating the surface area and the density, it was calculated that the asphaltene content in the first 15 µm layer was about 28wt%, leading to an increase of three times the original content of asphaltenes in this layer. This could explain why the surface showed more of a brittle behaviour.

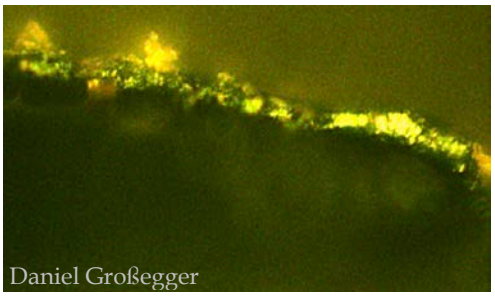

Figure 62: Cross section of liquid aged bitumen

Also other liquid ageing agents and a different concentration for hydrogen peroxide were used (Figure 63). A concentration of 15% hydrogen peroxide over 19 days is close to the spectra of 30% hydrogen peroxide over 19 days only a little bit less oxidised. The spectrum of nitric acid liquid aged bitumen (53,74% nitric acid) is noticeably similar to the spectrum of resins in appearance and intensity. If acids of smaller concentrations have the same effect is not verified. High concentration (exact concentration is unknown) of citric acid has had a very unexpected influence on the spectrum and is only included for the sake of completeness.

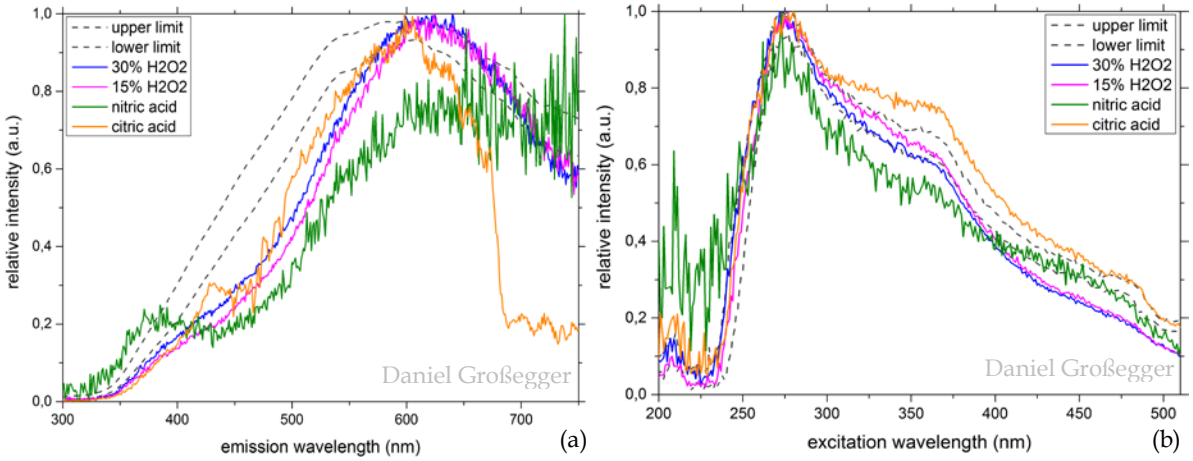

Figure 63: Liquid ageing with different acids: emission spectra (a) and excitation spectra (b)

5.2.3. Infrared spectroscopy

A comparison of base bitumen, laboratory long-term aged bitumen and liquid aged bitumen infrared spectra in the fingerprint region (see subsection 4.3.6.3) shows that during oxidation with air and hydrogen peroxides the ketone band and the sulphur oxide bands increase (Figure 64). The ketone band is more distinctive for the liquid aged sample. Additional peaks appear for the liquid aged sample. The shoulder at 1760 cm^{-1} indicates most likely

ketones on aromatic rings and carboxylic acids attached to aromatic rings, respectively. Also possible are carboxylate esters or peroxy acids. The peak 1211 cm^{-1} is correlated to the carboxylate ester band and ether band. Alcohol group bands are found to be correlated with the peak at 1124 cm^{-1}.

Bitumen consists of many different chemical species (see subsection 2.2.2) and so many different oxygen containing functional groups can occur during oxidation (ageing; 3.3). The above given identifications of the absorption peaks are considered as the main occurring functionalities. The broad peaks and adumbrated shoulders are likely to indicate additional group bands. It is noted that with different moieties the location of the band can shift and the peak width is also influenced by the chemical environment. The influence of the hydrogen peroxide stabiliser was not investigated, which could also result in an appearing peak in the infrared spectra, when the surface was not clean enough.

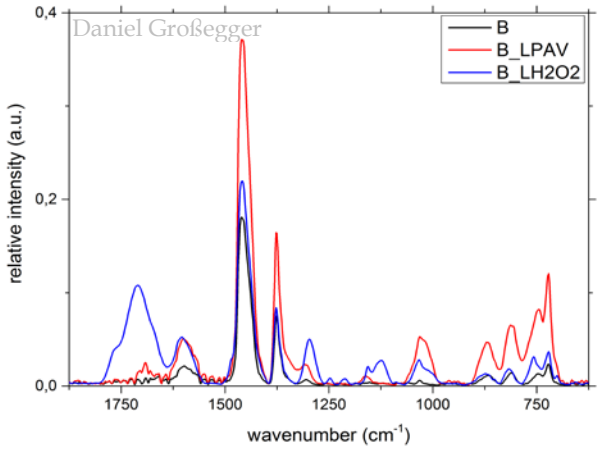

Figure 64: Infrared spectra in the fingerprint region of base bitumen B, laboratory long-term aged bitumen B_LPAV and liquid aged bitumen B_LH2O2

5.3. Brief insight in bitumen microstructure

This section is contributed to microstructure. The different atomic force microscopy techniques to visualise the microstructural features are not described in this thesis, since they were carried out by a colleague. A general short view of confocal laser scanning microscopy and atomic force microscopy is given in subsection 2.2.2.

Bitumen exhibits luminescence shown by fluorescence spectroscopy (see subsection 5.1.2 and 5.2.1). With confocal laser scanning microscopy a laser with defined wavelength (here 488 nm) excites one point and the luminescence signal is recorded (the detection ranged from 510 to 540 nm). Bitumen does not show a uniform signal, brighter elliptic spots were mapped (Figure 2). The excitation spectra reveal that at an excitation wavelength of 488 nm aromatics exhibits the highest signal intensity (Figure 43). Thus aromatic concentration is supposed to be higher in these areas. Whether the dimmer area consists of more asphaltenes or resins or whether the bright area encapsules cannot be stated with this technique.

Images of bitumen obtained by atomic force microscopy too reveal a structure. Three phases can be identified (labelled in Figure 3). One phase is corrugated (catana phase). The second phase encapsules the corrugated phase (peri-phase) and is itself embedded in the third

phase (para-phase). A comparison between confocal laser scanning microscopy images and atomic force microscopy images is difficult, due to different resolutions, but the bright spots are supposed to be about the same size as the peri-phase, but also catana phase is possible. Another possibility is that the para-phase fluctuates in concentration of fluorescence emitting molecules, allocating the bright spots distributed in the para-phase.

The structure observed by atomic force microscopy is time dependent (see subsections 2.2.2 and 3.4) and more structural features are present when the asphaltene fraction is increased, as it is during ageing (Figure 65). The catana phase and the peri-phase increase in size from non-aged to artificially long-term aged bitumen. The road sample bitumen does not feature the same structure as base bitumen and long-term aged bitumen. This could be due to the increased asphaltene concentration and decreased aromatic concentration or the extraction process from asphalt irreversible changed the structural features.

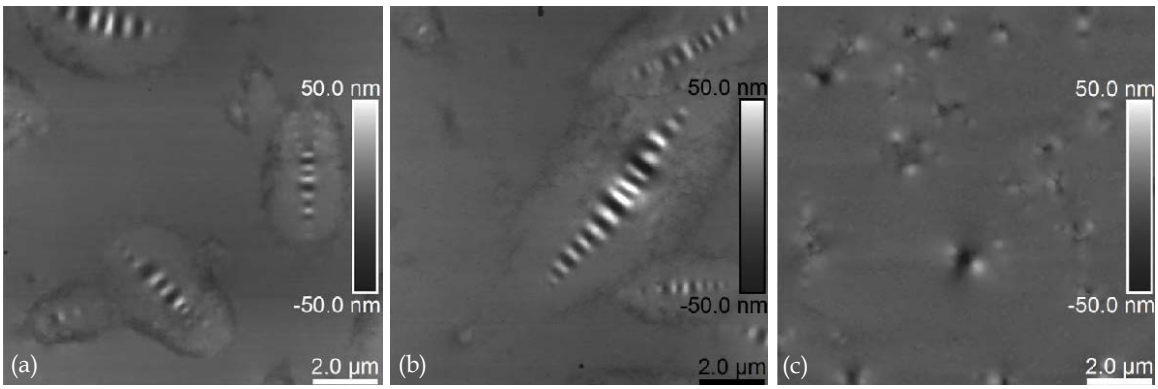

Figure 65: Atomic force microscopy topography images: base bitumen B (a), long-term aged bitumen B_LPAV (b) and road wearing course sample B_F282 (c) [18]

By scanning in peak force tapping mode correlation to mechanical properties can be made ("quantitative nonomechanical properties") [49]. Designed as a test measurement no calibration was done and so only relative proportion as coloured scale are given. Revealing that the catana phase has a higher penetration resistance (connected to Young's modulus [49], Figure 66a and b). The para-phase has a lesser penetration resistance (Figure 66a and b). The catana phase is expected to be composed of asphaltenes and resins, being more elastoplastic. Aromatics and saturates are viscous and are likely to be found in the para-phase. This correlates also well with the change in the fractional distribution. Additionally it seems that the peri-phase has a boundary of a lesser penetration resistance towards the para-phase. The road sample bitumen features several smaller "harder" spots. A direct comparison is not possible for these samples, but could reveal that the surface of the road sample has a general higher penetration resistance.

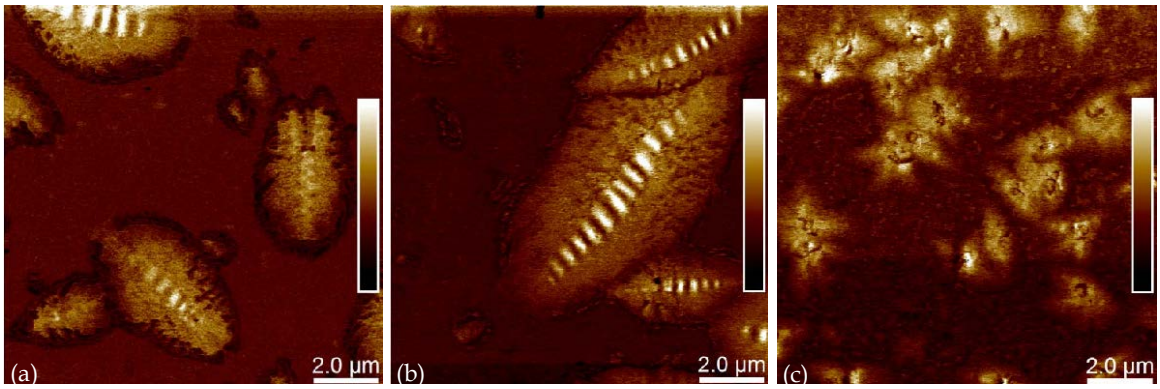

Figure 66: Atomic force microscopy images – penetration resistance: base bitumen B (a), long-term aged bitumen B_LPAV (b) and road wearing course sample B_F282 (c); bright is high value and dark is low value [18]

An overlay of topography and penetration resistance, and topography and adhesion is shown in Figure 67. The transition of penetration resistance and adhesion respectively, correlates with the topographic transition of the phases. The catana phase adheres lesser and the adhesion increases towards the para-phase. From experience, through microscope slide preparations, it can be said that saturates and aromatics are stickier and resins adhere strong to a surface once applied on it (second surface), otherwise it sticks to the spatula (first surface). With this additional information resins is likely to be in a higher concentration in the catana phase and peri-phase.

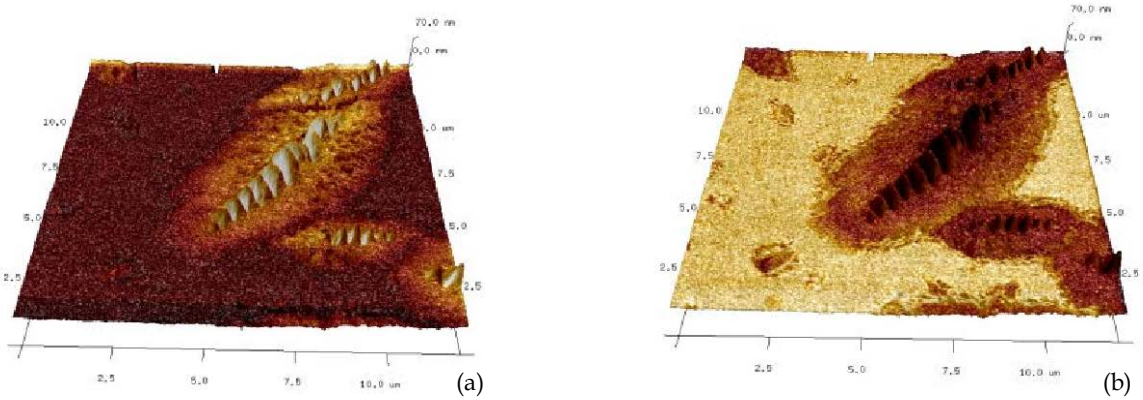

Figure 67: Atomic force microscopy image of artificially long-term bitumen B_LPAV: topography and penetration resistance (a), and topography and adhesion (b); bright is higher penetration resistance/higher adhesion and dark is lesser penetration resistance/lesser adhesion [18]

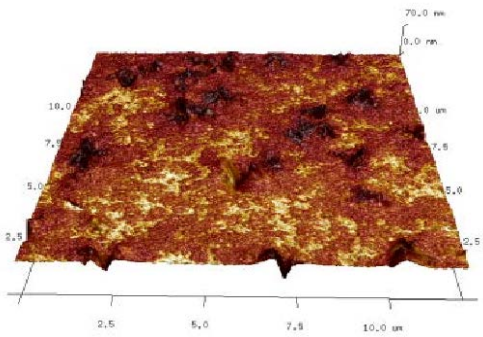

Figure 68: Atomic force microscopy image of road sample bitumen B_F282: topography and adhesion; bright is higher adhesion and dark is lesser adhesion [18]

The overlay topographic and adhesion image of the road sample bitumen revealed that the surface is less adhesive (Figure 68) and thus indicates increasing asphaltenes and decreasing aromatics diminish adhesion. Also with this the penetration resistance can be assumed to be higher and thus the surface is harder, which correlates with the increased stiffness of the bulk.

Fractions are not allocated to specific structural features. It is assumed that some features contain a greater amount of this fraction and a gradient of concentration exists in the surrounding, which is implied by the set cut points (method depending) for the fractions (see subsection 2.2.2).

Further studies of the fractions at room temperature by microscope revealed that asphaltenes are indissoluble in saturates and dissoluble in aromatics. The majority of resins is indissoluble in saturate and saturates gained a very faint reddish colour.

It cannot be said if the rough allocation of fractions is correct. Equipment with a higher resolution and additional samples would be necessary. A main part should be the investigation of the mechanism that leads to the structural features in bulk and surface. It has to be verified that the structural features present at the surface are a formation of structural features in the bulk.

6. Summary and conclusions

In the present thesis the fractional constituents were researched for non-aged and aged bitumen. The fractions were analysed in a gravimetrical, rheological and spectrochemical way. The aged bitumen was obtained once by field samples and second by laboratory ageing methods. Further spetrochemical methods were used to distinguish between non-aged and different aged bitumen.

It could be shown by separation into asphaltenes and maltenes (solubility separation) that the asphaltene fraction increases with progressing ageing stage. Further chromatographic separation of the maltenes by liquid column chromatography into saturates, aromatics and resins (separation due to polarity) revealed that the saturate content stayed unchanged during ageing. Aromatics decrease as asphaltenes and resins increase. The field aged bitumen form a test field already showed a fractional constituent as laboratory long-term aged bitumen, indicating an advanced oxidation during mixing in the asphalt mixing plant. As reference a bitumen sample from the wearing course of a 23,5 year old asphalt road was available. With 18,88wt% asphaltenes it contained more than twice of the investigated base bitumen with 9,20wt%. The reference had the same conventional testing method value range as the base bitumen. Standard laboratory aged bitumen is obtained by the use of air, higher temperatures and pressure for the last ageing stage. By using hydrogen peroxide nearly the same fractional distribution as long-term aged bitumen could be achieved by coincidence. The disadvantages for this liquid ageing method are the safety precautions and the longer duration for conducting it. Additional spectrochemical analysis revealed a different spectrum than for standard laboratory aged bitumen.

The comparison of the two studied base bitumens revealed that bitumen from the same producer with the same value range for needle penetration, differing in batch numbers, have different fractional distribution. The reason is the value range to characterise bitumen products. The obtained single fractions featured the same spectrochemical behaviour. The same was confirmed for the fractions of aged bitumen. Further comparison with literature and artificially generated bitumen from fractions verified that the fractional distribution, and hence the structural features, depends on the crude oil source and production treatment. And that classification numbers do not necessarily led to the same distribution and structural features respectively.

A chromatographic separation of asphaltenes showed that they are in the polarity range of aromatics and resins and are not the most polar fraction of bitumen.

The investigation of the single fractions showed that the colourless transparent saturates exhibit fluorescence and in the region of higher wavelength the exhibit light could be due to phosphorescence. The yellow to dark red coloured aromatics manifest the highest fluorescence intensity. Noticeable is the different excitation spectra, where the main peak is at about 478 nm, whereas the main peak for bitumen and maltenes is at about 275 nm. Aromatics have a main contribution to the fluorescence spectrum of bitumen, especially for the intensity. Resins show less and solid asphaltenes show no fluorescence. Two noticeable

peaks in their spectra at about 536 and 605 nm could be indicators for the ageing progress, due to their appearance in aged samples, but the possibility remains that they are introduced artefacts. If asphaltenes are dissolved, they do exhibit fluorescence. Depending on the concentration the intensity and spectral progression varies. Through the interaction of all fractions the spectrum of bitumen is created. Resins and asphaltenes diminish the exhibited fluorescence, indicated by their increasing content and the decrease of fluorescence intensity during ageing. As saturates are more or less unaffected by ageing their contribution to the fluorescence spectrum is assumed to be constant. By infrared spectroscopy some molecular structural changes could be shown. Saturates consist mainly of aliphatic hydrocarbons and only the last obtained fraction from the chromatographic separation contained aromatic rings, which could be due to the cut point between saturates and aromatics. Aromatic and resins include aromatic rings and oxygen, indicated by the ketone absorption band. Additionally sulphur was detected as sulphur oxides. Resins manifest slightly more relative absorption intensity for functionalities containing oxygen and sulphur, indicating a higher concentration of these for the resin fraction. Creep and creep recovery tests conducted with fractions and artificially generated bitumen from fractions showed that asphaltenes had a major impact on the mechanical and rheological behaviour of bitumen. Saturates and Aromatics were connected to a more viscose behaviour, whereas resins and asphaltenes contribute more to stiffness (elastoplastic behaviour).

Fluorescence spectroscopy is a possible way besides bitumen separation and mechanical/rheological methods to determine the oxidation state of bitumen from known base bitumen and references. The obtained spectra variation of one sample depends on preparation, geometry of the sample chamber, light source and operator. All these uncertainties are included in “belts”, due to restricted reproducibility, which typify 95% of all obtained normalised signals (repeated measurements). Laboratory aged samples showed decreasing fluorescence intensity for increasing ageing stages and also for increasing temperature and time of applied ageing methods. Preparation had a great influence on the signals, due to introducing a more oxidised surface after the sample was heated too high. The general trend of decreasing intensity with ageing duration was as well verified for the field aged samples. By normalising the spectra the intensity differences changes to a slope difference for emission. Normalised excitation spectra still showed a decreased intensity for higher wavelengths.

Laboratory liquid ageing was the attempt to simulated environmental conditions and to investigate the effects on the fractional composition. It primary changes the surface layer of bitumen and therefore spectrochemical methods are ideal, because the obtained information by fluorescence and infra red in allocated to the surface. It could be shown that light and air had already a slight influence on the surface and thus on the fluorescence signal. Hydrogen peroxide affects the surface without light exposure, but with light exposure the spectrum is changed significantly. The excitation spectra revealed that with increasing exposure duration the fluorescence intensity decreases as for aged bitumen. In addition the shoulder

at about 40 nm seems to vanish. The dissimilarity in the emission spectra between liquid aged and standard aged bitumen indicates a different mechanism for oxidation. A visible change happens to the surface, which turned grey or greenish and displayed a curly texture. The oxidation made the surface more brittle, which resulted in some cracks visualised by optical microscopy. Other acids used also changed the spectra. Nitric acid introduced changes on the surface that the spectra became similar to those of resins.

The ability of self-healing could be viewed as the changed surface of hydrogen peroxide treated bitumen sample slowly changed back to its black colour over duration of about a month.

A rough allocation of higher fraction concentration can be done for the surface, but further spectrochemical techniques with a higher space resolution are necessary for a clear allocation. The asphaltenes and resins are allocated in the catana phase and peri-phase. The para-phase consists mainly of saturates and aromatics. Aromatics act as solvent agency, which explains the encapsulation of the peri-phase seen by atomic force microscopy and the fluorescence spots featured with confocal laser scanning microscopy.

This thesis is a first step in trying to understand the mechanism of ageing and its connection to fractional distribution and structural features. The attempt of liquid ageing was to enhance processes occurring in the environment and to see whether reactions and products are the same as standard laboratory ageing methods and whether it is comparable to field ageing. The results indicated a different reaction mechanism for liquid aged bitumen. So further investigations of radicals generated by photochemical reactions are necessary to understand the occurring environmental processes.

7. List of tables

Table 1: Elemental analysis of crude oil and bitumen from various sources (wt%) [1,4–6] 3
Table 2: Code, description and treatment 17
Table 3: Snippet of atmospheric trace gases in dry air near ground level [24] 20
Table 4: Order of used eluents 40

8. List of figures

Figure 1: Flow chart of OMV refinery Schwechat; the production line for bitumen is marked purple [7] 6
Figure 2: Confocal laser scanning microscopy image of B_LPAV: fluorescence image (a) and optical image (b) 9
Figure 3: Atomic force microscopy images of B: topography (a, b) and cross profile of catana phase (c) [18] 10
Figure 4: Bitumen separation into various fractions [4] 10
Figure 5: Chromatographic column separation of maltenes obtained from B 11
Figure 6: Asphaltenes obtained from B_F282 12
Figure 7: Possible molecular structures of asphaltenes: $C_{57}H_{71}NOS$ (a), $C_{97}H_{129}NOS$ (b) and porphyrine (c) 12
Figure 8: Saturates obtain from B (a) and possible molecular structure: $C_{30}H_{62}$ (b) and $C_{38}H_{70}$ (c) 13
Figure 9: Possible molecular structure of aromatics: $C_{24}H_{34}$ (a) and $C_{27}H_{38}S$ (b) 14
Figure 10: Possible molecular structure of resins: $C_{42}H_{59}NO$ (a) and $C_{50}H_{82}S$ (b) 14
Figure 11: Asphalt microsection; the voids are filled with a polymer (blue) to provide stability during preparation 15
Figure 12: Needle penetration: probed samples (a) and development over time for the layer of the test field (b) (generated with data from [23]) 18
Figure 13: Phase angle: base bitumen, laboratory aged and first layer of test pieces at different time steps (a), layer of the 12 months test piece (b) (generated with data from [23]) 18
Figure 14: Schematic concept of tropospheric ozone generation [27] 22
Figure 15: Trend of ageing 26
Figure 16: Rolling Thins Film Oven Test: heating chamber with rotator, glass tube and air injection lance (a), filled glass tubes before (left) and after (right) treatment (b) [11] 28
Figure 17: Pressure Ageing Vessel: pressure vessel (a), frame with filled stainless steel pans (b) [11] 28
Figure 18: Liquid aged samples for chromatographic separation: 6,33 g (a) and 8,25 g (b) 30
Figure 19: Test field: with snow service (right) and without snow service (left) of unmodified (back) and modified (front) test pieces [23] 31
Figure 20: Measurement principles for needle penetration [23] 31
Figure 21: Correlation between complex modulus and phase angle (*Black* diagram) [38] 33
Figure 22: Creep behaviour of viscoelastic materials 33
Figure 23: Basic experimental set-up for column chromatography [39] 34
Figure 24: Development of chromatographic separation: pre-wetted (a), start of separation (b), advanced separation stage with no horizontal interface between the fractions (c) and column after separation (d) 41
Figure 25: Jablonski energy diagram [44] 43
Figure 26: Two prepared samples of saturates, aromatics, resins and asphaltenes (right to left) 44
Figure 27: Mean asphaltene fraction for different bitumen ageing stages 47

Figure 28: Weight per cent distribution of base bitumen fractions for different amount of used aluminium oxide: B (a) and B2 (b) 48
Figure 29: Fractional distribution related to test field..... 49
Figure 30: Fractional distribution of artificially aged bitumen..... 49
Figure 31: Weight per cent distribution of B (452 g aluminium oxide)..... 50
Figure 32: Weight per cent distribution and snap-cap vials of asphaltenes (obtained from B) separated by liquid column chromatography 51
Figure 33: Fluorescence spectra of saturates: emission (a) and excitation (b) 52
Figure 34: Fluorescence spectra of aromatics: emission (a) and excitation (b)..... 52
Figure 35: Fluorescence spectra of resins and asphaltenes: emission (a) and excitation (b) 53
Figure 36: Fluorescence spectra of asphaltenes dissolved in trichloroethene: emission (a) and excitation (b) 54
Figure 37: Weight per cent distribution of B2 (519 g aluminium oxide)..... 54
Figure 38: Infrared spectra of separated maltenes B2: staggered plot (a) and waterfall-development (b) 55
Figure 39: Infrared spectra fingerprint region of separated maltenes B2 56
Figure 40: Infrared spectra fingerprint region of separated maltenes B2 as waterfall-development 57
Figure 41: Infrared spectra: overview (a) and fingerprint region (b) of separated maltenes B_LPAV..... 58
Figure 42: Base bitumen and fractions of base bitumen B: overview emission spectra (a), zoomed emission spectra (b), overview excition spectra (c) and zoomed excitation spectra (d)..... 59
Figure 43: Infrared spectra fingerprint region of base bitumen and fractions of base bitumen B 59
Figure 44: Creep test of base bitumen, aged bitumen and its fractions (data from [35]) 60
Figure 45: Creep test of maltenes (data from [35]) 60
Figure 46: Creep tests of modified bitumen: base bitumen without saturates (a) and base bitumen with different amount of asphaltenes (b) (data from [35]) 61
Figure 47: Comparison of aged bitumen and artificially produced bitumen..... 62
Figure 48: Fluorescence spectra of water soluble compounds, dissolved and non-dissolved: emission spectra (a) and excitation spectra (b) 62
Figure 49: Change in fluorescence excitation spectrum by repeated measurements. 63
Figure 50: Comparison of analyte obtained form bitumen and maltenes: emission spectra (a) and excitation spectra (b)..... 63
Figure 51: Infrared spectrum of analyte: overview (a) and fingerprint region (b)..... 64
Figure 52: Ultraviolet and visible molecular absorption spectrum of the analyte dissolved in methanol..... 65
Figure 53: Influence of sample position onto the spectrum: sample chamber geometry (a), emission spectra (b), excitation spectra (c), normalised emission spectra (d) and normalised excitation spectra (e)..... 66
Figure 54: Fluorescence belt of base bitumen B: emission spectra (a) and excitation spectra (b) 67

Figure 55: Decreasing intensity during laboratory ageing: emission spectra (a), excitation spectra (b) and emission spectra of laboratory short-term aged bitumen at different temperatures (c) 68
Figure 56: Comparison between laboratory and field aged bitumen: emission spectra (a) and excitation spectra (b) 69
Figure 57: Water-stored sample: after 18 days (a), heat treated for measurements (similar to initial sample) (b) 69
Figure 58: Base bitumen B subjected to different storage conditions over 18 days: emission spectra (a) and excitation spectra (b) 70
Figure 59: Microscope images: non-aged bitumen (a) and light exposed bitumen (b) 70
Figure 60: Base bitumen B stored in hydrogen peroxide for different durations: emission spectra (a) and excitation spectra (b) 71
Figure 61: Laboratory liquid aged bitumen: microscope slide (a) and microscope images (b, c) 71
Figure 62: Cross section of liquid aged bitumen 72
Figure 63: Liquid ageing with different acids: emission spectra (a) and excitation spectra (b) 72
Figure 64: Infrared spectra in the fingerprint region of base bitumen B, laboratory long-term aged bitumen B_LPAV and liquid aged bitumen B_LH2O2 73
Figure 65: Atomic force microscopy topography images: base bitumen B (a), long-term aged bitumen B_LPAV (b) and road wearing course sample B_F282 (c) [18] 74
Figure 66: Atomic force microscopy images – penetration resistance: base bitumen B (a), long-term aged bitumen B_LPAV (b) and road wearing course sample B_F282 (c); bright is high value and dark is low value [18] 75
Figure 67: Atomic force microscopy image of artificially long-term bitumen B_LPAV: topography and penetration resistance (a), and topography and adhesion (b); bright is higher penetration resistance/higher adhesion and dark is lesser penetration resistance/lesser adhesion [18] 75
Figure 68: Atomic force microscopy image of road sample bitumen B_F282: topography and adhesion; bright is higher adhesion and dark is lesser adhesion [18] 75

9. References

[1] Asphalt Institute, Eurobitume. The Bitumen Industry – A Global Perspective Production, chemistry, use, specification and occupational exposure. second Edition. Asphalt Institute Inc. and European Bitumen Association-Eurobitume; 2011.

[2] GESTRATA. Asphalt Welten http://www.gestrata.at/publikationen/publ_archiv/GESTRATA_Image_Broschure.pdf (accessed March 13, 2015).

[3] Blab R. Skriptum konstruktiver Straßenbau. Institut für Verkehrswissenschaften; 2013.

[4] Lesueur D. The colloidal structure of bitumen: Consequences on the rheology and on the mechanisms of bitumen modification. Adv Colloid Interface Sci 2009;145:42–82.

[5] Simanzhenkov V, Idem R. Crude Oil Chemistry. Marcel Dekker, Inc.; 2003.

[6] Alvarez E, Marroquin G, Trejo F, Conteno G, Ancheyta J. Pyrolysis kinetics of atmospheric residue and its SARA fractions. Fuel 2011;90:3602–3607.

[7] OMV Refining & Marketing GmbH. No Title n.d. http://www.omv.at/SecurityServlet/secure?cid=1255754086633&lang=de&swa_id=1389125294636.365&swa_site=wps.vp.at (accessed February 23, 2015).

[8] Loibl A. private communication 2015.

[9] Masson J-F, Polomark GM, Collins P. Time-Dependent Microstructure of Bitumen and Its Fractions by Modulated Differential Scanning Calorimetry. Energy & Fuels 2002;16:470–476.

[10] Tittner D, Bailey RA. Encyclopedia of Chemistry. New York: Facts On File, Inc.; 2005.

[11] Hospodka M. Alterungsmechanismen von Bitumen und Simulation der Alterung im Labor. 2013.

[12] Redelius P, Soenen H. Relation between bitumen chemistry and performance. Fuel 2015;140:34–43.

[13] Sebor G, Blazek J, Nemer MF. Optimization of the preparative separation of petroleum maltenes by liquid adsorption chromatography. Journal of ChromatographyA 1999;847:323–330.

[14] Petersen JC. A Review of the Fundamentals of Asphalt Oxidation. Transportation Research Circular E-C140 2009.

[15] Guern M Le, Chailleux E, Farcas F, Dreessen S, Mabille I. Physico-chemical analysis of five hard bitumens: Identification of chemical species and molecular organization before and after artificial aging. Fuel 2010;89:3330–3339.

[16] Bearsley S, Forbes A, Haverkamp RG. Direct observation of the asphaltene structure in paving-grade bitumen using confocal laser-scanning microscopy. J Microsc 2004;215:149–155.

[17] Masson J-F, Leblond V, Margeson JC. Bitumen morphologies by phase-detection atomic force microscopy. Journal of Microscopy 2006;221:1–32.

[18] internal communication 2014.

[19] Redelius P. Asphaltenes in Bitumen , What They Are and What They Are Not. Raod Materials and Pavement Design 2009;10:25–43.

[20] Alboudwarej H, Beck J, Svrcek WY, Yarranton HW. Sensitivity of Asphaltene Properties to Separation Techniques. Energy & Fuels 2002;16:462–469.

[21] Ganeeva YM, Yusupova TN, Romanov G V. Asphaltene nano-aggregates: structure , phase transitions and effect on petroleum systems. Russian Chemical Reveviews 2011;80:993–1008.

[22] Masson J, Collins P, Polomark G. Steric Hardening and the Ordering of Asphaltenes in Bitumen. Energy & Fuels 2005;19:120–122.

[23] Stoyanova M. Untersuchungen der Feldalterung auf das rheologische Verhalten von Bitumen. 2014.

[24] Manaha SE. Fundamentals of Environmental Chemistry. second Edition. CRC Press LLC; 2001.

[25] Baird C, Cann M. Environmental Chemistry. fifth Edition. W. H. Freeman and Company; 2012.

[26] Roedel W, Wagner T. Physik unserer Umwelt: Die Atmosphäre. 4. Auflage. Springer-Verlag Berlin Heidelberg; 2011.

[27] Puxbaum H. lecture Luftchemie 2007.

[28] Naskar M, Reddy KS, Chaki TK, Divya MK, Deshpande AP. Effect of ageing on different modified bituminous binders : comparison between RTFOT and radiation ageing. Materials and Structures 2013;46:1227–1241.

[29] Boczkaj G, Przyjazny A, Kaminski M. Characteristics of volatile organic compounds emission profiles from hot road bitumens. Chemosphere 2014;107:23–30.

[30] Herrington PR. Diffusion and reaction of oxygen in bitumen films. Fuel 2012;94:86–92.

[31] Mouazen M, Poulesquen A, Bart F, Masson J, Charlot M, Vergnes B. Rheological , structural and chemical evolution of bitumen under gamma irradiation. Fuel Processing and Technology 2013;114:144–153.

[32] Durrieu F, Farcas F, Mouillet V. The influence of UV aging of a Styrene/Butadiene/Styrene modified bitumen: Comparison between laboratory and on site aging. Fuel 2007;86:1446–1451.

[33] DIN Deutsches Institut für Normungen e.V. Bitumen und bitumenhaltige Bindemittel - Betsimmung der Beständigkeit gegen Verhärtung unter Einfluss von Wärme und Luft - Teil 1: RTFOT-Verfahren. 2013. DIN EN 12607-1.

[34] DIN Deutsches Institut für Normungen e.V. Bitumen und bitumenhaltige Bindemittel - Beschleunigte Langzeit-Alterung mit einem Druckalterungsbehälter (PAV). 2012. DIN EN 14769.

[35] Hospodka M. private communication 2014.

[36] DIN Deutsches Institut für Normungen e.V. Bitumen und bitumenhaltige Bindemittel – Bestimmung der Nadelpenetration. 2013. DIN EN 1426.

[37] DIN Deutsches Institut für Normungen e.V. Bitumen und bitumenhaltige Bindemittel - Bestimmung des komplexen Schermoduls und des Phasenwinkels - Dynamisches Scherrheometer (DSR). 2012. DIN EN 14770.

[38] Hase M, Oelkers C. Rahmenbedingungen für DSR-Messungen an Bitumen. Straßenbau. Bundesanstalt für Straßenwesen; 2006.

[39] Braithwaite A, Smith FJ. Chromatographic Methods. fifth Edition. Dordrecht: Kluwer Acadamic Publishers; 1999.

[40] Kenkel J V. Analytical Chemistry for Technicians. third Edition. Boca Raton: CRC Press LLC; 2003.

[41] Skoog DA, West DM, Holler FJ, Crouch SR. Fundamentals of Analytical Chemistry. ninth Edition. Belmont: Brooks/Cole; 2014.

[42] ASTM International. Standard Test Methods for Separation of Asphalt into Four Fractions. 2001. ASTM D 4124-01.

[43] Engel T. Quantum Chemistry & Spectroscopy. third Edition. Pearson Education, Inc.; 2013.

[44] Herman B, Lakowicz JR, Murphy DB, Fellers TJ, Davidson MW. No Title n.d. http://www.olympusfluoview.com/theory/fluoroexciteemit.html (accessed February 23, 2015).

[45] Yang X, Kilpatrick P. Asphaltenes and Waxes Do Not Interact Synergistically and Coprecipitate in Solid Organic Deposits. Energy & Fuels 2005;19:1360–1375.

[46] Mouillet V, Farcas F, Besson S. Ageing by UV radiation of an elastomer modified bitumen. Fuel 2008;87:2408–2419.

[47] Hofko B, Eberhardsteiner L, Füssl J, Grothe H, Handle F, Hospodka M, et al. Impact of maltene and asphaltene fraction on mechanical behavior and microstructure of bitumen. Materials and Structures 2015;online January 31, 2015.

[48] Hollas JM. MODERN SPECTROSCOPY. fourth Edition. John Wiley & Sons Ltd; 2004.

[49] Das PK, Kringos N, Wallqvist V, Birgisson B. Micromechanical investigation of phase separation in bitumen by combining atomic force microscopy with differential scanning calorimetry results. Road Materials and Pavement Design 2013;14:25–37.

Appendix: Details on bitumen separation

bitumen: B

used amount of aluminium oxide: 452 g

initial weight: 11,82 g

fraction	weight [mg]	weight per cent [wt%]	uncertainty [wt%]
saturates 1	179,6	1,52	0,02
saturates 2	466,8	3,95	0,03
saturates 3	242,2	2,05	0,02
saturates 4	87,5	0,74	0,02
saturates 5	31,8	0,27	0,02
saturates 6	21,1	0,18	0,02
aromatics 1	2184,4	18,48	0,10
aromatics 2	1479	12,51	0,07
aromatics 3	1133,2	9,59	0,06
aromatics 4	495,8	4,19	0,03
aromatics 5	135,8	1,15	0,02
aromatics 6	85,2	0,72	0,02
aromatics 7	66,6	0,56	0,02
aromatics 8	51,7	0,44	0,02
aromatics 9	48,3	0,41	0,02
resins 1	882,6	7,47	0,05
resins 2	1573,8	13,31	0,08
resins 3	382,9	3,24	0,03
resins 4	112,2	0,95	0,02
resins 5	939,5	7,95	0,05
asphaltenes	1164,5	9,85	0,07

bitumen: B

used amount of aluminium oxide: 501 g

initial weight: 12,27 g

fraction	weight [mg]	weight per cent [wt%]	uncertainty [wt%]
saturates 1	105,2	0,86	0,02
saturates 2	434,5	3,54	0,03
saturates 3	292,8	2,39	0,03
saturates 4	132,9	1,08	0,02
saturates 5	56,6	0,46	0,02
saturates 6	30,4	0,25	0,02
aromatics 1	2150,4	17,53	0,10
aromatics 2	1381,7	11,26	0,07
aromatics 3	907,2	7,39	0,05
aromatics 4	644,8	5,26	0,04
aromatics 5	503,5	4,10	0,03
aromatics 6	210,8	1,72	0,02
aromatics 7	88,1	0,72	0,02
aromatics 8	63,0	0,51	0,02
aromatics 9	44,6	0,36	0,02
resins 1	1992,7	16,24	0,09
resins 2	866,1	7,06	0,05
resins 3	209,8	1,71	0,02
resins 4	101,3	0,83	0,02
resins 5	930,0	7,58	0,05
asphaltenes	1128,5	9,20	0,06

bitumen: B

used amount of aluminium oxide: 565 g

initial weight: 11,82 g

fraction	weight [mg]	weight per cent [wt%]	uncertainty [wt%]
saturates 1	3,9	0,03	0,02
saturates 2	77,4	0,65	0,02
saturates 3	394,5	3,34	0,03
saturates 4	253,0	2,14	0,03
saturates 5	125,3	1,06	0,02
aromatics 1	675,1	5,71	0,04
aromatics 2	2078,7	17,59	0,10
aromatics 3	845,3	7,15	0,05
aromatics 4	503,2	4,26	0,04
aromatics 5	211,6	1,79	0,02
aromatics 6	129,3	1,09	0,02
aromatics 7	113,4	0,96	0,02
aromatics 8	83,0	0,70	0,02
aromatics 9	74,4	0,63	0,02
resins 1	1258,2	10,64	0,07
resins 2	1975,8	16,72	0,10
resins 3	733,3	6,20	0,05
resins 4	470,1	3,98	0,04
resins 5	302,9	2,56	0,03
resins 5	191,7	1,62	0,02
resins 6	28,5	0,24	0,02
resins 7	22,9	0,19	0,02
asphaltenes	1230,0	10,41	0,51

bitumen: B2

used amount of aluminium oxide: 457 g

initial weight: 11,46 g

fraction	**weight [mg]**	**weight per cent [wt%]**	**uncertainty [wt%]**
saturates 1	384,6	3,36	0,03
saturates 2	306,6	2,68	0,03
saturates 3	102,2	0,89	0,02
saturates 4	56,2	0,49	0,02
aromatics 1	1729,0	15,09	0,09
aromatics 2	1398,1	12,20	0,08
aromatics 3	927,4	8,09	0,06
aromatics 4	424,7	3,71	0,04
aromatics 5	137,6	1,20	0,02
aromatics 6	107,0	0,93	0,02
aromatics 7	76,4	0,67	0,02
aromatics 8	70,1	0,61	0,02
aromatics 9	11,9	0,10	0,02
resins 1	69,0	0,60	0,02
resins 2	2687,4	23,45	0,14
resins 3	616,6	5,38	0,04
resins 4	136,0	1,19	0,02
resins 5	442,4	3,86	0,04
asphaltenes	1440,0	12,57	0,52

bitumen: B2

used amount of aluminium oxide: 519 g

initial weight: 14,07 g

fraction	weight [mg]	weight per cent [wt%]	uncertainty [wt%]
saturates 1	0,5	0,00	0,01
saturates 2	1,3	0,01	0,01
saturates 3	11,3	0,08	0,01
saturates 4	341,4	2,43	0,02
saturates 5	540,6	3,84	0,03
saturates 6	302,4	2,15	0,02
saturates 7	106,2	0,76	0,02
aromatics 1	1392,6	9,90	0,06
aromatics 2	1310,5	9,31	0,05
aromatics 3	1037,7	7,38	0,04
aromatics 4	600,5	4,27	0,03
aromatics 5	535,4	3,81	0,03
aromatics 6	449,2	3,19	0,03
aromatics 7	142,0	1,01	0,02
aromatics 8	79,1	0,56	0,02
resins 1	130,8	0,93	0,02
resins 2	1631,0	11,59	0,06
resins 3	1640,2	11,66	0,06
resins 4	836,1	5,94	0,04
resins 5	1091,3	7,76	0,05
asphaltenes	1810,0	12,86	0,43

bitumen: B_F000_A

used amount of aluminium oxide: 501 g

initial weight: 11,25 g

fraction	weight [mg]	weight per cent [wt%]	uncertainty [wt%]
saturates 1	11,2	0,10	0,02
saturates 2	186,6	1,66	0,02
saturates 3	453,6	4,03	0,04
saturates 4	192,3	1,71	0,03
saturates 5	57,6	0,51	0,02
saturates 6	25,7	0,23	0,02
aromatics 1	2528,9	22,48	0,14
aromatics 2	930,3	8,27	0,06
aromatics 3	532,1	4,73	0,04
aromatics 4	173,6	1,54	0,02
aromatics 5	84,4	0,75	0,02
aromatics 6	52,3	0,46	0,02
aromatics 7	51,0	0,45	0,02
aromatics 8	43,0	0,38	0,02
resins 1	1511,1	13,43	0,09
resins 2	1358,6	12,08	0,08
resins 3	550,1	4,89	0,04
resins 4	310,7	2,76	0,03
resins 5	369,6	3,29	0,03
resins 6	300,3	2,67	0,03
asphaltenes	1470,0	13,07	0,53

bitumen: B_F000_C

used amount of aluminium oxide: 604 g

initial weight: 11,91 g

fraction	weight [mg]	weight per cent [wt%]	uncertainty [wt%]
saturates 1	28,8	0,25	0,02
saturates 2	222,3	1,89	0,02
saturates 3	358,8	3,06	0,03
saturates 4	171,7	1,46	0,02
saturates 5	90,6	0,77	0,02
aromatics 1	2049,2	17,45	0,10
aromatics 2	1038,3	8,84	0,06
aromatics 3	845,2	7,20	0,05
aromatics 4	520,9	4,44	0,04
aromatics 5	248,0	2,11	0,03
aromatics 6	119,3	1,02	0,02
aromatics 7	75,2	0,64	0,02
aromatics 8	55,5	0,47	0,02
aromatics 1	18,9	0,16	0,02
resins 1	1478,7	12,60	0,08
resins 2	1537,2	13,09	0,08
resins 3	430,9	3,67	0,03
resins 4	284,8	2,43	0,03
resins 5	568,9	4,85	0,04
asphaltenes	1530,0	12,85	0,50

bitumen: B_F012_S1

used amount of aluminium oxide: 503 g

initial weight: 11,68 g

fraction	weight [mg]	weight per cent [wt%]	uncertainty [wt%]
saturates 1	90,4	0,77	0,02
saturates 2	426,6	3,65	0,03
saturates 3	294,7	2,52	0,03
saturates 4	127,1	1,09	0,02
saturates 5	57,0	0,49	0,02
aromatics 1	1780,0	15,24	0,09
aromatics 2	1132,3	9,69	0,07
aromatics 3	677,9	5,80	0,05
aromatics 4	454,1	3,89	0,04
aromatics 5	154,8	1,33	0,02
aromatics 6	73,4	0,63	0,02
aromatics 7	38,7	0,33	0,02
aromatics 8	40,2	0,34	0,02
resins 1	1765,8	15,12	0,09
resins 2	1230,9	10,54	0,07
resins 3	352,9	3,02	0,03
resins 4	281,5	2,41	0,03
resins 5	235,9	2,02	0,03
resins 6	556,3	4,76	0,04
asphaltenes	1710,0	14,64	0,51

bitumen: B_F282

used amount of aluminium oxide: 567 g

initial weight: 10,22 g

fraction	weight [mg]	weight per cent [wt%]	uncertainty [wt%]
saturates 1	0,0	0,00	0,02
saturates 2	139,4	1,36	0,03
saturates 3	383,6	3,75	0,04
saturates 4	199,9	1,96	0,03
saturates 5	76,6	0,75	0,02
saturates 6	44,6	0,44	0,02
aromatics 1	1728,2	16,91	0,12
aromatics 2	1072,1	10,49	0,08
aromatics 3	458,2	4,48	0,04
aromatics 4	151,9	1,49	0,03
aromatics 5	81,4	0,80	0,02
aromatics 6	64,7	0,63	0,02
aromatics 7	46,8	0,46	0,02
aromatics 8	35,8	0,35	0,02
aromatics 1	23,3	0,23	0,02
resins 1	1309,8	12,82	0,09
resins 2	1521,4	14,89	0,11
resins 3	101,5	0,99	0,02
resins 4	142,6	1,40	0,03
resins 5	421,6	4,13	0,04
asphaltenes	1930,0	18,88	0,59

bitumen: B_LRTFOT

used amount of aluminium oxide: 450 g

initial weight: 12,02 g

fraction	weight [mg]	weight per cent [wt%]	uncertainty [wt%]
saturates 1	6,6	0,05	0,02
saturates 2	416,9	3,47	0,03
saturates 3	417,3	3,47	0,03
saturates 4	122,2	1,02	0,02
saturates 5	42,1	0,35	0,02
saturates 6	30,2	0,25	0,02
aromatics 1	2445,3	20,34	0,12
aromatics 2	1718,4	14,30	0,09
aromatics 3	813,0	6,76	0,05
aromatics 4	199,8	1,66	0,02
aromatics 5	105,6	0,88	0,02
aromatics 6	74,6	0,62	0,02
aromatics 7	56,6	0,47	0,02
aromatics 8	50,2	0,42	0,02
resins 1	840,9	7,00	0,05
resins 2	1900,7	15,81	0,09
resins 3	470,7	3,92	0,03
resins 4	97,1	0,81	0,02
resins 5	125,5	1,04	0,02
resins 5	757,6	6,30	0,05
asphaltenes	1274,9	10,61	0,07

bitumen: B_LPAV

used amount of aluminium oxide: 451 g

initial weight: 13,25 g

fraction	weight [mg]	weight per cent [wt%]	uncertainty [wt%]
saturates 1	7,3	0,06	0,01
saturates 2	235,1	1,77	0,02
saturates 3	556,5	4,20	0,03
saturates 4	244,0	1,84	0,02
saturates 5	75,5	0,57	0,02
saturates 6	36,1	0,27	0,01
aromatics 1	2037,4	15,38	0,08
aromatics 2	1629,0	12,29	0,07
aromatics 3	937,0	7,07	0,05
aromatics 4	259,2	1,96	0,02
aromatics 5	90,9	0,69	0,02
aromatics 6	60,6	0,46	0,02
aromatics 7	48,1	0,36	0,02
aromatics 8	39,7	0,30	0,01
aromatics 1	25,4	0,19	0,01
resins 1	1210,1	9,13	0,05
resins 2	2050,5	15,48	0,08
resins 3	460,3	3,47	0,03
resins 4	135,0	1,02	0,02
resins 5	84,6	0,64	0,02
resins 6	969,2	7,31	0,05
asphaltenes	1966,9	14,84	0,08

bitumen: B_LH2O2

used amount of aluminium oxide: 498 g

initial weight: 13,45 g

fraction	weight [mg]	weight per cent [wt%]	uncertainty [wt%]
saturates 1	7,1	0,05	0,01
saturates 2	61,5	0,46	0,02
saturates 3	476,0	3,54	0,03
saturates 4	360,4	2,68	0,03
saturates 5	144,2	1,07	0,02
saturates 6	57,9	0,43	0,02
aromatics 1	1887,5	14,03	0,08
aromatics 2	1270,3	9,44	0,06
aromatics 3	909,1	6,76	0,04
aromatics 4	516,8	3,84	0,03
aromatics 5	263,4	1,96	0,02
aromatics 6	96,2	0,72	0,02
aromatics 7	63,3	0,47	0,02
aromatics 8	48,8	0,36	0,02
aromatics 1	15,2	0,11	0,01
resins 1	1648,7	12,26	0,07
resins 2	1916,0	14,25	0,08
resins 3	533,8	3,97	0,03
resins 4	939,3	6,98	0,04
asphaltenes	1901,4	14,14	0,08

asphaltenes

used amount of aluminium oxide: 153 g

initial weight: 2,01 g

fraction	weight [mg]	weight per cent [wt%]	uncertainty [wt%]
asphaltenes 1	52	2,58	0,09
asphaltenes 2	152,9	7,60	0,10
asphaltenes 3	653,2	32,46	0,12
asphaltenes 4	779	38,71	0,12
asphaltenes 5	201,3	10,00	0,10
asphaltenes 6	119,3	5,93	0,09
asphaltenes 7	16,6	0,82	0,09
asphaltenes 8	6,9	0,34	0,09
asphaltenes 9	1,1	0,05	0,09
Column hold-up	30,1	1,50	0,09

r